Mirosław Kozłowski

and

Janina Marciak-Kozłowska

From Quarks to Bulk Matter

Physics of the Causal Thermal Phenomena

Contents

Introduction

Three massive scientific waves are gathering momentum as we approach the end of the twentieth century. These waves are set to transform our lives in the twenty-first century to a far greater extent, than our parent's and grandparent's lives were changed by advances made during this century. Nanoscale science, information science and molecular biology are all rapidly developing into engineering disciplines, and each will be responsible for the start of at least one major industrial revolution during the next 20 years.

The book is mostly devoted to nanoscale science. Nanoscale science involves the study understanding and control of matter at the atomic level. In the late 1950s only the Nobel prize winning physicist Richard Feynman truly understood that it would be possible to observe and manipulate individual atoms [1]. Today hundreds of laboratories all over the world routinely use the scanning tunneling microscope (STM) – which was invented in the early 1980s by Gerd Binning and Heinrich Rohrer at IBM's Research Laboratory and Ruschlikon – to obtain topographic maps of material surfaces in which it is possible to identify individual atoms.

It may soon be possible to manufacture electrical contacts so tiny, that they would comprise just one, single atom, creating the ultimate in electronic miniaturization. E. Scheer and her multinational team created their

single-atom contacts using SMT [2]. The conductance for one atom of lead contacts was measured as the contact was stretched. It occurs that the conductance fell into in discrete steps. But perhaps most interesting of all, these single-atom contacts determine the conductance of the entire circuits in which they are placed. In other words, the quantum properties of atoms effectively determine the properties of an electronic circuit, which is a macroscopic object.

Recent years have seen significant advances in the characterization and manipulation of individual molecules. STM techniques allow for the study of single molecules on the surfaces, and optical techniques enable their characterization in complex condensed environments. Furthermore, the manipulation of molecules with STM may lead to the construction of artificial molecular machines [3].

An important scientific frontier is the application of X-ray pulses to investigate ultrafast structural dynamics (atomic motion and rearrangement), associated with phase transitions in solids, chemical reactions and rapid biological processes. The fundamental time scale for such motion is an atomic vibrational period, on the order of 100 fs. Such dynamics have been investigated to date primarily with visible pulses from mode-locked femtosecond lasers. That probe only extended electronic states providing indirect information about atomic structure. X-rays, on the other hand, interact with core electronic levels and can therefore provide direct information about atomic structure. Recently, 300-femtosecond synchrotron pulses were generated directly from an electron storage ring [4].

For the first few decades after the invention of the laser in 1960, the record for the shortest laser pulse fell by a factor of two every three years or so. Each development provided new insight into the microworld of atoms,

molecules and solids. In 1986, however, this trend essentially stopped, when the pulse length reached 6 femtoseconds. Only recently physicists at the Foundation for Research and Technology – Hellas (FORTH) on Crete have one new approach to break the femtosecond limits and measured 100 attosecond sharp feature [5].

The excitation of matter on the quark nuclear atomic, molecular or macroscopic level leads to transfer of energy. The response of the chunk of matter (atom, molecule or nanoparticle) is governed by the relaxation time τ.

In the book, we give the general definition of the relaxation time, which depends on coupling constants for electromagnetic, strong or gravitational interactions. It occurs, that for all interactions τ is not equal zero (though it scales from 10^{-43} s to the seconds).

The models of thermal processes with $\tau \neq 0$ we will call the causal models of the thermal phenomena, in the opposition to noncausal models with $\tau = 0$. The physical background for the differentiation of the causal and noncausal models stems from the observation, that for $\tau = 0$ velocity of the propagation of the interaction $v \to \infty$ and $v/c \to \infty$ ($c =$ light velocity) in complete disagreement with special relativity theory. In the book, we for short, define the causal thermal phenomena as the phenomena for which $\tau \neq 0$.

Nanoscience is located in length scale between atoms and small molecules on the one hand, and macroscopic matter on the other. It is regime into which we know very little. This state of affairs would not be of much concern if there were a desert of physical phenomena between the very large and the very small. But as we all know, there is *life in the desert.*

Contemporary there is considerable progress in the experimental nano-

science. Subfemtosecond lasers, scanning tunneling microscopy and atomic force microscopy allow us to measure nanoscale phenomena. The discovery of physical principles at nanoscale will reinforce the attack by biologists on the mysteries callular function. In any event the applicability of the science of nanoscale will not be limited to the world between angstroms and centimeters. Phenomena following similar principles may well be manifested in astrophysics, for example may be useful in explaining the origin of large-scale structure in the Universe [6].

The organization of the book is as follows: In Chapter 1 causal thermal phenomena in classical approximation are described. Chapter 2 is devoted to the study of quasi quantum description of causal thermal phenomena in quark, nucleon, atom and molecule gases. The gravitational causal thermal phenomena are described in Chapter 3. Chapter 4 presents the conclusions and perspectives of the study of causal thermal phenomena. Finally, Appendices encloses the preliminaries of partial differential equations (nomenclature and definitions) (A), and (B) the discussion of the heat transport paradox.

Bibliography for Introduction

[1] R. P. Feynman, *Engineering and Science*, (California Institute of Technology, February 1960).

[2] E. Scheer et al., *Nature* (9 July 1998).

[3] J. Uppenbrik and D. Clery, *Science* 283, (1999) 1667.

[4] R. W. Schoenlein et al., *Science* 287, (2000) 2237.

[5] N. A. Papadogiannis et al., *Phys. Rev. Lett.* 83, (1999) 4289.

[6] R. B. Laughlin and D. Pines, PNAS VOL 97, (2000) 28.

Chapter 1

Causal thermal phenomena, classical description

1.1 Fundamentals of the rapid thermal processes

The differential equations of thermal energy transfer should be hyperbolic so as to exclude action at distance; yet, the equations of irreversible thermodynamics — those of Navier-Stokes and Fourier are parabolic.[1]

When an ultrafast thermal pulse (e. g. femtosecond pulse) interacts with a metal surface, the excited electrons become the main carriers of the thermal energy. For a femtosecond thermal pulse, the duration of the pulse is of the same order as the electron relaxation time. In this case, the hyper-

[1]The classification of the partial differential equation can be found in Appendix A.

bolicity of the thermal energy transfer plays an important role.

Radiation deposition of energy in materials is a fundamental phenomenon to laser processing. It converts radiation energy into material's internal energy, which initiates many thermal phenomena, such as heat pulse propagation, melting and evaporation. The operation of many laser techniques requires an accurate understanding and control of the energy deposition and transport processes. Recently, radiation deposition and the subsequent energy transport in metals have been investigated with picosecond and femtosecond resolutions [1.1]–[1.7]. Results show that during high-power and short-pulse laser heating, free electrons can be heated to an effective temperature much higher than the lattice temperature, which in turn leads to both a much faster energy propagation process and a much smaller lattice-temperature rise than those predicted from the conventional radiation heating model. Corkum et al. [1.8] found that this electron-lattice nonequilibrium heating mechanism can significantly increase the resistance of molybdenum and copper mirrors to thermal damage during high-power laser irradiation when the laser pulse duration is shorter than one nanosecond. Clemens et al. [1.9] studied thermal transport in multilayer metals during picosecond laser heating. The measured temperature response in the first 20 ps was found to be different from predictions of the conventional Fourier model. Due to the relatively low temporal resolution of the experiment ($\sim 4\,\mathrm{ps}$), however, it is difficult to determine whether this difference is the result of nonequilibrium laser heating or is due to other heat conduction mechanisms, such as non-Fourier heat conduction, or reflection and refraction of thermal waves at interfaces. Heat is conducted in solids through electrons and phonons. In metals, electrons dominate the heat conduction, while in insulators and semiconductors, phonons are the major heat

Table 1.1: General Features of Heat Carriers

	Free Electron	Phonon
Generation	ionization or excitation	lattice vibration
Propagation media	vacuum or media	media only
Statistics	Fermion	Boson
Dispersion	$E = \hbar^2 q^2/(2m)$	$E = E(q)$
Velocity ($\mathrm{m} \cdot \mathrm{s}^{-1}$)	$\sim 10^6$	$\sim 10^3$

carriers. Table 1.1 lists important features of the electrons and phonons.

The traditional thermal science, or macroscale heat transfer, employs phenomenological laws, such as Fourier's law, without considering the detailed motion of the heat carriers. Decreasing dimensions, however, have brought an increasing need for understanding the heat transfer processes from the microscopic point of view of the heat carriers. The response of the electron and phonon gases to the external perturbation initiated by laser irradiation can be described with the help of a memory function of the system. To that aim, let us consider the generalized Fourier law [1.10]–[1.13]:

$$q(t) = -\int_{-\infty}^{t} K(t-t')\nabla T(t')\,dt', \tag{1.1}$$

where $q(t)$ is the density of a thermal energy flux, $T(t')$ is the temperature of electrons and $K(t-t')$ is a memory function for thermal processes. The density of thermal energy flux satisfies the following equation of heat conduction:

$$\frac{\partial}{\partial t}T(t) = \frac{1}{\rho c_v}\nabla^2 \int_{-\infty}^{t} K(t-t')T(t')\,dt', \tag{1.2}$$

where ρ is the density of charge carriers and c_v is the specific heat of electrons in a constant volume. We introduce the following equation for the memory function describing the Fermi gas of charge carriers:

$$K(t-t') = K_1 \lim_{t_0 \to 0} \delta(t-t'-t_0). \tag{1.3}$$

In this case, the electron has a very "short" memory due to thermal disturbances of the state of equilibrium. Combining Eqs. (1.3) and (1.2) we obtain

$$\frac{\partial}{\partial t} T = \frac{1}{\rho c_v} K_1 \nabla^2 T. \tag{1.4}$$

Equation (1.4) has the form of the parabolic equation for heat conduction (PHC). Using this analogy, Eq. (1.4) may be transformed as follows:

$$\frac{\partial}{\partial t} T = D_T \nabla^2 T, \tag{1.5}$$

where the heat diffusion coefficient D_T is defined as follows:

$$D_T = \frac{K_1}{\rho c_v}. \tag{1.6}$$

From Eq. (1.6), we obtain the relation between the memory function and the diffusion coefficient

$$K(t-t') = D_T \rho c_v \lim_{t_0 \to 0} \delta(t-t-t_0'). \tag{1.7}$$

In the case when the electron gas shows a "long" memory due to thermal disturbances, one obtains for memory function

$$K(t-t') = K_2. \tag{1.8}$$

When Eq. (1.8) is substituted to the Eq. (1.2) we obtain

$$\frac{\partial}{\partial t} T = \frac{K_2}{\rho c_v} \nabla^2 \int_{-\infty}^{t} T(t')\, dt. \tag{1.9}$$

Differentiating both sides of Eq. (1.9) with respect to t, we obtain

$$\frac{\partial^2 T}{\partial t^2} = \frac{K_2}{\rho c_v} \nabla^2 T. \tag{1.10}$$

Equation (1.10) is the hyperbolic wave equation describing thermal wave propagation in a charge carrier gas in a metal film. Using a well-known form of the wave equation,

$$\frac{1}{v^2} \frac{\partial^2 T}{\partial t^2} = \nabla^2 T, \tag{1.11}$$

and comparing Eqs. (1.10) and (1.11), we obtain the following form for the memory function:

$$K(t - t') = \rho c_v v^2 \tag{1.12}$$

$$v = \text{finite}, \; v < \infty.$$

As the third case, "intermediate memory" will be considered:

$$K(t - t') = \frac{K_3}{\tau} \exp\left[-\frac{(t - t')}{\tau}\right], \tag{1.13}$$

where τ is the relaxation time of thermal processes. Combining Eqs. (1.13) and (1.2) we obtain

$$c_v \frac{\partial^2 T}{\partial t^2} + \frac{c_v}{\tau} \frac{\partial T}{\partial t} = \frac{K_3}{\rho \tau} \nabla^2 T \tag{1.14}$$

and

$$K_3 = D_\tau c_v \rho. \tag{1.15}$$

Thus, finally,

$$\frac{\partial^2 T}{\partial t^2} + \frac{1}{\tau} \frac{\partial T}{\partial t} = \frac{D_T}{\tau} \nabla^2 T. \tag{1.16}$$

Equation (1.16) is the hyperbolic equation for heat conduction (HHC), in which the electron gas is treated as a Fermion gas. The diffusion coefficient D_T can be written in the form [1.14]

$$D_T = \frac{1}{3} v_F^2 \tau, \tag{1.17}$$

where v_F is the Fermi velocity for the electron gas in a semiconductor. Applying Eq. (1.17) we can transform the hyperbolic equation for heat conduction, Eq.(1.16), as follows:

$$\frac{\partial^2 T}{\partial t^2} + \frac{1}{\tau} \frac{\partial T}{\partial t} = \frac{1}{3} v_F^2 \nabla^2 T. \tag{1.18}$$

Let us denote the velocity of disturbance propagation in the electron gas as s:

$$s = \sqrt{\frac{1}{3}} v_F. \tag{1.19}$$

Using the definition of s, Eq. (1.18) may be written in the form

$$\frac{1}{s^2} \frac{\partial^2 T}{\partial t^2} + \frac{1}{\tau s^2} \frac{\partial T}{\partial t} = \nabla^2 T. \tag{1.20}$$

For the electron gas, treated as the Fermi gas, the velocity of sound propagation is described by the equation [1.15]

$$v_S = \left(\frac{P_F^2}{3 m m^*} \left(1 + F_0^S \right) \right)^{1/2}, \qquad P_F = m v_F, \tag{1.21}$$

where m is the mass of a free (non-interacting) electron and m^* is the effective electron mass. Constant F_0^S represents the magnitude of carrier-carrier interaction in the Fermi gas. In the case of a very weak interaction, $m^* \to m$ and $F_0^S \to 0$, so according to Eq. (1.21),

$$v_S = \frac{m v_F}{\sqrt{3} m} = \sqrt{\frac{1}{3}} v_F. \tag{1.22}$$

To sum up, we can make a statement that for the case of weak electron-electron interaction, sound velocity $v_s = \sqrt{1/3}v_F$ and this velocity is equal to the velocity of thermal disturbance propagation s. From this we conclude that the hyperbolic equation for heat conduction Eq. (1.20), is identical as the equation for second sound propagation in the electron gas:

$$\frac{1}{v_S^2}\frac{\partial^2 T}{\partial t^2} + \frac{1}{\tau v_S^2}\frac{\partial T}{\partial t} = \nabla^2 T. \tag{1.23}$$

Using the definition expressed by Eq. (1.17) for the heat diffusion coefficient, Eq. (1.23) may be written in the form

$$\frac{1}{v_S^2}\frac{\partial^2 T}{\partial t^2} + \frac{1}{D_T}\frac{\partial T}{\partial t} = \nabla^2 T. \tag{1.24}$$

The mathematical analysis of Eq. (1.23) leads to the following conclusions:

1. In the case when $v_S^2 \to \infty$, τv_S^2 is finite, Eq. (1.24) transforms into the parabolic equation for heat diffusion:

$$\frac{1}{D_T}\frac{\partial T}{\partial t} = \nabla^2 T. \tag{1.25}$$

2. In the case when $\tau \to \infty$, v_S is finite, Eq. (1.24) transforms into the wave equation:

$$\frac{1}{v_S^2}\frac{\partial^2 T}{\partial t^2} = \nabla^2 T. \tag{1.26}$$

Equation (1.26) describes propagation of the thermal wave in the electron gas. From the point of view of theoretical physics, condition $v_S \to \infty$ violates the special theory of relativity. From this theory we know that there is a limited velocity of interaction propagation and this velocity $v_{\mathrm{lim}} = c$,

where c is the velocity of light in a vacuum. Multiplying both sides of Eq. (1.24) by c^2, we obtain

$$\frac{c^2}{v_S^2}\,\frac{\partial^2 T}{\partial t^2}+\frac{c^2}{D_T}\,\frac{\partial T}{\partial t}=c^2\nabla^2 T, \tag{1.27}$$

Denoting $\beta = v_S/c$, Eq. (1.27) may be written in the form

$$\frac{1}{\beta^2}\,\frac{\partial^2 T}{\partial t^{2\,2}}+\frac{1}{\tilde{D}_T}\,\frac{\partial T}{\partial t}=c^2\nabla^2 T, \tag{1.28}$$

where $\tilde{D}_T = \tau\beta^2$, $\beta < 1$. On the basis of the above considerations, we conclude that the heat conduction equation, which satisfies the special theory of relativity, acquires the form of the partial hyperbolic Eq. (1.28). The rejection of the first component in Eq. (1.28) violates the special theory of relativity.

1.2 The relaxation dynamics of the ultrafast thermal pulses

Heat transport during fast laser heating of solids has become a very active research area due to the significant applications of short pulse lasers in the fabrication of sophisticated microstructures, synthesis of advanced materials, and measurements of thin film properties. Laser heating of metals involves the deposition of radiation energy on electrons, the energy exchange between electrons, and the lattice, and the propagation of energy through the media.

The theoretical predictions showed that under ultrafast excitation conditions the electrons in a metal can exist out of equilibrium with the lattice

for times of the order of the electron energy relaxation time [1.2, 1.5]. Model calculations suggest that it should be possible to heat the electron gas to temperature T_e of up to several thousand degrees for a few picoseconds while keeping the lattice temperature T_l relatively cold. Observing the subsequent equilibration of the electronic system with the lattice allows one to directly study electron-phonon coupling under various conditions.

Several groups have undertaken investigations relating dynamics' changes in the optical constants (reflectivity, transmissivity) to relative changes in electronic temperature. But only recently, the direct measurement of electron temperature has been reported.

The temperature of hot electron gas in a thin gold film ($l = 300$ Å) was measured, and a reproducible and systematic deviation from a simple Fermi-Dirac (FD) distribution for short time $\Delta t \sim 0.4\,\mathrm{ps}$ were obtained. As stated in Ref. [1.5], this deviation arises due to the finite time required for the nascent electrons to equilibrate to a FD distribution. The nascent electrons are the electrons created by the direct absorption of the photons prior to any scattering.

In papers [1.10, 1.13], the relaxation dynamics of the electron temperature with the hyperbolic heat conduction equation (HHC), Eq.(1.24), was investigated. Conventional laser heating processes which involve a relatively low-energy flux and long laser pulse have been successfully modeled in metal processing and in measuring thermal diffusivity of thin films [1.16]. However, applicability of these models to short-pulse laser heating is questionable [1.2, 1.5, 1.10, 1.11, 1.12, 1.13]. As it is well known, the Anisimov model [1.16] does not properly take into account the finite time for the nascent electrons to relax to the FD distribution. In the Anisimov model, the Fourier law for heat diffusion in the electron gas is assumed. However,

the diffusion equation is valid only when relaxation time is zero, $\tau = 0$, and velocity of the thermalization is infinite, $v \to \infty$.

The effects of ultrafast heat transport can be observed in the results of front-pump back probe measurements [1.2, 1.5]. The results of these type of experiments can be summarized as follows. Firstly, the measured delays are much shorter than would be expected if heat were carried by the diffusion of electrons in equilibrium with the lattice (tens of picoseconds). This suggests that heat is transported via the electron gas alone, and that the electrons are out of equilibrium with the lattice on this time scale. Secondly, since the delay increases approximately linearly with the sample thickness, the heat transport velocity can be extracted, $v_h \simeq 10^8\,\mathrm{cm}\cdot\mathrm{s}^{-1} = 1\,\mu\mathrm{m}\cdot\mathrm{ps}^{-1}$. This is of the same order of magnitude as the Fermi velocity of electrons in gold, $1.4\ \mu\mathrm{m}\cdot\mathrm{ps}^{-1}$.

1.3 The thermal inertia of materials heated with ultrafast laser pulses

According to the constitutive relation in the thermal wave model, heat flux $\vec{q}$ obeys the relation [1.10]–[1.13]

$$\vec{q}(\vec{r}, t+\tau) = -k\nabla T(\vec{r}, t), \tag{1.29}$$

where τ is the relaxation time (a phase lag) and k is the thermal conductivity. The temperature gradient established in the material at time t results in a heat flux that occurred at a later time $t+\tau$ due to the insufficient time of response. For combining with the energy equation, however, all the physical quantities involved must correspond to the same instant of time.

The Taylor's series expansion is thus applied to the heat flux $\vec{q}$ in Eq. (1.29) to give

$$\vec{q}(\vec{r},t) + \frac{\partial \vec{q}(\vec{r},t)}{\partial t}\,\tau + \frac{\partial^2 \vec{q}(\vec{r},t)}{\partial t^2}\,\frac{\tau^2}{2} = -k\nabla T(\vec{r},t). \tag{1.30}$$

In the linearized thermal wave theory, the phase lag is assumed to be small and the higher-order terms in Eq. (1.30) are neglected. By retaining only the first-order term in τ, Eq. (1.30) becomes

$$\vec{q}(\vec{r},t) + \tau\,\frac{\partial \vec{q}(\vec{r},t)}{\partial t} = -k\nabla T(\vec{r},t) \tag{1.31}$$

After combining Eq. (1.31) with the energy conservation equation

$$-\nabla \cdot \vec{q} = \rho C_v\,\frac{\partial T}{\partial t} \tag{1.32}$$

one obtains the HHC, Eq. (1.24).

Equation (1.31) can be compared to the equation of the motion for particle with mass m in a resistive medium,

$$\gamma \vec{v} + m\,\frac{d\vec{v}}{dt} = \vec{P}(\vec{r},t), \tag{1.33}$$

where γ is a resistive coefficient, $\vec{v}$ denotes the velocity, and $\vec{P}(\vec{r},t)$ is the external force. Comparing Eqs. (1.31) and (1.33) we conclude the correspondence

$$\begin{aligned} -\nabla T(\vec{r},t) &\longrightarrow \vec{P}(\vec{r},t) \\ \vec{q}(\vec{r},t) &\longrightarrow \vec{v} \\ k^{-1} &\longrightarrow \gamma \\ \frac{\tau}{k} &\longrightarrow m \end{aligned} \tag{1.34}$$

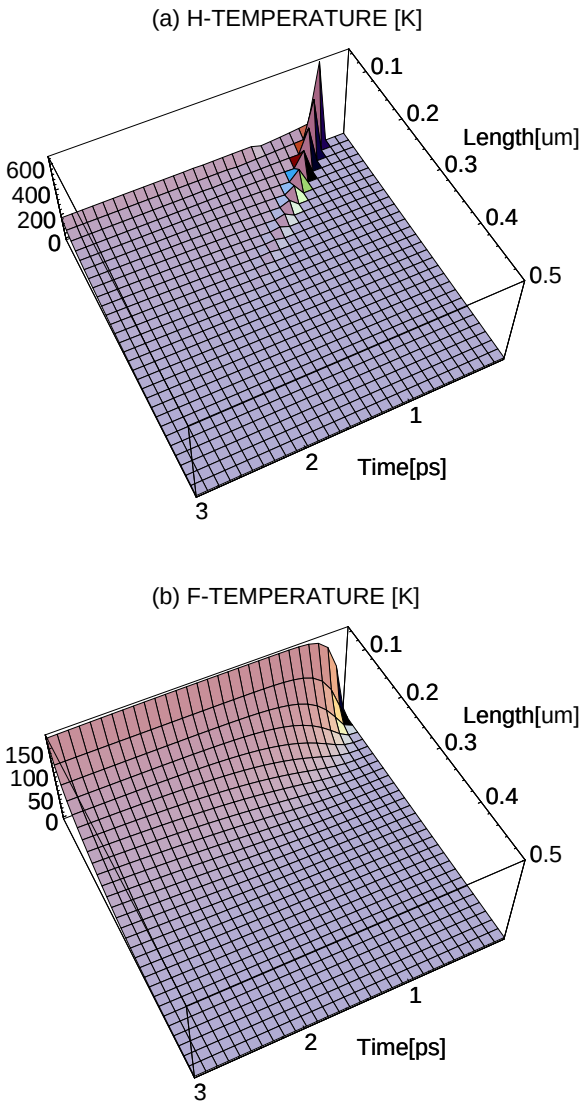

Figure 1.1: (a) The solution of HHC for $v_S = 0.15\,\mu\mathrm{m}\cdot\mathrm{ps}^{-1}$, $\tau = 0.12\,\mathrm{ps}$, Δt-pulse duration$= 0.06\,\mathrm{ps}$. (b) The solution of PHC for the same values of v_S, τ and $\Delta t = 0.06\,\mathrm{ps}$.

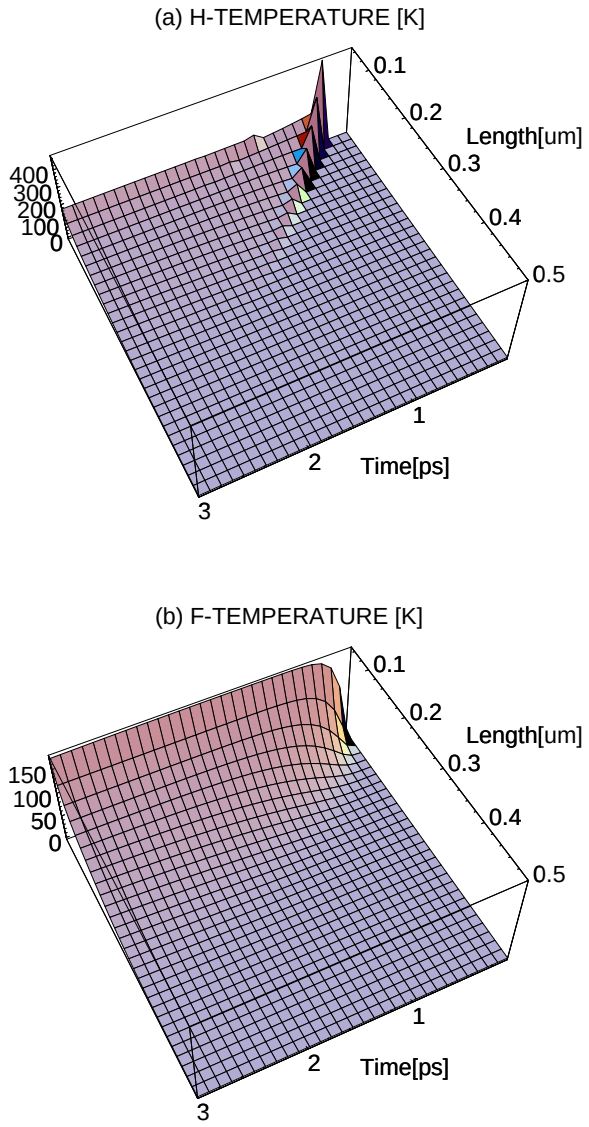

Figure 1.2: (a) The same as in Fig. 1.1(a) but with Δt-pulse duration= 0.1 ps. (b) The same as in Fig. 1.1(b), but with $\Delta t = 0.1$ ps.

For the steady-state case, Eq. (1.33) reduces to

$$\gamma \vec{v} = \vec{P}(\vec{r}, t) \tag{1.35}$$

and Eq. (1.30) reduces to the Fourier law.

From the relations, given by Eq. (1.34), we conclude that the greater relaxation time corresponds to the greater mass $\equiv$ greater inertia. It seems quite resonable to treat the relaxation time as the measure of the degree of the thermal inertia. In papers [1.10]–[1.13], it was shown that for the thermal processes with characteristic time $\Delta t \geq \tau$, the heat transfer is well described by Fourier law. In another way, for $\Delta t \geq \tau$ the thermal processes can be called inertia-free processes. On the other hand, for thermal processes with $\Delta t < \tau$ the thermal inertia plays an important role.

In Figs. 1.1 and 1.2, the 3D solutions of HHC and PHC equation are presented. The solutions are obtained for $v_S = 0.15\,\mu\mathrm{m} \cdot \mathrm{ps}^{-1}$ and $\tau = 0.12\,\mathrm{ps}$ [1.13] and for $\Delta t = 0.06\,\mathrm{ps}$ and $0.1\,\mathrm{ps}$. As can be easily seen, the solutions of HHC equations (Figs. 1.1(a) and 1.2(a)) show the retardation of the response of the system to the external thermal perturbation. The temperature surface shows the effect of the thermal inertia. Moreover, the shorter the Δt, the more localized is the temperature surface. For the solution of PHC (Figs. 1.1(b) and 1.2(b)) the instant heating of the system is observed without any signature of the inertia of the system, and the temperature in system is smeared out.

1.4 Causal transport of hot electrons

The effects of ultrafast heat transport can be observed in the results of front-pump back probe measurements [1.5]. The results of these type of experiments can be summarized as follows: Firstly, the measured delays are much shorter than would be expected if the heat were carried by the diffusion of electrons in equilibrium with the lattice (tens of picoseconds). This suggests, that the heat is transported via the electron gas alone, and that the electrons are out of equilibrium with the lattice on this time scale. Secondly, since the delay increases approximately linearly with the sample thickness, the heat transport velocity can be extracted $v_h \simeq 10^8\,\mathrm{cm}\cdot\mathrm{s}^{-1} = 1\,\mu\mathrm{m}\cdot\mathrm{ps}^{-1}$. This is of the same order of magnitude as the Fermi velocity of electrons in Au, $1.4\,\mu m\cdot ps^{-1}$.

Since the heat moves at a velocity comparable to v_F — Fermi velocity of the electron gas, it is natural to question exactly how the transport takes place. Since those electrons which lie close to the Fermi surface are the principal contributors to transport, the heat-carrying electrons move at v_F. In the limit of lengths longer than the momentum relaxation length, λ, the random walk behavior is averaged and the electron motion is subject to a diffusion equation. Conversely, on a length scale shorter than λ, the electrons move ballistically with velocity close to v_F.

The importance of the ballistic motion may be appreciated by considering the different hot-electron scattering lengths reported in the literature. The electron-electron scattering length in Au, λ_{ee} has been calculated in Ref. [1.17]. They find that $\lambda_{ee} \sim (E - E_F)^2$ for electrons close to the Fermi level. For 2-eV electrons $\lambda_{ee} \approx 35\,\mathrm{nm}$ increasing to 80 nm for 1-eV. The electron-phonon scattering length λ_{ep} is usually inferred from conductivity

data. Using Drude relaxation times, λ_{ep} can be computed, $\lambda_{ep} \approx 42\,\mathrm{nm}$ at 273 K. This is shorter than λ_{ee}, but of the same order of magnitude. Thus, we would expect that both electron-electron and electron-phonon scattering are important on this length scale. However, since conductivity experiments are steady state measurements, the contribution of phonon scattering in a femtosecond regime experiment such as pump-probe ultrafast lasers, is uncertain.

In the usual electron-phonon coupling model [1.16], one describes the metal as two coupled subsystems, one for electrons and one for phonons. Each subsystem is in local equilibrium so the electrons are characterized by a FD distribution at temperature T_e and the phonon distribution is characterized by a Bose-Einstein distribution at the lattice temperature T_l. The coupling between the two systems occurs via the electron-phonon interaction. The time evolution of the energies in the two subsystems is given by the coupled parabolic differential equations (Fourier law). For ultrafast lasers, the duration of pump pulse is of the order of relaxation time in metals [1.5]. In that case, the parabolic heat conduction equation is not valid and hyperbolic heat conduction must be used (1.24)

$$\frac{1}{v_S^2}\,\frac{\partial^2 T}{\partial t^2} + \frac{1}{D_T}\,\frac{\partial T}{\partial t} = \nabla^2 T, \qquad D_T = \tau v_S^2. \tag{1.36}$$

In Eq. (1.36), v_S is the thermal wave speed, τ is the relaxation time and D_T denotes the thermal diffusivity. In the following, Eq. (1.36) will be used to describe the heat transfer in the thin gold films.

To that aim, we define: T_e is the electron gas temperature and T_l is the lattice temperature. The governing equations for nonstationary heat

transfer are

$$\frac{\partial T_e}{\partial t} = D_T \nabla^2 T - \frac{D_T}{v_S^2}\,\frac{\partial^2 T_e}{\partial t^2} - G(T_e - T_l), \qquad \frac{\partial T_l}{\partial t} = G(T_e - T_l), \quad (1.37)$$

where D_T is the thermal diffusivity, T_e is the electron temperature, T_e is the lattice temperature, and G is the electron-phonon coupling constant. In the following, we will assume that on subpicosecond scale the coupling between electron and lattice is weak and Eq. (1.37) can be replaced by the following equations (1.24):

$$\frac{\partial T_e}{\partial t} = D_T \nabla^2 T - \frac{D_T}{v_S^2}\,\frac{\partial^2 T_e}{\partial t^2}, \qquad T_l = \text{constant}. \quad (1.38)$$

Equation (1.38) describes nearly ballistic heat transport in a thin gold film irradiated by an ultrafast ($\Delta t < 1\,\text{ps}$) laser beam. The solution of Eq. (1.38) for 1 D is given by [1.10]–[1.13]:

$$\begin{aligned} T(x,t) \;=\; & \frac{1}{v_s}\int dx'\, T(x',0)\left[e^{-t/2\tau}\,\frac{1}{t_0}\,\Theta(t-t_0)\right. \\ & + e^{-t/2\tau}\,\frac{1}{2\tau}\left\{I_0\left(\frac{(t^2-t_0^2)^{1/2}}{2\tau}\right)\right. \\ & \left.\left. + \frac{t}{(t^2-t_0^2)^{1/2}}\,I_1\left(\frac{(t^2-t_0^2)^{1/2}}{2\tau}\right)\right\}\Theta(t-t_0)\right], \end{aligned} \quad (1.39)$$

where v_s is the velocity of second sound, $t_0 = (x - x')/v_s$ and I_0 and I_1 are modified Bessel functions and $\Theta(t - t_0)$ denotes the Heaviside function. We are concerned with the solution to Eq. (1.39) for a nearly delta function temperature pulse generated by laser irradiation of the metal surface. The pulse transferred to the surface has the shape:

$$\begin{aligned} \Delta T_0 &= \frac{\beta \rho_E}{C_V v_s\,\Delta t} \qquad \text{for} \qquad 0 \le x < v_s\,\Delta t, \\ \Delta T_0 &= 0 \qquad\quad \text{for} \qquad x \ge v_s\,\Delta t \end{aligned} \quad (1.40)$$

In Eq. (1.40), ρ_E denotes the heating pulse fluence, β is the efficiency of the absorption of energy in the solid, $C_V(T_e)$ is electronic heat capacity, and Δt is duration of the pulse. With $t = 0$ temperature profile described by Eq. (1.40) yields:

$$T(l,t) = \frac{1}{2}\,\Delta T_0 e^{-t/2\tau}\Theta(t-t_0)\Theta(t_0+\Delta t-t) + \frac{\Delta t}{4\tau}\,\Delta T_0 e^{-\tau/2\tau}\left\{I_0(z)+\frac{t}{2\tau}\,\frac{1}{z}\,I_1(z)\right\}\Theta(t-t_0), \quad (1.41)$$

where $z = (t^2 - t_0^2)^{1/2}/2\tau$ and $t = l/v_s$. The solution to Eq. (1.38), when there are reflecting boundaries, is the superposition of the temperature at l from the original temperature and from image heat source at $\pm 2nl$. This solution is:

$$T(l,t) = \sum_{i=0}^{\infty} \Delta T_0 e^{-t/2\tau}\Theta(t-t_i)\Theta(t_i+\Delta t-t) + \Delta T_0\,\frac{\Delta t}{2\tau}\,e^{-t/2\tau}\left\{I_0(z_i)+\frac{t}{2\tau}\,\frac{1}{z_i}\,I_1(z_i)\right\}\Theta(t-t_i), \quad (1.42)$$

where $t_i = t_0,\ 3t_0,\ 5t_0,\ t_0 = l/v_0$. For gold, $C_V(T_e) = C_e(T_e) = \gamma T_e$,$\gamma = 71.5\,\mathrm{J\,m^{-3}\,K^{-2}}$ and Eq. (1.40) yields:

$$\Delta T_0 = \frac{1.4\times 10^5 \rho_E \beta}{v_s \Delta t T_e} \qquad \text{for} \qquad 0 \le x \le v_s\Delta t$$
$$\Delta T_0 = 0 \qquad \text{for} \qquad x \ge v_s\Delta t, \quad (1.43)$$

where ρ_E is measured in $\mathrm{m\,J\cdot cm^{-2}}$, v_s in $\mu\mathrm{m}\cdot\mathrm{ps^{-1}}$, and Δt in ps. For $T_e = 300\,\mathrm{K}$:

$$\Delta T_0 = \frac{4.67\times 10^2 \beta \rho_E}{v_s \Delta t} \qquad \text{for} \qquad 0 \le x \le v_s\Delta t$$
$$\Delta T_0 = 0 \qquad \text{for} \qquad x \ge v_s\Delta t \quad (1.44)$$

The model calculations (formulae 1.41–1.44) were applied to the description of the experimental results presented in paper [1.5] and a fairly good agreement of the theoretical calculations and experimental results was obtained [1.13].

1.5 Velocity of thermal waves

One of the best models in mathematical physics is Fourier's model for heat conduction in solids. Despite the excellent agreement obtained between theory and experiment, the Fourier model contains several inconsistent implications. The most important is that the model implies an infinite speed of propagation for heat. Despite such an unacceptable notion of energy transport in solids, the classical diffusion theory gives quite reliable results for most situations encountered in modern thermal engineering. However, there are situations, such as those dealing with extremely short time responses, where the classical diffusion model breaks down and the wave nature of heat propagation becomes dominant. For femtosecond laser pulses the hyperbolicity of the thermal energy transfer plays an important role. The consequence of the hyperbolicity of the master equations for heat transfer is the existence of the thermal waves. Considering the importance of the thermal wave in future engineering applications and simultaneously the lack of a simple physics presentation of the thermal wave for the reader, a new insight into the hyperbolic heat conduction equation is presented. A new form of HHC equation is obtained which properly takes into account the relativistic nature of the ultrafast heat transport.

The earliest recorded speculations of the existence of a propagating temperature wave was advanced by Nernst [1.18] in 1917. He suggested that

in good thermal conductors, at low temperature, heat may have sufficient "inertia" to give rise to an "oscillating discharge". In the early fifties it was shown by Dingle [1.19], Ward and Wilks [1.20] and London [1.21], that a density fluctuation in a phonon gas would propagate as a thermal wave — a second sound wave — provided that "losses" from the wave were negligible. In one of their papers, Ward and Wilks [1.22] indicated they would attempt to look for a second sound wave in sapphire crystals. No results of their experiments were published. Then, for nearly a decade, the subject of "thermal wave" lay dormant. Interest was revived in the sixties, primarily through the efforts of J. A. Krumhansl, R. A. Guyer and C. C. Ackerman. In the paper by Ackerman and Guyer [1.23] the thermal wave in dielectric solids was experimentally and theoretically investigated. They found a value for the thermal wave velocity in LiF at a very low temperature $T \sim 1$ K, of $v_s \sim 100 - 300$ ms^{-1}. In insulators and semiconductors phonons are the major heat carriers. In metals electrons dominate. For long thermal pulses, i.e., when the pulse duration, Δt, is larger than the relaxation time, τ, for thermal processes, $\Delta t \gg \tau$, the heat transfer in metals is well described by Fourier diffusion equation. The advent of modern ultrafast lasers opens up the possibility investigating a new mechanism of thermal transport — the thermal wave in an electron gas heated by lasers. The effect of an ultrafast heat transport can be observed in the results of front pump back probe measurements [1.2, 1.5]. The results of this type of experiments can be summarized as follows. Firstly, the measured delays are much shorter than it would be expected if the heat were carried by the diffusion of electrons in equilibrium with the lattice (tens of picoseconds). This suggests that the heat is transported via the electron gas alone, and that the electrons are out of equilibrium with the lattice within this time scale. Secondly, since the

delay increases approximately linearly with the sample thickness, the heat transport velocity can be determined, $v_h \sim 10^8$ cm s^{-1} $= 1\mu$m ps^1. This is of the same order of magnitude as the Fermi velocity of electrons in Au, 1.4 μm ps^{-1}.

In the papers [1.2, 1.12], the heat transport in a thin metal film (Au) was investigated with the help of the hyperbolic heat conduction equation. It was shown that when the memory of the hot electron gas in metals is taken into account, then the HHC is the dominant equation for heat transfer. The hyperbolic heat conduction equation for heat transfer in an electron gas has the form (1.24)

$$\frac{1}{\left(\frac{1}{3}v_F^2\right)}\frac{\partial^2 T}{\partial t^2} + \frac{1}{\tau\left(\frac{1}{3}v_F^2\right)}\frac{\partial T}{\partial t} = \nabla^2 T \tag{1.45}$$

If we consider an infinite electron gas, then the Fermi velocity can be calculated[2]

$$v_F \cong bc \tag{1.46}$$

In Eq. (1.46), c is the light velocity in vacuum and $b \sim 10^{-2}$. Considering Eq. (1.46), Eq. (1.45) can be written in a more elegant form:

$$\frac{1}{c^2}\frac{\partial^2 T}{\partial t^2} + \frac{1}{c^2\tau}\frac{\partial T}{\partial t} = \frac{b^2}{3}\nabla^2 T \tag{1.47}$$

In order to derive the Fourier law from Eq. (1.47), we are forced to break the special theory of relativity and put in Eq. (1.47) $c \to \infty$, $\tau \to 0$. In addition, it can be demonstrated from HHC in a natural way, that in electron gas the heat propagation with velocity $v_h \sim v_F$ in the accordance with the results of the pump probe experiments [1.23, 1.2].

[2]The detailed discussion of the formula (1.46) in Chapter 2

1.6 The thermal wave as the solution of HHC

The importance of the existence of thermal waves in engineering applications was investigated in the paper [1.12]. The propagation of the thermal front in metals has attracted a lot of attention and presents a unique feature of thermal wave propagation.

Considering the importance of the thermal wave in future engineering applications and simultaneously the lack of the simple physics presentation of the thermal wave for engineering audience in the following we present the main results concerning the wave nature of heat transfer.

Hence, we discuss Eq. (1.47) in more detail. Firstly, we observe that the second derivative term dominates when:

$$c^2(\Delta t)^2 < c^2 \Delta t \tau \tag{1.48}$$

i.e., when $\Delta t < \tau$. This implies that for very short heat pulses we have a hyperbolic wave equation of the form:

$$\frac{1}{c^2}\frac{\partial^2 T}{\partial t^2} = \frac{b^2}{3}\nabla^2 T \tag{1.49}$$

and the velocity of the thermal wave is given by

$$v_{th} \sim \frac{1}{\sqrt{3}}\frac{c}{b}, \qquad b \sim 10^{-2}. \tag{1.50}$$

The velocity v_{th} Eq. (1.50) is the velocity of the thermal wave in an infinite Fermi gas of electrons, which is free of all impurities. The thermal wave, which is described by the solution of Eq. (1.49), does not interact with the crystal lattice. It is the maximum value of the thermal wave obtainable in an infinite free electron gas. If we consider the opposite case to that in Eq. (1.48)

$$c^2(\Delta t)^2 > c^2 \tau \Delta t \tag{1.51}$$

i.e., when

$$\Delta t > \tau \tag{1.52}$$

then, one obtains from Eq. (1.47):

$$\frac{1}{c^2\tau}\frac{\partial T}{\partial t} = \frac{b^2}{3}\nabla^2 T \tag{1.53}$$

Eq. (1.53) is the parabolic heat conduction equation–Fourier equation.

The solutions of Eq. (1.47) for the following input parameters: $\tau = 0.12$ ps, $v_{th} = 0.15$ μm ps^{-1}, $\Delta t = 0.02$ ps, 0.06 ps, 0.1 ps are presented in Figs. 1.3–1.5.

The value of the thermal wave velocity v_h is taken from paper [1.13]. Isotherms are presented as a function of the thin film thickness (length) l [μm] and the delay times. The mechanism of heat transfer on a nanometer scale, can be divided according to Fig. 1.3 ($\Delta t = 0.02$ ps) into three stages: a heat wave for $t \sim Lv_{th}^{-1}$, mixed heat transport for $Lv_{th}^{-1} < t < 3L_{th}^{-1}$ and diffusion for $t > 3Lv_{th}^{-1}$. The thermal wave moves in a manner described by the hyperbolic differential partial equation, $x = v_{th}t$. For $t < xv_{th}^{-1}$ the system is undisturbed by an external heat source (laser beam).For longer heat pulses, Figs. 1.4–1.5 the evidence of the thermal wave is gradually reduced — but the retardation of the thermal pulse is still evident. In Fig. 1.6 the solution of the parabolic heat conduction (1.53) is presented. In this case, contrary to the solution of the HHC, heating of the film starts at $t = 0$.

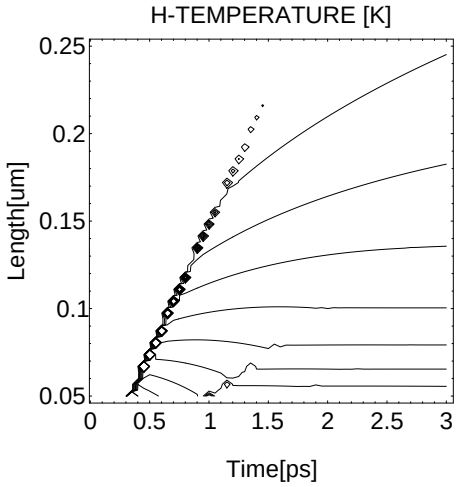

Figure 1.3: The solution of the HHC Eq. (1.47) "H-Temperature" for thermal wave velocity $v_{th} = 0.15\ \mu\mathrm{m\,ps}^{-1}$, relaxation time $\tau = 0.1$ ps, and pulse duration $\Delta t = 0.02$ ps.

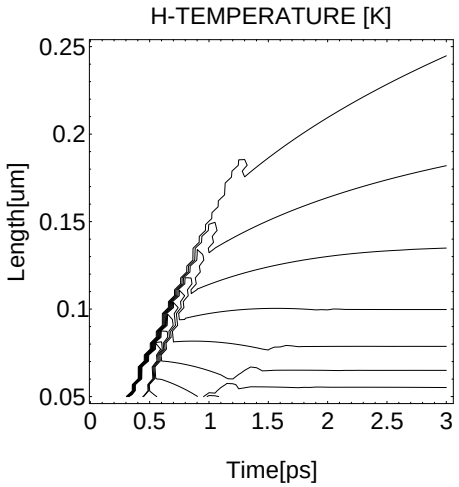

Figure 1.4: The same as in Fig. 1.3 but for $\Delta t = 0.06$ ps.

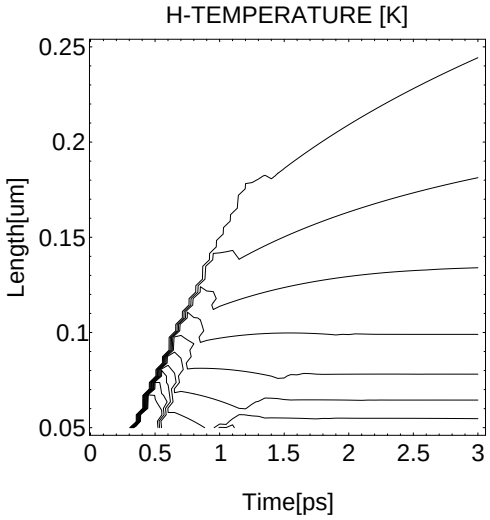

Figure 1.5: The same as in Fig. 1.3 but for $\Delta t = 0.1$ ps.

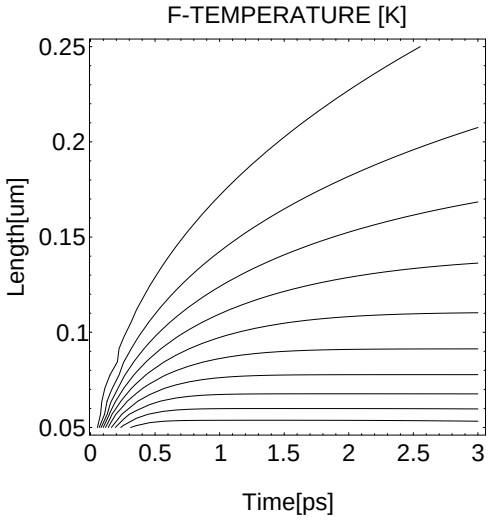

Figure 1.6: The solution of parabolic heat conduction equation (1.53) Fourier law. "F-Temperature" for $v_{th} = 0.15\ \mu\mathrm{m\,ps^{-1}}$, $\tau = 0.12$ ps, $\Delta t = 0.02$ ps.

1.7 Slowing and dephasing of the thermal waves

If heat is released in a body of gas liquid or solid, a thermal flux transported by heat conduction appears. The pressure gradients associated with the thermal gradients set a gas or liquid in motion, so that additional energy transport occurs through convection. In particular, at sufficiently large energy releases, shock waves are formed in a gas or liquid which transport thermal energy at velocities larger that the speed of sound. Below the critical energy release, nearly pure thermal wave may propagate owing to heat conduction in a gas or liquid with other transport mechanisms being negligible [1.24]. Solids metals provide an ideal test medium for the study of thermal waves, since they are practically incompressible at temperature below their melting point and the thermal wave pressures are small compared to the classic pressure (produced by repulsion of the atoms in the lattice) up to large energy releases. In accordance with this picture, the speed of sound in a metal is independent of temperature and given by $c_s = (E/\rho)^{1/2}$ where E is the elasticity modulus and ρ is the density.

Using the path-integral method developed in paper [1.25], the solution of the HHC can be obtained. It occurs, that the velocity of the thermal wave in medium is lower than the velocity of the initial thermal wave. The slowing of the thermal wave is caused by the scattering of heat carriers in medium. The scatterings also change the phase of the initial thermal wave.

In one-dimensional flow of heat in metals, the hyperbolic heat transport equation is given by (1.18)

$$\tau \frac{\partial^2 T}{\partial t^2} + \frac{\partial T}{\partial t} = D_T \frac{\partial^2 T}{\partial x^2}, \qquad D_T = \frac{1}{3} v_F^2 \tau, \tag{1.54}$$

where τ denotes the relaxation time, D_T is the diffusion coefficient and T is the temperature. Introducing the non-dimensional spatial coordinate $z = x/\lambda$, where $\lambda = \lambda/2\pi$ denotes the reduced mean free path, Eq. (1.54) can be written in the form:

$$\frac{1}{v'^2}\frac{\partial^2 T}{\partial t^2} + \frac{2a}{v'^2}\frac{\partial T}{\partial t} = \frac{\partial^2 T}{\partial z^2} \tag{1.55}$$

where

$$v' = \frac{v}{\lambda} \qquad a = \frac{1}{2\tau} \tag{1.56}$$

In Eq. (1.56) v denotes the velocity of heat propagation [1.3], $v = (D/\tau)^{1/2}$.

In the paper by C. De Witt-Morette and See Kit Fong [1.25], the path–integral solution of Eq. (1.55) was obtained. It was shown, that for the initial condition of the form:

$$\begin{aligned} T(z,0) &= \Phi(z) \qquad \text{an "arbitiary" function} \\ \left.\frac{\partial T(z,t)}{\partial t}\right|_{t=0} &= 0 \end{aligned} \tag{1.57}$$

the general solution of the Eq. (1.54) has the form:

$$\begin{aligned} T(z,t) &= \frac{1}{2}\left[\Phi(z,t) + \Phi(z,-t)\right] e^{-at} \\ &\quad + \frac{a}{2} e^{-at} \int_0^t d\eta [\Phi(z,\eta) + \Phi(z,-\eta)] \\ &\quad + [I_0(a(t^2-\eta^2)^{1/2}) + \frac{t}{(t^2-\eta^2)^{1/2}} I_1(a(t^2-\eta^2)^{1/2})] \end{aligned} \tag{1.58}$$

In Eq. (1.58), $I_0(x)$ and $I_1(x)$ denote the modified Bessel function of zero and first order respectively.

Let us consider the propagation of the initial thermal wave with velocity v', i.e.,

$$\Phi(z - v't) = sin(z - v't) \tag{1.59}$$

In that case, the integral in (1.58) can be computed analytically, $\Phi(z,\ t) + \Phi(z,\ -t) = 2sinzcos(v'\ t)$ and the integrals on the right-hand side of (1.58) can be done explicitly [1.25]; we obtain:

$$F(z,t) = e^{-at}\left[\frac{a}{w_1}sin(w_1 t) + cos(w_1 t)\right] sinz, \qquad v' \geq a \tag{1.60}$$

and

$$F(z,t) = e^{-at}\left[\frac{a}{w_2}sinh(w_2 t) + cosh(w_2 t)\right] sinz, \qquad v' < a \tag{1.61}$$

where $w_1 = (v'^2 - a^2)^{1/2}$ and $w_2 = (a^2 - v'^2)^{1/2}$.

In order to clarify the physical meaning of the solutions given by formulas (1.60) and (1.61), we observe that $v' = v/\lambda$ and w_1 and w_2 can be written as:

$$\begin{aligned} v_1 = \lambda w_1 &= v\left(1 - \left(\frac{1}{2\tau\omega}\right)^2\right)^{1/2}, \qquad 2\tau\omega > 1 \\ v_2 = \lambda w_2 &= v\left(\left(\frac{1}{2\tau\omega}\right)^2 - 1\right)^{1/2}, \qquad 2\tau\omega < 1 \end{aligned} \tag{1.62}$$

where ω denotes the pulsation of the initial thermal wave. From formula (1.62), it can be concluded that we can define the new effective thermal wave velocities v_1 and v_2. Considering formulas (1.61) and (1.62), we observe that the thermal wave with velocity v_2 is very quickly attenuated in time. It occurs that when $\omega^{-1} > 2\tau$, the scatterings of the heat carriers diminish the thermal wave.

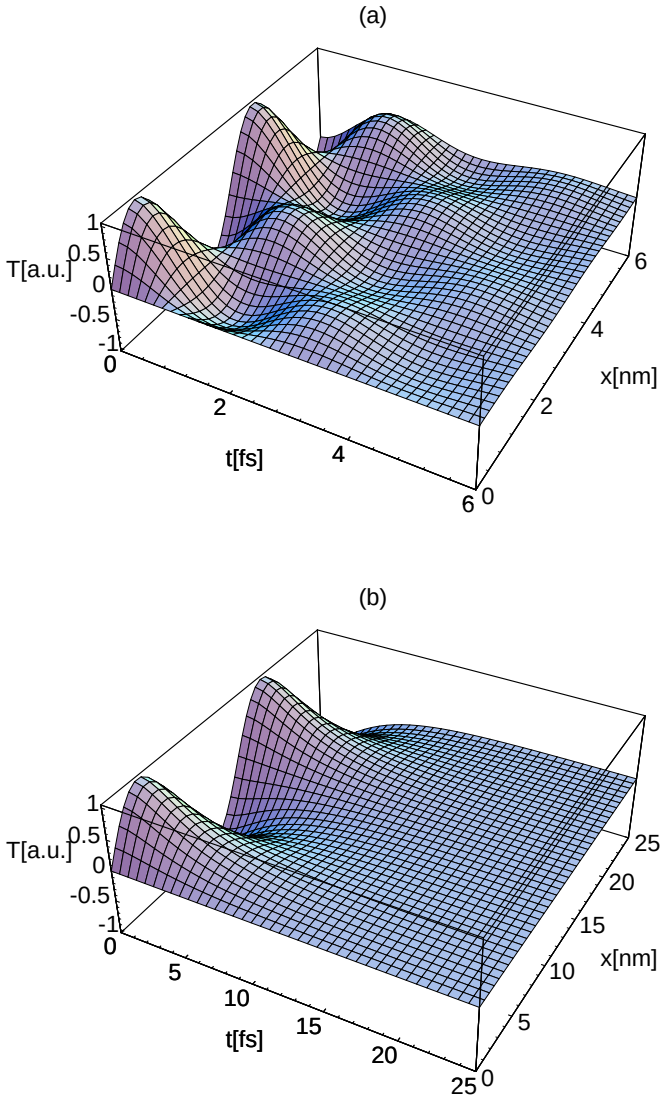

Figure 1.7: (a) Solution of HHC Eq. (1.54) for the following input parameters $v = 1$ nm fs^{-1}, $\tau = 1$ fs, $\omega\tau = 2$. (b) Solution of HHC equation for the following input parameters $v = 1$ nm fs^{-1}, $\tau = 1$ fs, $\omega\tau = 0.45$.

It is interesting to observe that in the limit of a very short relaxation time, i.e., when $\tau \to 0$, $v_2 \to \infty$, because for $\tau \to 0$ Eq. (1.54) is the Fourier parabolic equation.

It can be concluded, that for $\omega^{-1} > 2\tau$, the Fourier equation is relevant equation for the description of the thermal phenomena in metals. For $\omega^{-1} < 2\tau$, the scatterings are slower than in the preceding case and attenuation of the thermal wave is weaker. In that case, $\tau \neq 0$ and v_1 is always finite:

$$v_1 = v\left(1 - \left(\frac{1}{2\tau\omega}\right)^2\right)^{1/2} < v \tag{1.63}$$

For $\tau \to \infty$, i.e., for very rare scatterings $v_1 \to v$ and Eq. (1.54) is a nearly free thermal wave equation. For τ finite the $v_1 < v$ and thermal wave propagates in the medium with smaller velocity than the velocity of the initial thermal wave.

Considering the formula (1.60), one can define the change of the phase of the initial thermal wave β, i.e.:

$$Tan[\beta] = \frac{a}{w_1} = \frac{1}{2\tau\omega}\frac{1}{\sqrt{1 - \frac{1}{4\tau^2\omega^2}}}, \qquad 2\tau\omega > 1 \tag{1.64}$$

We conclude that the scatterings produce the change of the phase of the initial thermal wave. For $\tau \to \infty$ (very rare scatterings), $Tan[\beta] = 0$.

In Figs. 1.7 (a) and (b), the solutions of the Eq. (1.54) for the following input parameters are presented. In Fig. 1.7 (a) $v = 1$ nm fs^{-1} [1.3], $\tau = 1$ fs, $\omega\tau = 2$ and the solution of the Eq. (1.54), formula (1.60) represent the damped thermal wave which propagates with velocity $v_1 = 0.97v$. Fig. 1.7 (b) represent the solution of Eq. (1.54) formula (1.61) for the following input parameters $v = 1$ nm fs^{-1} and $\omega\tau = 0.45$. In that case, the thermal wave is very quickly attenuated and the solutions of Eq. (1.54), formula (1.61) represent the diffusion of the initial thermal wave.

Bibliography for Chapter 1

[1.1] G. L. Eesley. *Phys. Rev. Lett.* 51, (1983) 2140.

[1.2] S. D. Brorson, J. G. Fujimoto, and E. P. Ippen, *Phys. Rev. Lett.* 59, (1987) 1962.

[1.3] H. E. Elsayed-Ali, T. Juhasz, G. O. Smith, and W. E. Bron, *Phys. Rev. B* 43, (1991) 4488.

[1.4] T. Juhasz, H. E. Elsayed-Ali, X. H. Hu, and W. E. Bron, *Phys. Rev. B* 45, (1992) 13819.

[1.5] W. S. Fann, R. Storz, H. W. K. Tom, and J. Bokor, *Phys. Rev. Lett.* 68, (1992) 2834.

[1.6] W. S. Fann, R. Storz, H. W. K. Tom, and J. Bokor. *Phys. Rev. B* 46, (1992) 13592.

[1.7] R. H. M. Groeneveld, *Femtosecond Spectroscopy on Electrons and Phonons in Noble Metals*, Ph. D. thesis, (Van der Waals—Zeeman Laboratory, University of Amsterdam 1992).

[1.8] P. B. Corkum, F. Brunel, and N. K. Sherman, *Phys. Rev. Lett.* 61, (1988) 2886.

[1.9] B. M. Clemens, G. L. Eesley, and A. C. Paddock, *Phys. Rev. B* 37, (1988) 1085.

[1.10] J. Marciak-Kozłowska, *Int. J. Thermophysics* 14, (1993) 593.

[1.11] J. Marciak-Kozłowska, *J. Phys. Ch. Solids* 55, (1994) 721.

[1.12] J. Marciak-Kozłowska *Lasers in Engineering* 4, (1995) 57.

[1.13] J. Marciak-Kozłowska, *Int. J. Thermophysics* 16, (1995) 1989

[1.14] Ch. Kittel and H. Kroemer, *Thermal Physics*, (W. H. Freeman and Company, San Francisco, 1980).

[1.15] D. Pines and P. Nozieres, *The Theory of Quantum Liquids*, (Benjamin, New York, 1966).

[1.16] S. J. Anisimov, B. L. Kapoliovich, and T. L. Pereleman, *Sov. Phys. JETP* 39, (1975) 375.

[1.17] W. F. Królikowski, W. E. Spicer, *Phys. Rev. B* 1, (1970) 478.

[1.18] W. Nernst, *Die Theoretischen Grundlagen des Wärmestatzes*, (Knapp, Halle 1917).

[1.19] R. B. Dingle, *Proc. Phys. Soc. (London)* A65, (1952) 374.

[1.20] J. C. Ward, J. Wilks, *Phil. Mag.* 42, (1951) 314.

[1.21] F. London, *Superfluids* VOL. II p. 101, (J. Wiley and Sons, New York, 1954).

[1.22] J. C. Ward, J. Wilks, *Phil. Mag.* 43, (1952) 48.

[1.23] C. C. Ackerman, R. A. Guyer, *Annals of Physics* 50, (1968) 128.

[1.24] Ya. B. Zeldovich, A. S. Kompaneets, *Collection Dedicated to the Seventieth Birthday of Academician A. F. Joffe*, (Izd. Akad. Nauk SSR, 1959), p. 61.

[1.25] C. De Witt-Morette, See Kit Fong, *Phys. Rev. Lett.* 19, (1989) 2201.

Chapter 2

Causal thermal phenomena, quantal description

2.1 Discretization of the thermal excitation in high excited matter

There is an impressive amount of literature on hyperbolic heat transport in matter [2.1]-[2.5]. In Chapter 1 we developed the new hyperbolic heat transport equation which generalizes the Fourier heat transport equation for the rapid thermal processes. The hyperbolic heat conduction equation (HHC) for the fermionic system has be written in the form (1.23)

$$\frac{1}{\left(\frac{1}{3}v_F^2\right)}\,\frac{\partial^2 T}{\partial t^2}+\frac{1}{\tau\left(\frac{1}{3}v_F^2\right)}\,\frac{\partial T}{\partial t}=\nabla^2 T, \tag{2.1}$$

where T denotes the temperature, τ the relaxation time for the thermal disturbance of the fermionic system, and v_F is the Fermi velocity.

In what follows we develop the new formulation of the HHC, considering the details of the two fermionic systems: electron gas in metals and the nucleon gas.

For the electron gas in metals, the Fermi energy has the form

$$E_F^e = (3\pi)^2 \frac{n^{2/3}\hbar^2}{2m_e}, \tag{2.2}$$

where n denotes the density and m_e electron mass. Considering that

$$n^{-1/3} \sim a_B \sim \frac{\hbar^2}{me^2}, \tag{2.3}$$

and a_B = Bohr radius, one obtains

$$E_F^e \sim \frac{n^{2/3}\hbar^2}{m_e} \sim \frac{\hbar^2}{ma^2} \sim \alpha^2 m_e c^2, \tag{2.4}$$

where c = light velocity and $\alpha = 1/137$ is the fine-structure constant for electromagnetic interaction. For the Fermi momentum p_F we have

$$p_F^e \sim \frac{\hbar}{a_B} \sim \alpha m_e c, \tag{2.5}$$

and, for Fermi velocity v_F,

$$v_F^e \sim \frac{p_F}{m_e} \sim \alpha c. \tag{2.6}$$

Formula (2.6) gives the theoretical background for the result presented in Chapter 1. Comparing formulas (1.46) and (2.6) it occurs that $b = \alpha$. Considering formula (2.6), Eq. (1.47) can be written as

$$\frac{1}{c^2}\frac{\partial^2 T}{\partial t^2} + \frac{1}{c^2\tau}\frac{\partial T}{\partial t} = \frac{\alpha^2}{3}\nabla^2 T. \tag{2.7}$$

As seen from (2.7), the HHC equation is a relativistic equation, since it takes into account the finite velocity of light.

For the nucleon gas, Fermi energy equals

$$E_F^N = \frac{(9\pi)^{2/3}\hbar^2}{8mr_0^2}, \tag{2.8}$$

where m denotes the nucleon mass and r_0, which describes the range of strong interaction, is given by

$$r_0 = \frac{\hbar}{m_\pi c}, \tag{2.9}$$

wherein m_π is the pion mass. From formula (2.9), one obtains for the nucleon Fermi energy

$$E_F^N \sim \left(\frac{m_\pi}{m}\right)^2 mc^2. \tag{2.10}$$

In analogy to the Eq. (2.4), formula (2.10) can be written as

$$E_F^N \sim \alpha_s^2 mc^2, \tag{2.11}$$

where $\alpha_s = \frac{m_\pi}{m} \cong 0.15$ is the fine-structure constant for strong interactions. Analogously, we obtain the nucleon Fermi momentum

$$p_F^N \sim \frac{\hbar}{r_0} \sim \alpha_s mc \tag{2.12}$$

and the nucleon Fermi velocity

$$v_F^N = \frac{pF}{m} \sim \alpha_s c, \tag{2.13}$$

and HHC for nucleon gas can be written as

$$\frac{1}{c^2}\frac{\partial^2 T}{\partial t^2} + \frac{1}{c^2\tau}\frac{\partial T}{\partial t} = \frac{\alpha_s^2}{3}\nabla^2 T. \tag{2.14}$$

In the following, the procedure for the discretization of temperature $T(\vec{r},t)$ in hot fermion gas will be developed. First of all, we introduce the reduced de Broglie wavelength

$$\begin{aligned} \lambda\!\!\!^{-e}_{B} &= \frac{\hbar}{m_e v_h^e}, \qquad v_h^e = \frac{1}{\sqrt{3}}\,\alpha c, \\ \lambda\!\!\!^{-N}_{B} &= \frac{\hbar}{m v_h^N}, \qquad v_h^N = \frac{1}{\sqrt{3}}\,\alpha_s c, \end{aligned} \tag{2.15}$$

and the mean free paths λ^e and λ^N

$$\lambda^e = v_h^e \tau^e, \qquad \lambda^N = v_h^N \tau^N. \tag{2.16}$$

In view of formulas (2.15) and (2.16), we obtain the HHC for electron and nucleon gases

$$\frac{\lambda\!\!\!^{-e}_{B}}{v_h^e}\,\frac{\partial^2 T^e}{\partial t^2} + \frac{\lambda\!\!\!^{-e}_{B}}{\lambda^e}\,\frac{\partial T}{\partial t} = \frac{\hbar}{m_e}\,\nabla^2 T^e, \tag{2.17}$$

$$\frac{\lambda\!\!\!^{-N}_{B}}{v_h^N}\,\frac{\partial^2 T^N}{\partial t^2} + \frac{\lambda\!\!\!^{-N}_{B}}{\lambda^N}\,\frac{\partial T^N}{\partial t} = \frac{\hbar}{m}\,\nabla^2 T^N. \tag{2.18}$$

Equations (2.17) and (2.18) are the hyperbolic partial differential equations which are the master equations for heat propagation in Fermi electron and nucleon gases. In the following, we will study the quantum limit of heat transport in the fermionic systems. We define the quantum heat transport limit as follows:

$$\lambda^e = \lambda\!\!\!^{-e}_{B}, \qquad \lambda^N = \lambda\!\!\!^{-N}_{B}. \tag{2.19}$$

In that case, Eqs. (2.17) and (2.18) have the form

$$\tau^e\,\frac{\partial^2 T^e}{\partial t^2} + \frac{\partial T^e}{\partial t} = \frac{\hbar}{m_e}\,\nabla^2 T^e, \tag{2.20}$$

$$\tau^N\,\frac{\partial^2 T^N}{\partial t^2} + \frac{\partial T^N}{\partial t} = \frac{\hbar}{m}\,\nabla^2 T^N, \tag{2.21}$$

where

$$\tau^e = \frac{\hbar}{m_e (v_h^e)^2}, \qquad \tau^N = \frac{\hbar}{m (v_h^N)^2}. \tag{2.22}$$

Equations (2.20) and (2.21) define the master equation for quantum heat transport (QHT). Having the relaxation times τ^e and τ^N, one can define the "pulsations" ω_h^e and ω_h^N

$$\omega_h^e = (\tau^e)^{-1}, \qquad \omega_h^N = (\tau^N)^{-1}, \tag{2.23}$$

or

$$\omega_h^e = \frac{m_e (v_h^e)^2}{\hbar}, \qquad \omega_h^N = \frac{m (v_h^N)^2}{\hbar},$$

i.e.,

$$\begin{aligned} \omega_h^e \hbar &= m_e (v_h^e)^2 = \frac{m_e \alpha^2}{3} c^2, \\ \omega_h^N \hbar &= m (v_h^N)^2 = \frac{m \alpha_s^2}{3} c^2. \end{aligned} \tag{2.24}$$

The formulas (2.24) define the Planck-Einstein relation for heat quanta E_h^e and E_h^N

$$\begin{aligned} E_h^e &= \omega_h^e \hbar = m_e (v_h^e)^2, \\ E_h^N &= \omega_h^N = m_N (v_h^N)^2. \end{aligned} \tag{2.25}$$

The heat quantum with energy $E_h = \hbar\omega$ can be named the *heaton*, in complete analogy to the *phonon*, *magnon*, *roton*, etc. For τ^e, $\tau^N \to 0$, Eqs. (2.20) and (2.24) are the Fourier equations with quantum diffusion coefficients D^e and D^N

$$\frac{\partial T^e}{\partial t} = D^e \nabla^2 T^e, \qquad D^e = \frac{\hbar}{m_e}, \tag{2.26}$$

$$\frac{\partial T^N}{\partial t} = D^N \nabla^2 T^N, \qquad D^N = \frac{\hbar}{m}. \tag{2.27}$$

The quantum diffusion coefficients D^e and D^N were introduced for the first time by E. Nelson [2.6].

For finite τ^e and τ^N, for $\Delta t < \tau^e$, $\Delta t < \tau^N$, Eqs. (2.20) and (2.21) can be written as

$$\frac{1}{(v_h^e)^2}\,\frac{\partial^2 T^e}{\partial t^2} = \nabla^2 T^e, \tag{2.28}$$

$$\frac{1}{(v_h^N)^2}\,\frac{\partial^2 T^N}{\partial t^2} = \nabla^2 T^N. \tag{2.29}$$

Equations (2.28) and (2.29) are the wave equations for quantum heat transport (QHT). For $\Delta t > \tau$, one obtains the Fourier equations (2.26) and (2.27).

In what follows, the dimensionless form of the QHT will be used. Introducing the reduced time t' and reduced length x',

$$t' = t/\tau, \qquad x' = \frac{x}{v_h \tau}, \tag{2.30}$$

one obtains, for QHT,

$$\frac{\partial^2 T^e}{\partial t^2} + \frac{\partial T^e}{\partial t} = \nabla^2 T^2, \tag{2.31}$$

$$\frac{\partial^2 T^N}{\partial t^2} + \frac{\partial T^N}{\partial t} = \nabla^2 T^N \tag{2.32}$$

and, for QFT,

$$\frac{\partial T^e}{\partial t} = \nabla^2 T^e, \tag{2.33}$$

$$\frac{\partial T^N}{\partial t} = \nabla^2 T^N. \tag{2.34}$$

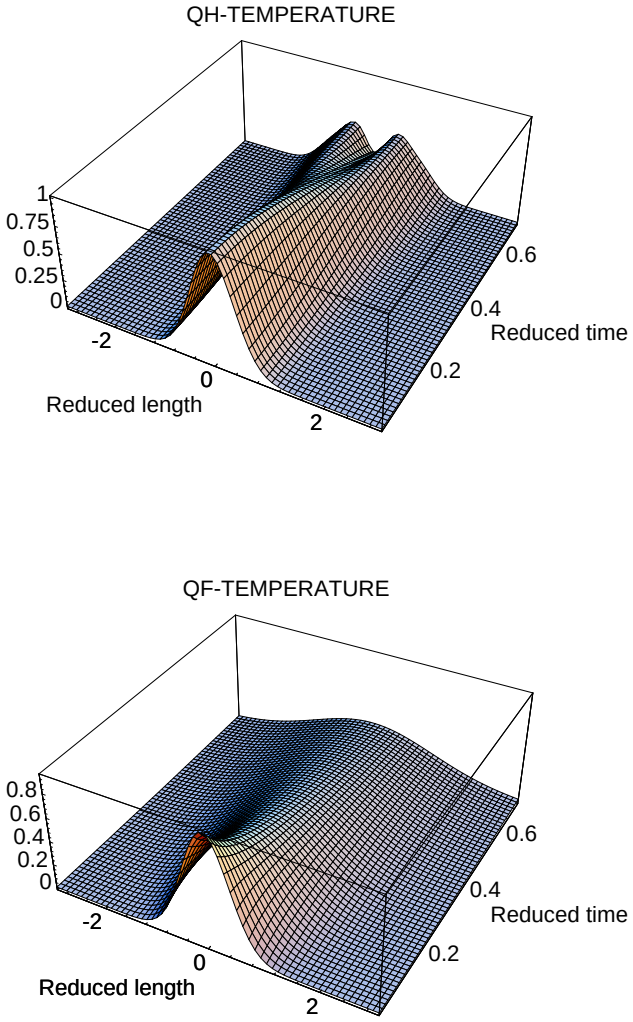

Figure 2.1: (a) The numerical solution of the QHT (2.31) for the initial Gaussian temperature profile (2.35). (b) The numerical solution of the QFT (2.33) for the initial Gaussian temperature profile (2.35).

In Figs. 2.1 (a) and 2.1 (b), the solution of QHT and QFT, respectively, for the initial Gaussian temperature pulse

$$T(0,x') = \exp(-3x'^2), \qquad \left.\frac{\partial T(t'x')}{\partial t'}\right|_{t'=0} = 0 \tag{2.35}$$

are presented. Isotherms are presented as the functions of the reduced length and reduced time (2.30). As can be seen from Fig. 2.1 (a) the initial Gaussian temperature pulse (2.35) propagates as the thermal wave to the left and right with the same velocity ("two arms" picture represents the front of the thermal wave). By contrast, in the case of QFT (Fig. 2.1 (b)), the heat transfer is the heat diffusion from the thermal Gaussian source.

The possible interpretation of the heaton energies can be stated as follows. For an electron gas, we obtain from formulas (2.15) and (2.25), for $m_e = 0.51\,\mathrm{MeV}/c^2$, and $v_h = (1/\sqrt{3})\alpha c$,

$$E_h^e = 9\,\mathrm{eV}, \tag{2.36}$$

which is of the order of the Rydberg energy. For nucleon gases ($m = 938\,\mathrm{MeV}/c^2$, $\alpha_s = 0.15$) one finds, from formulas (2.15) and (2.25),

$$E_h^N \sim 7\,\mathrm{MeV} \tag{2.37}$$

i.e., the average binding energy of the nucleon in the nucleus ("boiling" temperature for the nucleus).

When the ordinary matter (on the atomic level) or nuclear matter (on the nucleus level) is excited with short temperature pulses ($\Delta t \sim \tau$), the response of the matter is discrete. The matter absorbs the thermal energy in the form of the quanta E_h^e or E_h^N.

It is quite natural to pursue the study of the thermal excitation to the subnucleon level, i.e., quark matter. In the following, we generalize the

QHT equation (2.7) for quark gas in the form

$$\frac{1}{c^2}\,\frac{\partial^2 T^q}{\partial t^2}+\frac{1}{c^2\tau}\,\frac{\partial T^q}{\partial t}=\frac{(\alpha_s^q)^2}{3}\,\nabla^2 T^q, \tag{2.38}$$

with α_s^q denoting the fine-structure constant for strong quark-quark interaction, v_h^q the thermal velocity

$$v_h^q=\frac{1}{\sqrt{3}}\,\alpha_s^q c, \tag{2.39}$$

and τ is relaxation time for quark gas.

Analogously to electron and nucleon gases, we obtain for quark heaton

$$E_h^q=\frac{m_q}{3}(\alpha_s^q)^2c^2, \tag{2.40}$$

where m_q denotes the mass of the average quark mass. For a quark gas, the average quark mass can be calculated according to formula [2.7]

$$\begin{aligned} m_q &= \frac{1}{3}(m_u+m_d+m_s) \\ &= \frac{1}{3}(350+350+550)\,\mathrm{MeV}=417\,\mathrm{MeV}, \end{aligned} \tag{2.41}$$

where m_u, m_d, m_s denotes the mass of the up, down and strange quark, respectively. For the calculation of the α_s^q we consider the decays of the baryon resonances. For strong decay of the $\Sigma^o(1385\,\mathrm{MeV})$ resonance

$$K^- + p \to \Sigma^o(1385\,\mathrm{MeV}) \to \Lambda + \pi^0,$$

the width $\Gamma \sim 36\,\mathrm{MeV}$ and lifetime

$$\tau_s=\frac{\hbar}{\Gamma}\sim 10^{-23}\,\mathrm{s}.$$

For electromagnetic decay,

$$\Sigma^0(1192\,\mathrm{MeV}) \to \Lambda + \gamma,$$

$\tau_e \sim 10^{-19}$ s. Considering that

$$\left(\frac{\alpha_s^q}{\alpha}\right) \sim \left(\frac{\tau_e}{\tau_s}\right)^{1/2} \sim 100,$$

one obtains for α_s^q the value

$$\alpha_s^q \sim 1. \tag{2.42}$$

Substituting formulas (2.41) and (2.42) into (2.40), one finds

$$E_h^q \sim 139\,\mathrm{MeV} \sim \mathrm{m}_\pi, \tag{2.43}$$

where m_π denotes the π-meson mass. It occurs that where one attempts to "melt" the nucleon in order to obtain the free quark gas, the energy of the heaton is equal to the π-meson mass (which consists of two quarks). It is the simple presentation of *quark confinement.*

The contemporary results of the investigation of have ion interactions seems to support the above considerations. With the advent of ultra-relativistic heavy-ion collisions in the laboratory, at CERN and Brookhaven a new interdisciplinary field has emerged from the traditional domains of particle physics and nuclear physics. In combining methods and concepts from both areas, the study of heavy-ion interactions at very high energies a new and orginal approach in investigating the properties of matter and its interactions. Combining the elementary-interactions aspect of high energy physics with the macroscopic-matter aspect of nuclear physics, the subject of heavy-ion collisions is the study of *bulk matter* consisting of strongly interacting particles (hadrons). Thermodynamics would be an ideal language to be used in this field, so that complex multiparticle states can be described in terms of a few macroscopic variables: temperature, density, etc.

For the first time the discretization of the temperature field in high excited hadronic matter was described in paper [2.57]. It is interesting

to observe that the linear dependence of the temperature on the mass of *hadrons* emitted in S+S, Pb+Pb reactions was described in paper [2.58]. This observation supports the existence of the *heaton* in hadron gas excited to high temperature ($T \sim 200$ MeV).

2.2 Brownian representation of quantum heat transport in attosecond domain

The advent of the ultrashort duration laser pulses particularly those in attosecond (10^{-18} s) domain [2.8] open new experimental possibilities in the study of the details of the quantum heat transport, e.g. the quantum path of the heat carriers.

The quantum heat transport equation (QHT), formulas (2.20), (2.21) describe the quantum limit of heat transport. From a mathematical point of view, the Eqs. (2.20), (2.21) are the telegrapher type equation. In paper [2.9], it was shown that the hyperbolic diffusion equation (telegrapher equation) can be obtained within the frame of the correlated random walk (CRW) theory of the Brownian motion. As was shown in paper [2.9], the average displacement of the Brownian particle is described by the formula

$$< x^2 >= \frac{2\hbar\tau}{m_e}\left[t/\tau - \left(1 - e^{-t/\tau}\right)\right]. \qquad (2.44)$$

In deriving the Eq. (2.44), the diffusion coefficient $D = \hbar/m$ was used, according to formula (2.26). Eq. (2.44) has important consequences for the understanding the quantum heat transport. Can we define the trajectory of the *heatons*? To find the answer, let us discuss the two time limits of the Eq. (2.44). First of all, let us assume $t >> \tau$. Then, from formula, one

obtains

$$< x^2 > \cong \frac{2\hbar\tau}{m_e}\left(\frac{t}{\tau} - 1\right) = \frac{2\hbar}{m_e}\, t. \tag{2.45}$$

Equation (2.45) describes the quantum diffusion of the *heatons* with quantum diffusion coefficient $D = \hbar/m$, i.e.:

$$< x^2 >= 2Dt. \tag{2.46}$$

It is interesting to observe, that Eq. (2.46) can be interpreted as describing the random walk of a Brownian particles (*heatons*) and that the *heaton* path has fractal dimension $d_f = 2$, because the "mass" segment with duration t is related to the "radius" x by the relation (2.46) [2.10]

$$t \sim x^{d_f}. \tag{2.47}$$

The fractal dimension of the quantum path was investigated by Abbot and Wise [2.11]. They showed that the observed path of a particle in quantum mechanics is a fractal curve with the Hausdorff dimension two.

For $t \sim \tau$, one obtains from Eq. (2.44)

$$< x^2 > \cong \frac{2\hbar\tau}{m}\left(t/\tau - \left(1 - 1 + t/\tau - \frac{t^2}{2\tau^2}\right)\right) = \frac{\hbar}{m\tau}\, t^2, \tag{2.48}$$

which in view of formula (2.22) gives

$$< x^2 >= v_h^2 t^2. \tag{2.49}$$

Equation (2.49) describes the free motion of a *heaton* with velocity $v_h = \frac{1}{\sqrt{3}}\,\alpha c$ and considering Eq. (2.47), the path of quantum particle has a fractal dimension $d_f = 1$ i.e. the straight line. Now, we show that the analogy between quantum paths and random walks of quantum particles (*heaton*)

can be extended. As was shown in paragraph 2.1, for $\Delta t < \tau$ the QHT has the form of the quantum wave equation

$$\tau \frac{\partial^2 T}{\partial t^2} = \frac{\hbar}{m_e} \nabla^2 T \tag{2.50}$$

i.e.

$$\frac{1}{v_h^2} \frac{\partial^2 T}{\partial t^2} = \nabla^2 T. \tag{2.51}$$

The maximum value of the thermal wave velocity can be equal c – the velocity of light

$$v_h = c. \tag{2.52}$$

In that case, the relaxation time is described by formula

$$\tau_r = \frac{\hbar}{m v_h^2} \qquad \longrightarrow \qquad \frac{\hbar}{mc^2}. \tag{2.53}$$

The relaxation time τ_r, for $v_h = c$ is given by

$$\tau_r = \Lambda / c, \tag{2.54}$$

where Λ denotes the reduced Compton wave length for electron,

$$\Lambda = \frac{\hbar}{m_e c}. \tag{2.55}$$

Having established the expression for relaxation time τ_r the "pulsation" ω_r can be defined as

$$\omega_r = \tau_r^{-1} = \frac{mc^2}{\hbar} \tag{2.56}$$

i.e.

$$E_h^e = \omega_r \hbar = m_e c^2. \tag{2.57}$$

Considering that $m_e = 0.511\,\mathrm{MeV}/c^2$, the *heaton* internal energy can be calculated

$$E_h^e = 0.511\,\mathrm{MeV}, \tag{2.58}$$

and diffusion coefficient $D = \hbar/m$ can be written as

$$D = \frac{\hbar}{m} = \frac{\hbar}{mc}c = \Lambda c. \tag{2.59}$$

It is well known from quantum electrodynamics that quantum void fluctuations create and destroy virtual electron-positon pairs. These virtual electron-positon pairs have a characteristic lifetime of the order Λ/c. This is the typical time scale over which collisions occur between the *heaton* and the virtual electron-positon pairs. It is clear that the Compton wavelength Λ can be identified as the new mean free path since it is the typical distance covered by the virtual pair before its anihilation. The Eq. (2.59) for diffusion coefficient relates the D to Λ in the same manner as in kinetic theory of gases i.e.

$$D = \lambda_e v \qquad \longrightarrow \qquad D = \Lambda c. \tag{2.60}$$

For the relativistic regime, the average displacement $< x^2 >$ has the form of equations (2.46) and (2.48)

$$< x^2 >= 2Dt \tag{2.61}$$

for $t >> \tau_r$ and,

$$< x^2 >= c^2 t^2$$

for $t < \tau_r$.

As in nonrelativistic regime, for $t >> \tau_r$ the quantum path has the fractal dimension $d_f = 2$ and for $t < \tau_r$ the quantum path is the straight line but now with velocity $v_h = c$.

The advent of ultrashort duration pulses, particularly those in attosecond domain, has opened up new experimental possibilities in the study of structure of the matter in subnanometer scale. Conditions in this new field

of investigation are markedly different from those in for longer pulse duration. The distinction being that at longer pulse duration ($\sim 1\,\mathrm{ps}$) excited particles and their surroundings have had sufficient time to approach thermal equilibrium. For temporal resolution $\sim 1\,\mathrm{fs}$, it is possible to resolve the dynamics of the nonequilibrium excited carrier. The time resolution of the order 1 attosecond ($10^{-18}\,\mathrm{s}$) offers the possibilities of observing the path of the quantum heat carriers — *heatons*.

For a temporal resolution Δt of the order of the relaxation time $\tau \sim 10^{-17}\,\mathrm{s}$, the erratic Brownian motion of the individual *heatons* for $\Delta t >> \tau$ can be observed. For $\Delta t < \tau$, the *heatons* move along straight lines. Lasers with attosecond laser pulses open up quite new possibilities for studying these discrete thermal phenomena. For the contemporary laser technology, the time resolution Δt of the order of relaxation time $\tau_r \sim 10^{-21}\,\mathrm{s}$ (formula (2.58)) is out of technological possibilities. Nevertheless, it is important to take into account the fact that for $\Delta t \leq 10^{-21}\,\mathrm{s}$ the *heatons* move with the velocity of the light! It is worthwhile to realize that there exist models of elementary particles in which it is assumed that the electron propagates with the speed of light with certain chirality, except that at random times it flips both the direction of propagation (by 180°) and handedness, the rate of such flips is precisely the mass m (in units $\hbar = c = 1$) [2.12]–[2.15]. In the frame of the model developed in the present paper, the relaxation time for the interaction of *heatons* with voids is described by the formula (2.58) as $\tau = \hbar/mc^2$.

2.3 The fundamental solution of the quantum heat transport equation

In what follows, we will describe the one-dimension hyperbolic heat transfer with the help of Eqs. (2.20) and (2.21). To that aim, let us consider the following transformation of the temperature field $T(x,t)$

$$T(x,t) = e^{-\frac{t}{2\tau^{e,N}}} U^{e,N}(x,t). \tag{2.62}$$

When applied Eq. (2.62) to the Eqs. (2.20) and (2.21) one obtains the new QHT

$$\frac{\partial^2 U^{e,N}(x,t)}{\partial t^2} - (v_h^{e,N})^2 \frac{\partial^2 U^{e,N}(x,t)}{\partial x^2} - \frac{1}{4(\tau^{e,N})^2} U^{e,N}(x,t) = 0. \tag{2.63}$$

For the Cauchy boundary conditions

$$U^{e,N}(x,0) = f^{e,N}(x), \qquad \left.\frac{\partial U^{e,N}(x,t)}{\partial t}\right|_{t=0} = g^{e,N}(x), \tag{2.64}$$

the solution of Eq. (2.63) has the form [2.16]

$$\begin{aligned} U^{e,N}(x,t) &= \frac{f^{e,N}(x - v_h^{e,N}t) + f^{e,N}(x + v_h^{e,N}t)}{2} \\ &+ \frac{1}{2v_h^{e,N}} \int_{x - v_h^{e,N}t}^{x + v_h^{e,N}t} g(\zeta) I_0 \left[\frac{1}{2\tau^{e,N} v_h^{e,N}} \sqrt{(v_h^{e,N}t)^2 - (x-\zeta)^2} \right] d\zeta \\ &+ \frac{t}{2\tau^{e,N}} \int_{x - v_h^{e,N}t}^{x + v_h^{e,N}t} f(\zeta) \frac{I_1 \left[\frac{1}{2\tau^{e,N} v_h^{e,N}} \sqrt{(v_h^{e,N}t)^2 - (x-\zeta)^2} \right]}{\sqrt{(v_h^{e,N}t)^2 - (x-\zeta)^2}} d\zeta, \end{aligned} \tag{2.65}$$

and the solutions of Eqs. (2.20), (2.21) are

$$T^{e,N}(x,t) = e^{-t/2\tau^{e,N}} U^{e,N}(x,t). \tag{2.66}$$

For $\tau^{e,N} \to \infty$ (ballistic quantum heat transport) Eq. (2.63) can be written as

$$\frac{\partial^2 U^{e,N}}{\partial t^2} - (v_h^{e,N})^2 \frac{\partial^2 U^{e,N}}{\partial x^2} = 0 \tag{2.67}$$

and for Cauchy boundary conditions (2.64) the wave equation (2.67) has the solution [2.16]

$$U^{e,N}(x,t) = \frac{1}{2}\left[f^{e,N}(x + v_h^{e,N}t) + f(x - v_h^{e,N}t)\right] + \frac{1}{2v_h^{e,N}} \int_{x-v_h^{e,N}t}^{x+v_h^{e,N}t} g(\zeta)d\zeta. \tag{2.68}$$

In that case the solutions of Eqs. (2.20) and (2.21) are

$$T^{e,N}(x,t) = U^{e,N}(x,t). \tag{2.69}$$

Both solutions (2.66) and (2.69) exhibit the domains of dependence and influence on the hyperbolic equations. These domains which characterize the maximum speed at which disturbances or signals travel are determined by the principal parts of the given equations (i.e. the second derivative terms) and do not depend on the lower order terms. These results show that the QHT and the wave equation have identical domains of dependence and influence.

Now, let us consider the static field limit $U^{e,N}(x,t) \to V^{e,N}(x)$ of the Eq. (2.63)

$$\begin{aligned} \frac{\partial^2 V^e(x)}{\partial x^2} &= -\frac{1}{4}\left(\frac{m_e v_h^e}{\hbar}\right)^2 V^e(x), \\ \frac{\partial^2 V^N(x)}{\partial x^2} &= -\frac{1}{4}\left(\frac{m v_h^N}{\hbar}\right)^2 V^N(x). \end{aligned} \tag{2.70}$$

If we require spherically symmetric solutions of Eqs. (2.70), i.e. one that solely depends upon $|\vec{r}|$ (in 3 dimension) then we can write

$$\nabla^2 V^e(r) = -\frac{1}{4}\left(\frac{m_e v_h^e}{\hbar}\right)^2 V^e(r),$$

$$\nabla^2 V^N(r) = -\frac{1}{4}\left(\frac{m v_h^N}{\hbar}\right)^2 V^N(r). \tag{2.71}$$

The spherically symmetric solutions of Eq. (2.71) are

$$\begin{aligned} V^e(r) &= -\frac{g^e}{r} e^{-r/R^e}, \\ V^N(r) &= -\frac{g^N}{r} e^{-r/R^N}. \end{aligned} \tag{2.72}$$

where $g^{e,N}$ denotes the coupling constants ("charges") for electromagnetic and strong interactions respectively. The parameters R^e and R^N are the ranges of the interactions. Following formula (2.72), one obtains

$$\begin{aligned} R^e &= \frac{2\hbar}{m_e v_h^e}, \\ R^N &= \frac{2\hbar}{m_N v_h^N}. \end{aligned} \tag{2.73}$$

For electromagnetic interactions, the range R^e can be written in the form

$$R^e \cong \frac{2\hbar}{m_e v_F^e} \sim \frac{2\hbar}{P_F^e} \sim \frac{2}{k_F^e}. \tag{2.74}$$

where k_F^e denotes the Fermi wave vector for the electrons. Substituting formula (2.74) to Eq. (2.72), the potential $V^e(r)$ can be written as

$$V^e(r) = -\frac{g^e}{r} e^{-\frac{r k_F}{2}}. \tag{2.75}$$

Formula (2.75) is the well known equation for Debye – Hückl Coulomb potential with screening [2.17, 2.18], where g^e is equal $\alpha\hbar c$.

For strong interactions, potential $V^N(r)$ has the form of the Yukawa nucleon – nucleon potential [2.19]

$$V^N(r) = -\frac{g^N}{r} e^{-\frac{r}{R^N}}, \qquad g^N = \alpha_s \hbar c, \tag{2.76}$$

with the range R^N, where

$$R^N = \frac{2\hbar}{m v_h^N} = \frac{2\hbar}{m_N \alpha_s c}, \tag{2.77}$$

where $\alpha_s = m_\pi m_N^{-1}$ is the fine-structure constant for strong interactions. In that case, formula (2.77) can be written as

$$R^N = \frac{2\hbar}{m_\pi c}, \tag{2.78}$$

i.e. R^N is of the order of Compton wavelength for meson π, which defines the range of strong interactions. Following formulas (2.25), (2.73), (2.74), (2.78) the numerical values for *heaton* energies E^N and ranges of interactions are calculated and presented in Table 2.1.

Table 2.1: The ranges and heaton energies for electromagnetic and strong interactions

Fermions	R^e, R^N [m]	E^e, E^N [eV]
electrons	10^{-10}	~ 10
nucleons	10^{-15}	$\sim 10^7$

In Fig. 2.2(a) the Debye – Hückl potential, formula (2.75) is presented (thick curve). In the same figure, the Coulomb potential (thin curve) is also presented. The nucleon – nucleon Yukawa potential, formulas (2.76), (2.78) is presented in Fig. 2.2(b). As it is well known [2.19] for $r < 0.8\,\mathrm{fm}$ the nucleon – nucleon potential has the hard core term. In Fig. 2.2(b) the hard core term is represented by the vertical line.

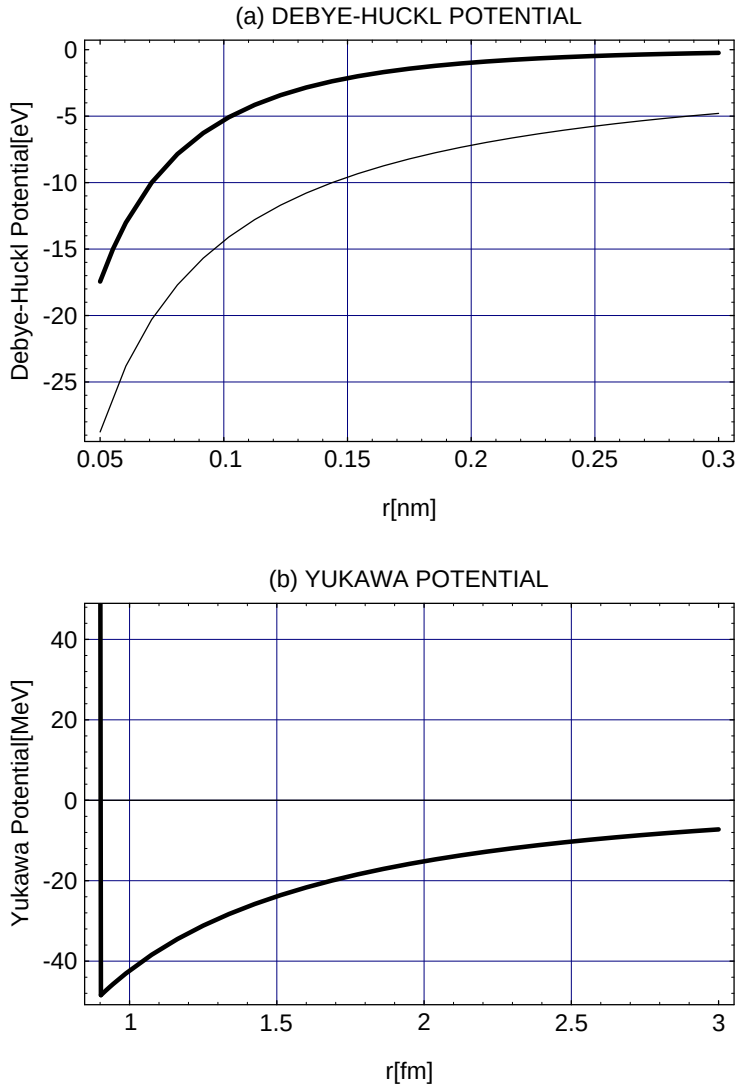

Figure 2.2: (a) The Debye – Hückl potential, formula (2.75) — thick curve and Coulomb potential — thin curve. (b) The Yukawa potential, formula (2.76) with hard core term.

The formulas (2.76) and (2.78), which describe the range of strong force can be formulated in the spirit of Skyrme model [2.20]. Skyrme introduced a model of nucleons as distributions of pion fields. In our case, the strong force is mediated by meson π, which is a "part" of nucleon, i.e. $m_\pi \approx 0.15m$.

2.4 The distortionless quantum thermal waves

Efficient conversion of electromagnetic energy to particle energy is of fundamental importance in many areas of physics. The nature of intense, short pulse laser interactions with single atoms and solid targets has been subject of extensive experimental and theoretical investigation over the last 15 years [2.21]. Recently, the interaction of femtosecond laser pulses with Xe clusters was investigated [2.22, 2.23] and strong X-ray emission and multi-keV electron generation were observed. Such experiments have become possible, owing to recently developed high peak power lasers which are based on chirped pulse amplification and are capable of producing focused light intensity of up to $10^{14} - 10^{19}\,\mathrm{Wcm}^{-2}$.

In intensely irradiated clusters, optically and collisionally ionized electrons undergo rapid collisional heating for short time (< 1ps) before the cluster disintegrates in the laser field. Charge separation of the hot electrons inevitably leads to a very fast expansion of the cluster ions. Both electrons and ions ultimately reach a velocity given by the speed of sound of the cluster plasma [2.24].

When the intense laser pulse interacts with atomic clusters ionization to very high charge states is observed [2.24]. The high Coulomb field cer-

tainly influences the thermal processes in clusters. In the chapter, the new QHT equation is formulated in which the external — not only thermal forces are included. The solution of the new QHT for Cauchy boundary conditions will be derived. The condition for the distortionless propagations of the thermal wave will be formulated.

Now, we develop the generalized quantum heat transport equation which includes the potential term. In this way, we use the analogy between the Schrödinger equation and quantum heat transport equations (2.31), (2.32). Let us consider, for the moment, the parabolic heat transport equation i.e. the Eqs. (2.33), (2.34), with the second derivative term omitted [2.25, 2.26]

$$\frac{\partial T}{\partial t} = \frac{\hbar}{m}\nabla^2 T. \tag{2.79}$$

When the real time $t \to \frac{it}{2}$ and $T \to \Psi$, Eq. (2.79) has the form of a free Schrödinger equation

$$i\hbar\frac{\partial \Psi}{\partial t} = -\frac{\hbar^2}{2m}\nabla^2\Psi. \tag{2.80}$$

The complete Schrödinger equation has the form

$$i\hbar\frac{\partial \Psi}{\partial t} = -\frac{\hbar^2}{2m}\nabla^2\Psi + V\Psi, \tag{2.81}$$

where V denotes the potential energy. When we go back to real time $t \to -2it$ and $\Psi \to T$, the new parabolic quantum heat transport is obtained

$$\frac{\partial T}{\partial t} = \frac{\hbar}{m}\nabla^2 T - \frac{2V}{\hbar}T. \tag{2.82}$$

Equation (2.82) describes the quantum heat transport for $\Delta t > \tau$. For heat transport initiated by ultrashort laser pulses, when $\Delta t \leq \tau$ one obtains the generalized quantum hyperbolic heat transport equation

$$\tau\frac{\partial^2 T}{\partial t^2} + \frac{\partial T}{\partial t} = \frac{\hbar}{m}\nabla^2 T - \frac{2V}{\hbar}T. \tag{2.83}$$

Considering that $\tau = \hbar/mv^2$ [2.25, 2.26], Eq. (2.83) can be written as follows:

$$\frac{1}{v^2}\frac{\partial^2 T}{\partial t^2} + \frac{m}{\hbar}\frac{\partial T}{\partial t} + \frac{2Vm}{\hbar}T = \nabla^2 T. \tag{2.84}$$

Equation (2.84) describes the heat flow when apart from the temperature gradient, the potential energy V operates.

In the following, we consider the one-dimensional heat transfer phenomena, i.e.

$$\frac{1}{v^2}\frac{\partial^2 T}{\partial t^2} + \frac{m}{\hbar}\frac{\partial T}{\partial t} + \frac{2Vm}{\hbar}T = \frac{\partial^2 T}{\partial x^2}. \tag{2.85}$$

For quantum heat transfer equation (2.85), we seek solution in the form

$$T(x,t) = e^{-t/2\tau}u(x,t). \tag{2.86}$$

After substitution of Eq. (2.86) into Eq. (2.85), one obtains

$$\frac{1}{v^2}\frac{\partial^2 u}{\partial t^2} - \frac{\partial^2 u}{\partial x^2} + q\,u(x,t) = 0, \tag{2.87}$$

where

$$q = \frac{2Vm}{\hbar^2} - \left(\frac{mv}{2\hbar}\right)^2. \tag{2.88}$$

In the following, we will consider the constant potential energy $V = V_0$. The general solution of Eq. (2.87) for Cauchy boundary conditions,

$$u(x,0) = f(x), \qquad \left.\frac{\partial u(x,t)}{\partial t}\right|_{t=0} = F(x), \tag{2.89}$$

has the form [2.27]

$$u(x,t) = \frac{f(x-vt) + f(x+vt)}{2} + \frac{1}{2}\int_{x-vt}^{x+vt} \Phi(x,t,z)dz, \tag{2.90}$$

where

$$\Phi(x,t,z) = \frac{1}{v}F(z)J_0\left(\frac{b}{v}\sqrt{(z-x)^2-v^2t^2}\right) + btf(z)\frac{J_0'(\frac{b}{v}\sqrt{(z-x)^2-v^2t^2})}{\sqrt{(z-x)^2-v^2t^2}},$$

$$b = \left(\frac{mv^2}{2\hbar}\right)^2 - \frac{2Vm}{\hbar^2}v^2 \tag{2.91}$$

and $J_0(z)$ denotes the Bessel function of the first kind. Considering formulas (2.86), (2.87), (2.88) the solution of Eq. (2.85) describes the propagation of the distorted thermal quantum waves with characteristic lines $x = \pm vt$. We can define the distortionless thermal wave as the wave which preserves the shape in the field of the potential energy V_0. The condition for conserving the shape can be formulated as

$$q = \frac{2Vm}{\hbar^2} - \left(\frac{mv}{2\hbar}\right)^2. \tag{2.92}$$

When Eq. (2.92) holds, Eq. (2.87) has the form

$$\frac{\partial^2 u(x,t)}{\partial t^2} = v^2\frac{\partial^2 u}{\partial x^2}. \tag{2.93}$$

Equation (2.93) is the quantum wave equation with the solution (for Cauchy boundary conditions (2.89))

$$u(x,t) = \frac{f(x-vt)+f(x+vt)}{2} + \frac{1}{2v}\int_{x-vt}^{x+vt} F(z)dz. \tag{2.94}$$

It is quite interesting to observe, that condition (2.92) has an analog in the classical theory of the electrical transmission line. In the context of the transmission of an electromagnetic field, the condition $q = 0$ describes the Heaviside distortionless line. Eq. (2.92) — the distortionless condition — can be written as

$$V_0\tau \sim \hbar, \tag{2.95}$$

We can conclude, that in the presence of the potential energy V_0 one can observe the undisturbed quantum thermal wave only when the Heisenberg uncertainty relation for thermal processes (2.95) is fulfilled.

The generalized quantum heat transport equation (GQHT) (2.85) leads to the generalized Schrödinger equation. After the substitution $t \to it/2$, $T \to \Psi$ in Eq. (2.85), one obtains the generalized Schrödinger equation (GSE)

$$i\hbar\frac{\partial\Psi}{\partial t} = -\frac{\hbar^2}{2m}\nabla^2\Psi + V\Psi - 2\tau\hbar\frac{\partial^2\Psi}{\partial t^2}. \tag{2.96}$$

Considering that $\tau = \hbar/mv^2 = \hbar/m\alpha^2c^2$ ($\alpha = 1/137$ is the fine-structure constant for electromagnetic interactions) Eq. (2.96) can be written as

$$i\hbar\frac{\partial\Psi}{\partial t} = -\frac{\hbar^2}{2m}\nabla^2\Psi + V\Psi - \frac{2\hbar^2}{m\alpha^2c^2}\frac{\partial^2\Psi}{\partial t^2}. \tag{2.97}$$

One can conclude, that for time period $\Delta t < \hbar/m\alpha^2c^2 \sim 10^{-17}$ s the description of quantum phenomena needs some revision. On the other hand, for $\Delta t > 10^{-17}$ in GSE the second derivative term can be omitted and as the result the SE is obtained, i.e.

$$i\hbar\frac{\partial\Psi}{\partial t} = -\frac{\hbar^2}{2m}\nabla^2\Psi + V\Psi. \tag{2.98}$$

It is quite interesting to observe, that GSE was discussed also in papers [2.25, 2.28] in the context of the sub-quantal phenomena.

Concluding, a study of the interactions of the attosecond laser pulses with matter can shed the light on the applicability of the SE to the study of the ultrashort sub-quantal phenomena. The structure of the Eq. (2.87) depends on the sign of the parameter q. For quantum heat transport phenomena with electrons as the heat carriers parameter q is the function of potential barrier height (V_0) and velocity v. Considering that velocity v

equals [2.25]

$$v = \frac{1}{\sqrt{3}}\alpha c = 1.26\,\frac{\mathrm{nm}}{\mathrm{fs}}, \tag{2.99}$$

parameter q can be calculated for typical barrier height $V_0 \geq 0$. In Fig. 2.3 the parameter q as the function of V_0 is calculated. For $q < 0$, i.e., when V_0 <1.125 eV, Eq. (2.87) is the *modified telegrapher's equation* [2.14].

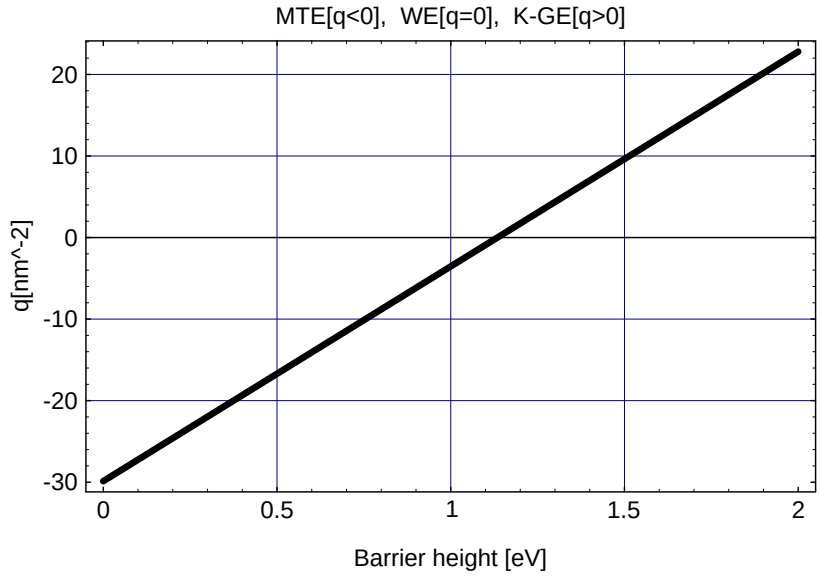

Figure 2.3: Parameter q (formula (2.88)) as the function of the barrier height (eV).

For Cauchy initial condition

$$u(x,o) = f(x), \qquad \frac{\partial u(x,o)}{\partial t} = g(x), \tag{2.100}$$

the solution of the Eq. (2.87) has the form

$$\begin{aligned} u(x,t) &= \frac{f(x-vt)+f(x+vt)}{2} \\ &+ \frac{1}{2v}\int_{x-vt}^{x+vt} g(\zeta) I_0\left[\sqrt{-q(v^2t^2-(x-\zeta)^2)}\right] d\zeta \\ &+ \frac{(v\sqrt{-q})t}{2}\int_{x-vt}^{x+vt} f(\zeta)\frac{I_1\left[\sqrt{-q(v^2t^2-(x-\zeta)^2)}\right]}{\sqrt{v^2t^2-(x-\zeta)^2}} d\zeta. \end{aligned} \tag{2.101}$$

When $q > 0$ Eq. (2.87) is the *Klein-Gordon equation* (K-G) [2.14] well known from application to elementary particle and nuclear physics.

For Cauchy initial condition (2.100), the solution of (K-G) equation can be written as

$$\begin{aligned} u(x,t) &= \frac{f(x-vt)+f(x+vt)}{2} \\ &+ \frac{1}{2v}\int_{x-vt}^{x+vt} g(\zeta) J_0\left[\sqrt{q(v^2t^2-(x-\zeta)^2)}\right] d\zeta \\ &- \frac{v\sqrt{q}t}{2}\int_{x-vt}^{x+vt} f(\zeta)\frac{J_0\left[\sqrt{q(v^2t^2-(x-\zeta)^2)}\right]}{\sqrt{v^2t^2-(x-\zeta)^2}} d\zeta. \end{aligned} \tag{2.102}$$

Both solutions (2.101) and (2.102) exhibit the domains of dependence and influence on *modified telegrapher's equation* and *Klein–Gordon Equation.* These domains, which characterize the maximum speed at which thermal disturbance travel are determined by the principal parts of the given equation (i.e., the second derivative terms) and do not depend on the lower order terms. It can be concluded that these equation and the wave equation (for $m = 0$) have identical domains of dependence and influence.

2.5 Metastable thermal quantum states

The concept of metastable states in quantum mechanics dates back to the beginning of the century. The interaction between a quantum system and an external electromagnetic field was described by Planck using the concept of a metastable state. The metastable is distinguished from a stationary state which is "infinitely" long lived. The metastable state is an unstable state and has finite lifetime [2.28].

In this paragraph, the metastable thermal states created in quantum structures by the ultrashort thermal pulses are investigated. When the ultrashort laser pulses interact with an inhomogeneous quantum structure, the potential energy barriers on the edges of discontinuities influence the thermal energy transport.

The master equation which describes the thermal perturbation propagation is the Klein-Gordon equation (2.87), with $q > 0$ which is the hyperbolic partial differential equation. In complete analogy to the quantum Klein-Gordon equation, the thermal Klein-Gordon equation has the periodic solution – thermal waves. For the thermal wave which propagates in an inhomogeneous structure the transmission and the reflection phenomena as well as formation of metastable state can be investigated.

The existence of metastable thermal states can be very important in the modeling of the thermal energy dissipation in quantum inhomogeneous structures, in which ultrashort electromagnetic pulses generate the ultrashort thermal harmonic perturbations.

The generalized heat transport equation, which includes the potential has the form

$$\frac{1}{v^2}\frac{\partial^2 T}{\partial t^2} + \frac{m}{\hbar}\frac{\partial T}{\partial t} + \frac{2Vm}{\hbar^2}T = \nabla^2 T. \tag{2.103}$$

For constant potential barrier $V = V_0$ and in the case of the one-dimensional heat transfer phenomena, Eq. (2.103) can be written as

$$\frac{1}{v^2}\frac{\partial^2 T}{\partial t^2} + \frac{m}{\hbar}\frac{\partial T}{\partial t} + \frac{2V_0 m}{\hbar^2}T = \frac{\partial^2 T}{\partial x^2}. \tag{2.104}$$

In the generalized quantum heat transport equation (2.104), we seek a solution in the form

$$T(x,t) = e^{-t/2\tau}u(x.t), \tag{2.105}$$

where the relaxation time, τ, equals

$$\tau = \frac{\hbar}{mv^2}. \tag{2.106}$$

After substituting Eqs. (2.105) and (2.106) into Eq. (2.104), one obtains

$$\frac{1}{v^2}\frac{\partial^2 u}{\partial t^2} - \frac{\partial^2 u}{\partial x^2} + qu(x,t) = 0, \tag{2.107}$$

where

$$q = \frac{2V_0 m}{\hbar^2} - \left(\frac{mv}{2\hbar}\right)^2. \tag{2.108}$$

For $q > 0$, Eq. (2.108) is the Klein-Gordon equation. In the following, we will consider the heat transport through the double Dirac delta potential barrier

$$V_0(x) = a\delta(x) + a\delta(x-d), \tag{2.109}$$

where a is the barrier strength and d is the barrier separation. Let $u(x,t)$ determine harmonic plane thermal wave

$$u(x,t) = e^{-i\omega t}\phi(x). \tag{2.110}$$

The function $\phi(x)$ fulfills the time independent equations

$$\frac{\hbar^2}{2m}\frac{d^2\phi(x)}{dx^2} + \phi(x)\left[\frac{(\hbar\omega)^2}{2mv^2} + \frac{mv^2}{8}\right] = 0 \tag{2.111}$$

when $V_0 = 0$, and

$$\frac{\hbar^2}{2m}\frac{d^2\phi(x)}{dx^2} + \phi(x)\left[\frac{(\hbar\omega)^2}{2mv^2} + \frac{mv^2}{8} - V_0\right] = 0 \tag{2.112}$$

when $V_0 \neq 0$.

In the potential free region, the plane harmonic thermal wave $\phi(x)$ has the form

$$\phi(x) = e^{ikx}. \tag{2.113}$$

After substituting Eq. (2.113) into Eq. (2.111) one obtains

$$-k^2 + \frac{2m\Omega^2}{\hbar^2} = 0; \qquad k = \left(\frac{2m\Omega^2}{\hbar^2}\right)^{1/2}, \tag{2.114}$$

where

$$\Omega^2 = \frac{mv^2}{8} + \frac{(\hbar\omega)^2}{2mv^2}. \tag{2.115}$$

The solution of Eq. (2.112) in three different regions can be expressed as follows:

$$\begin{aligned} \phi_I(x) &= e^{ikx} + Re^{-ikx} \qquad x \leq 0, \\ \phi_{II}(x) &= Ae^{ikx} + Be^{-ikx} \qquad 0 \leq x \leq d, \\ \phi_{III}(x) &= Ce^{ikx} \qquad x \geq d. \end{aligned} \tag{2.116}$$

Here R and C are the reflection and transmission amplitudes respectively. The transmission coefficient equals $|C|^2$. The boundary conditions at $x = 0$ and $x = d$ are used to determine the amplitude C and the transmission coefficient $|C|^2$. At the locations of the delta barriers, the wave functions $\phi(x)$ are continuous, that is

$$\phi_I(0) = \phi_{II}(0), \qquad \phi_{II}(d) = \phi_{III}(d). \tag{2.117}$$

The slope of the wave functions at $x = 0$ and $x = d$ is discontinuous, and it can be shown by carrying out the following integrals:

$$\lim_{\eta\to 0}\int_{-\eta}^{\eta}\left[-\frac{\hbar^2}{2m}\frac{d^2}{dx^2}+a\delta(x)+a\delta(x-d)\right]\phi(x)dx=\lim_{\eta\to 0}\int_{-\eta}^{\eta}\Omega^2\phi(x)dx, \tag{2.118}$$

or

$$-\frac{\hbar^2}{2m}\left[\phi'_{II}(0)-\phi'_{I}(0)\right]+a\phi_I(0)=0 \tag{2.119}$$

and

$$\lim_{\eta\to 0}\int_{d-\eta}^{d+\eta}\left[-\frac{\hbar^2}{2m}\frac{d^2}{dx^2}+a\delta(x)+a\delta(x-d)\right]\phi(x)dx=\lim\int_{d-\eta}^{d+\eta}\Omega^2\phi(x)dx, \tag{2.120}$$

or

$$-\frac{\hbar^2}{2m}\left[\phi'_{III}(d)-\phi'_{II}(d)\right]+a\phi_{III}(d)=0. \tag{2.121}$$

From Eqs. (2.119) and (2.121), the discontinuity of the first-order derivatives at $x = 0$, and d can be observed.

By substituting Eqs. (2.116) into Eqs. (2.117), (2.119) and (2.121) one obtains

$$\begin{aligned}
1+R&=A+B,\\
Ae^{ikd}+Be^{-ikd}&=Ce^{ikd},\\
\tfrac{\hbar^2}{2m}\left[ikA-Bik-ik+Rik\right]+a(1+R)&=0,\\
-\tfrac{\hbar^2}{2m}\left[ikCe^{ikd}-ikAe^{ikd}+Bike^{-ikd}\right]+aCe^{ikd}&=0
\end{aligned} \tag{2.122}$$

When the dimensionless parameter $\epsilon = 2ma/k\hbar^2$ is defined, Eqs. (2.122)

can be written as

$$\begin{aligned} 1 + R &= A + B, \\ Ae^{ikd} + Be^{-ikd} &= Ce^{ikd}, \\ A - B - 1 + R - \tfrac{\epsilon}{i}(1 + R) &= 0, \\ -Ae^{ikd} + Be^{-ikd} + Ce^{ikd}(1 - \tfrac{\epsilon}{i}) &= 0. \end{aligned} \tag{2.123}$$

After rearrangement of the Eqs. (2.123), transmission amplitude C can be calculated

$$C = \frac{4}{[\epsilon^2 e^{2ikd} + (i\epsilon + 2)^2]}. \tag{2.124}$$

With the transmission amplitude C, (formula 2.124), we can define the transmission coefficient, K

$$K = |C|^2. \tag{2.125}$$

For a quantum two-barrier structure (2.109) the residence time r, the time which harmonic thermal pulse spends inside the structure, can be defined as

$$r = \frac{d}{Kv}. \tag{2.126}$$

The residence time, formula (2.126), was first defined by B. R. Mottelson [2.29] in connection with tunneling phenomena in nuclear physics.

In Figs. 2.4 and 2.5, the residence time and the ratio of the residence time r, (2.126), to the relaxation time τ, (2.106), of the thermal harmonic pulse are presented.

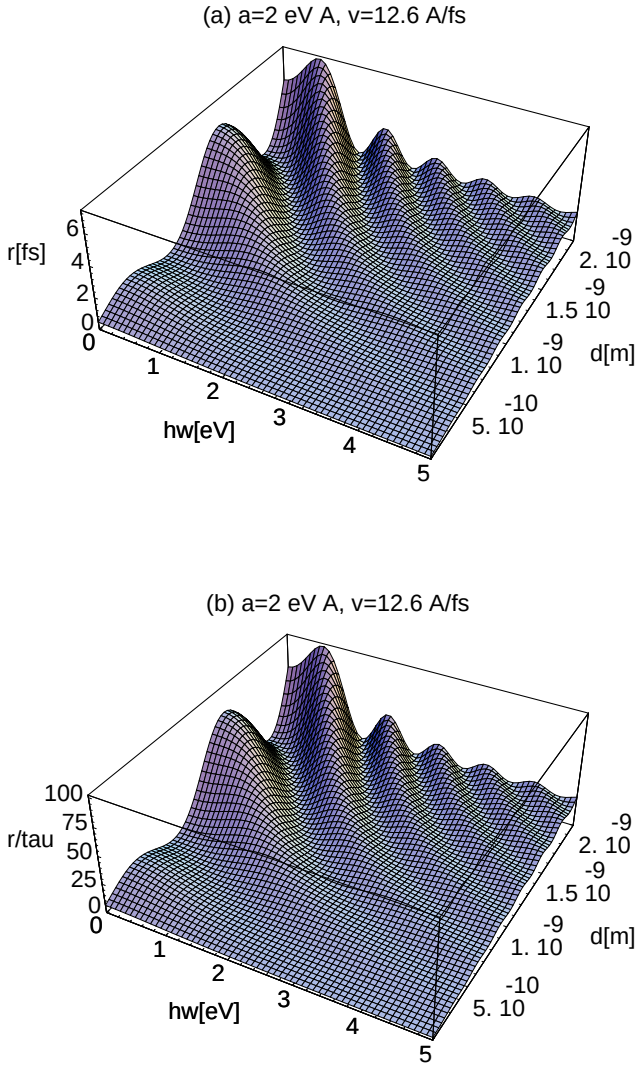

Figure 2.4: (a) The residence time, r, formula (2.126) for double – barrier structure with $a = 2$ eVA and $v = 1.26$ nm/fs. (b) The ratio r/τ for the double – barrier structure.

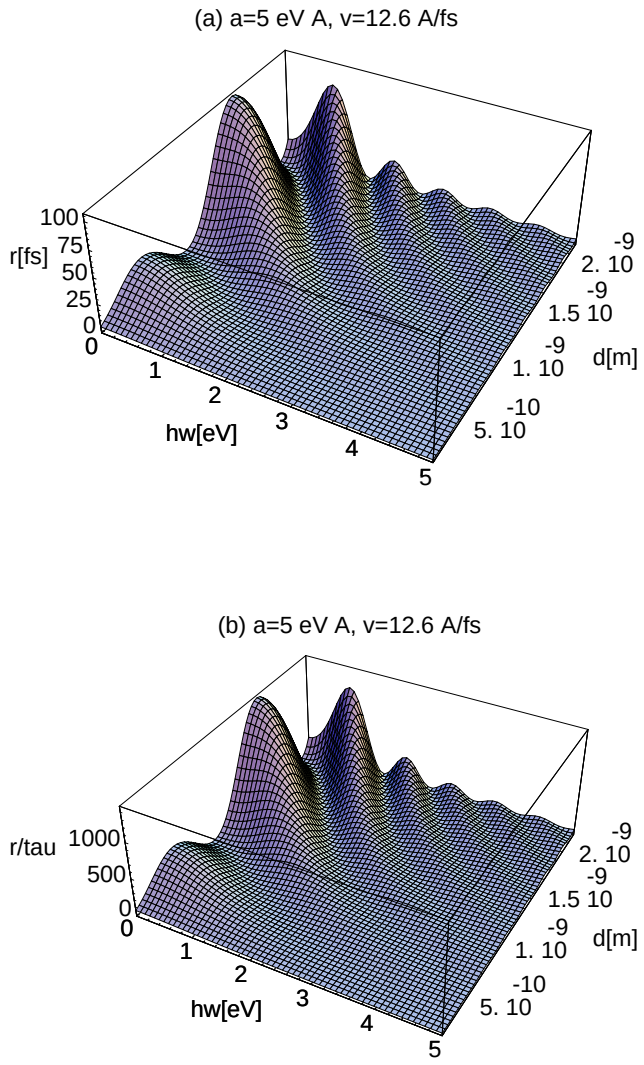

Figure 2.5: (a), (b) The same as in Figs. 2.4(a), (b) but for $a = 5$ eVA.

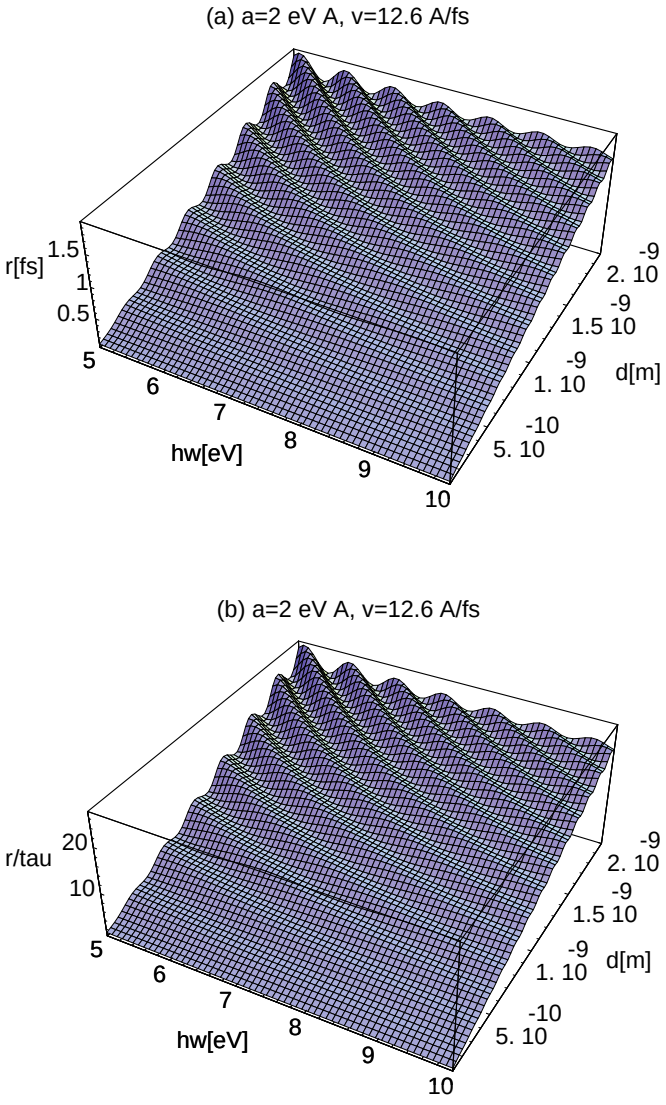

Figure 2.6: (a), (b) The same as in Figs. 2.4(a), (b).

In Fig. 2.4(a), the residence time was calculated for the quantum structure with potential

$$V(x) = 2\text{eV}\text{Å}\delta(x) + 2\text{eV}\text{Å}\delta(x-d) \tag{2.127}$$

and the thermal wave velocity $v = 1.26$ nm/fs $= 12.6$ AAfs. The resonant peaks corresponding to the metastable states become broadened at higher energy indicating the decreasing lifetime of the metastable thermal states. In Fig. 2.4(b), the ratio r/τ for the same quantum potential (2.127) was calculated.

The results for quantum structure

$$V(x) = 5\text{eV}\text{Å}\delta(x) + 5\text{eV}\text{Å}\delta(x-d) \tag{2.128}$$

are presented in Figs. 2.5(a), (b).

It is quite interesting to observe, that for thermal harmonic pulse with an energy $\hbar\omega < 5$ eV, the residence time depends strongly on potential strength parameter a and linear dimension d of the quantum structure. Moreover, for discrete values of thermal harmonic pulse energy the metastable (with long residence time) states are generated. In these metastable states, the thermal energy is stored inside the structure and is not transmitted outward. In complete analogy to the quantum mechanics for greater energy of the thermal harmonic pulse, the quantum structure is transparent for thermal pulse. The results for $\hbar\omega > 5$ eV are presented in Figs. 2.6(a), (b). In that case, we observe small "ripples" on the smooth background. The background is described by the traversal time, d/v.

2.6 Quantum heat transport on the molecular scale

Molecular electronics is a new field of science and technology, which is evolving from the convergence of ideas from chemistry, physics, biology, electronics and information technology [2.30, 2.31, 2.32]. It considers, on the one hand molecular materials for electronic/optoelectronic applications, on the other hand attempts to build electronics with molecules at the molecular level. It is this second viewpoint which concerns us here: describing the heat transport at the level of single or few molecules.

The heat and charge transport phenomena on the molecular scale are the quantum phenomena and electrons constitute the charge and heat carriers. We argue, that to describe the heat transport phenomena on the molecular level the quantum heat transport equation is a natural reference equation.

The quantum heat transport equation for the atomic scale has the form (2.20, 2.21)

$$\tau\frac{\partial^2 T}{\partial t^2}+\frac{\partial T}{\partial t}=D\nabla^2 T, \tag{2.129}$$

where τ is the relaxation time, D is the heat diffusion coefficient and T denotes temperature. For the atomic scale heat transport, the relaxation time equals

$$\tau=\frac{\hbar}{mv_h^2}, \qquad v_h=\frac{1}{\sqrt{3}}\alpha c, \tag{2.130}$$

where m is the electron mass and v_h is the velocity of the heat perturbation. Moreover, on the atomic level the temperature field $T(r)$ is quantized by a quantum heat of energy, the *heaton*. The *heaton* energy equals

$$E_h=m_e v_h^2. \tag{2.131}$$

Due to formula (2.131), the *heaton* energy is the interaction energy of electromagnetic field with electrons (through the coupling constant α).

At the molecular level we seek energy of interactions of the electromagnetic field with a molecule. This energy is described by the formula [2.33]

$$E_h^m = \alpha^2 \frac{m_e}{m_p} m_e c^2, \tag{2.132}$$

where m_e, m_p are the masses of electron and proton, respectively.

Considering the general formula for *heaton* energy (2.131), one obtains from formula (2.132) for velocity of the thermal perturbation

$$v_h = \alpha c \left(\frac{m_e}{m_p} \right)^{1/2}. \tag{2.133}$$

Comparison of formulas (2.130) and (2.133) shows, that v_h scales with ratio $(m_e/m_p)^{1/2}$ when the atomic scale is changed to the molecular scale; v_h is the Fermi velocity for molecular gas.

Quantum heat transport equation (2.129) has as a solution, for short time scale, (short in comparison to relaxation time τ) the heat waves which propagate with velocity v_h. One can say that on the molecular level, the heat waves are slower in comparison to the atomic scale.

From formulas (2.130) and (2.133), the relaxation time can be calculated

$$\tau = \frac{m_p}{m_e} \frac{\hbar}{m_e c^2 \alpha^2}. \tag{2.134}$$

It occurs, that relaxation time on the molecular scale is longer (ratio m_p/m_e) than the atomic relaxation time. For standard values of the constants of the Nature

$$\alpha = \frac{1}{137}, \qquad m_e = 0.511\,\mathrm{MeV/c^2}, \qquad m_p = 938\,\mathrm{MeV/c^2}, \tag{2.135}$$

one obtains the following numerical values for v_h, τ and E_h: $v_h = 0.05\,\mathrm{nm/fs}$, $\tau = 44\,\mathrm{fs}$ and $E_h = 10^{-2}$ eV. With those values of v_h and τ, the mean free path

$$\lambda = \tau v_h \tag{2.136}$$

can be calculated and $\lambda = 2.26\,\mathrm{nm}$. It is interesting to observe, that in the structure of the biological cells, some elements have the dimension of the order of the nanometer [2.30].

With the help of the *heaton* energy one can define the *heaton temperature*, i.e., the characteristic temperature of the heat transport on the molecular scale, viz.:

$$T_m = \alpha^2 \frac{m_e}{m_p} m_e c^2\, 1.16\, 10^{10}\,\mathrm{K} \approx 10^{-3} \alpha^2 m_e c^2 \sim 316\,\mathrm{K}. \tag{2.137}$$

This defines what we generally term "room temperature". At temperatures far below T_m, the hydrogen bond becomes very rigid and the flexibility of atomic configurations is weakened. Most substances are liquid or solid below T_m. Biology occurs in environments with ambient temperature within an order or magnitude or so of T_m.

In Figs. 2.7, 2.8, the results of the theoretical calculations for the quantum heat transport on the molecular scale are presented. In Fig.2.7(a) the solution of Eq. (2.129) in one-dimension case

$$\tau \frac{\partial^2 T}{\partial t^2} + \frac{\partial T}{\partial t} = D \frac{\partial^2 T}{\partial x^2}, \tag{2.138}$$

for the following input parameters $v_h = 0.05\,\mathrm{nm/fs}, \tau = 44\,\mathrm{fs}, T_0 = 300\,\mathrm{K}$ (initial temperature) and Δt duration of laser pulse $= 0.2\,\tau$ is presented.

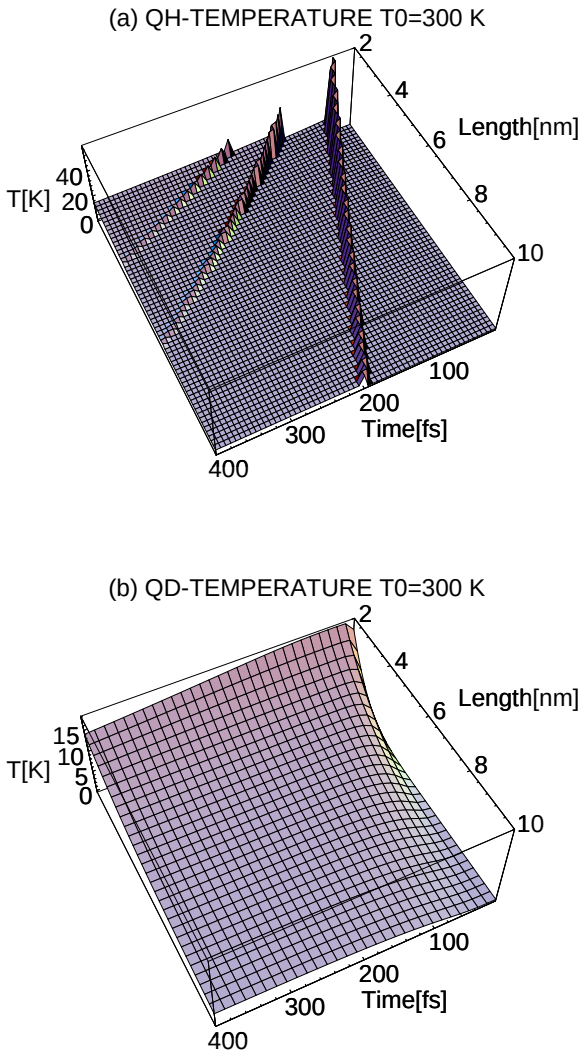

Figure 2.7: (a) The solution of QHT equation (2.138) for the following input parameters $v_h = 5\ 10^{-2}\,\mathrm{nm/fs}, \tau = 44\,\mathrm{fs}, T_0 = 300\,\mathrm{K}$ and $\Delta t = 0.2\tau$. (b) The solution of QPT (2.139) with the same input parameters.

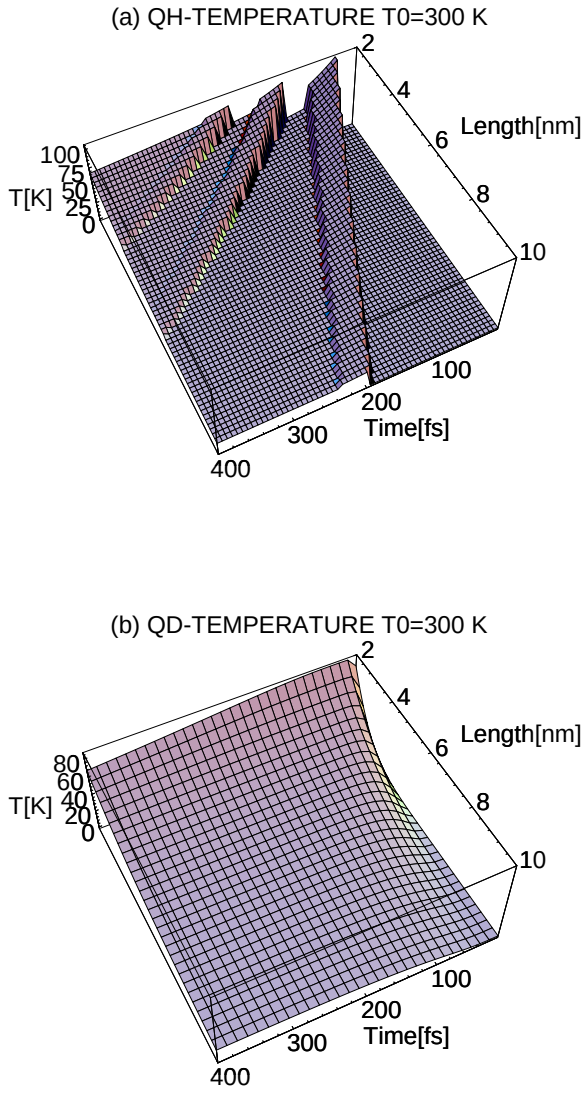

Figure 2.8: (a, b) The same as in Fig. 2.7(a, b) but for $\Delta t = \tau$.

In Fig. 2.7(b) the solution of quantum parabolic heat transport equation (QHT), (Fourier equation)

$$\frac{\partial T}{\partial t} = D\frac{\partial^2 T}{\partial x^2} \tag{2.139}$$

with the same input parameters is presented.

In Figs. 2.8(a, b), the solutions of Eqs. (2.138), (2.139) for the same input parameter but for $\Delta t = \tau$ are presented.

From the analysis of the solutions of hyperbolic and parabolic quantum heat transport equation, the following conclusions can be drawn. In the case of QHT equation the thermal wave dominates the heat transport for $\Delta t = 0.2\ \tau,\ \tau$. The finite value of v_h involves the delay time for the response of the molecular system on the initial temperature change. In the case of QPT, instantaneous diffusion heat transport is observed. From the technological point of view, the strong localization of thermal energy in the front of thermal wave is very important.

2.7 Electron thermal relaxation in metallic nanoparticles

Clusters and aggregates of atoms in the nanometer size (currently called nanoparticles) are systems intermediate in several respects, between simple molecules and bulk materials and have been objects of intensive work [2.34]–[2.36]. The main motivation for the growing interest in these systems is related to the possibility of tailoring, to a considerable extent, their physical behavior on the basis of the size [2.37, 2.38].

In paper [2.34], the novel experimental approach to investigate the dif-

ferent mechanism leading to the electron thermalization in nanoparticles was presented. The femtosecond pump-probe measurements on gallium nanoparticles in both the liquid and solid phases was performed. The samples were prepared by evaporation – condensation of high purity gallium in ultrahigh vacuum on sapphire substrates. The nanoparticle shape was of a truncated sphere. The measurements were performed on three gallium samples with radii $r = 5$ nm, 7nm and 9 nm. Transient transmissivity and reflectivity measurements were performed by using a standard pump-probe configuration. The laser system consists of a Ti: sapphire laser with chirped pulse amplification which provides pulses of 150 fs duration at 780 nm with an energy up to 750 μJ at 1 kHz repetition rate.

The main results of the paper [2.34] are: (i) the temporal behavior of the electron energy relaxation is similar in both phases, (ii) the time constant for thermal relaxation is of the order 600 – 1600 fs.

In this paper, we investigate the thermal relaxation phenomena in the nanoparticles in the frame of quantum heat transport equation formulated in papers [2.39, 2.40]. In paper [2.39], the thermal inertia of materials heated with laser pulses faster than the characteristic relaxation time was investigated. It was shown, that in the case of the ultrashort laser pulses the hyperbolic heat conduction (HHC) must be used. For Ga nanoparticles the mean free path of the electron is larger than the maximum radius of the nanoparticles [2.34]. Moreover, the mean free path is of the order of the de Broglie wave length. In that case, the classical hyperbolic heat conduction equation (HHC) must be replaced by quantum hyperbolic heat transport equation (QHT) (2.20)

$$\tau^e \frac{\partial^2 T^e}{\partial t^2} + \frac{\partial T^e}{\partial t} = \frac{\hbar}{m_e} \nabla^2 T^e, \tag{2.140}$$

where T^e denotes the temperature of the electron gas in nanoparticle, τ^e is the relaxation time and m_e denotes the electron mass. The relaxation time τ^e is defined as

$$\tau^e = \frac{\hbar}{m_e v_h^2}, \tag{2.141}$$

where v_h is the thermal pulse propagation velocity

$$v_h = \frac{1}{\sqrt{3}}\alpha c. \tag{2.142}$$

In formula (2.142) α is the fine-structure constant, $\alpha = e^2/\hbar c$ and c denotes the light velocity in vacuum. Both parameters τ^e and v_h completely characterize the thermal energy transport on the atomic scale and can be named as "*atomic relaxation time*" and *"atomic" heat velocity.*

Both τ^e and v_h are build up from constant of Nature, $e, \hbar, m_e, c$. Moreover, on the atomic scale there is no shorter time period than τ_e and smaller velocity build from constant of the Nature. In consequence, one can name τ^e and v_h as *elementary relaxation time* and *elementary velocity*, which characterize heat transport in the elementary building block of matter, the atom.

In the following, starting with elementary τ^e and v_h, we intend to describe thermal relaxation processes in nanoparticles which consist of the N atoms (molecules) each with elementary τ^e and v_h. To that aim, we use the Pauli-Heisenberg inequality [2.41]

$$\Delta r \Delta p \geq N^{\frac{1}{3}}\hbar, \tag{2.143}$$

where r denotes characteristic dimension of the nanoparticle and p is the momentum of energy carriers. The Pauli-Heisenberg inequality expresses the basic property of the N-fermionic system. In fact, compared to the

standard Heisenberg inequality

$$\Delta r \Delta p \geq \hbar, \tag{2.144}$$

we notice that, in this case the presence of the large number of identical fermions forces the system either to become spatially more extended for fixed typical momentum dispension, or to increase its typical momentum dispension for a fixed typical spatial extension. We could also say that for a fermionic system in its ground state, the average energy per particle increases with the density of the system.

A picturesque way of interpreting the Pauli-Heisenberg inequality is to compare Eq. (2.143) with Eq. (2.144) and to think of the quantity on the right hand side of it as the "effective fermionic Planck constant"

$$h^f(N) = N^{\frac{1}{3}}\hbar. \tag{2.145}$$

We could also say that antisymmetrization, which typifies fermionic amplitudes amplifies those quantum effects which are affected by Heisenberg inequality. It does so to a degree, what becomes significant if the number N of identical fermions is large [2.41].

According to formula 2.145, we recalculate the relaxation time τ, formula (2.141) and thermal velocity v_h, formula (2.142) for nanoparticle consisting N fermions

$$\hbar \to \hbar^f(N) = N^{\frac{1}{3}}\hbar \tag{2.146}$$

and obtain

$$v_h^f = \frac{e^2}{\hbar^f(N)} = \frac{1}{N^{\frac{1}{3}}} v_h, \tag{2.147}$$

$$\tau^f = \frac{\hbar^f}{m(v_h^f)^2} = N\tau. \tag{2.148}$$

Number N particles in nanoparticle (sphere with radius r) can be calculated according to the formula (we assume that density of nanoparticle does not differ too much from bulk material)

$$N = \frac{\frac{4\pi}{3} r^3 \rho A Z}{\mu} \tag{2.149}$$

and for spherical with semiaxes a, b, c

$$N = \frac{\frac{4\pi}{3} abc \rho A Z}{\mu}, \tag{2.150}$$

where ρ is the density of the nanoparticle, A is the Avogardo number, μ is the molecular mass of particles in grams and Z is the number of the valence electrons.

With formulas (2.147) and (2.148), we calculated de Broglie wave length λ_B^f and mean free path λ_{mfp}^f for nanoparticles

$$\lambda_B^f = \frac{\hbar^f}{m v_{th}^f} = N^{\frac{2}{3}} \lambda_B, \tag{2.151}$$

$$\lambda_{mfp}^f = v_{th}^f \tau_{th}^f = N^{\frac{2}{3}} \lambda_{mfp}, \tag{2.152}$$

where λ_B and λ_{mfp} denote the de Broglie wave length and mean free path for heat carriers in nanoparticles.

In the following, we will study the thermal relaxation process in gallium particles [2.34]. For Ga, density $\rho = 5.9$ g/cm^3 and $\mu = 70$ g. In Fig. 2.9 we present the calculation of the relaxation time τ^f formula (2.148) and thermal wave velocity v_{th}^f (2.147) for Ga nanoparticles, when axes $a = b = r$ and $c = dr, d \leq 1$ (symmetric spheroid). In that case

$$N = \frac{\frac{4\pi}{3} d r^3 \rho A Z}{\mu}. \tag{2.153}$$

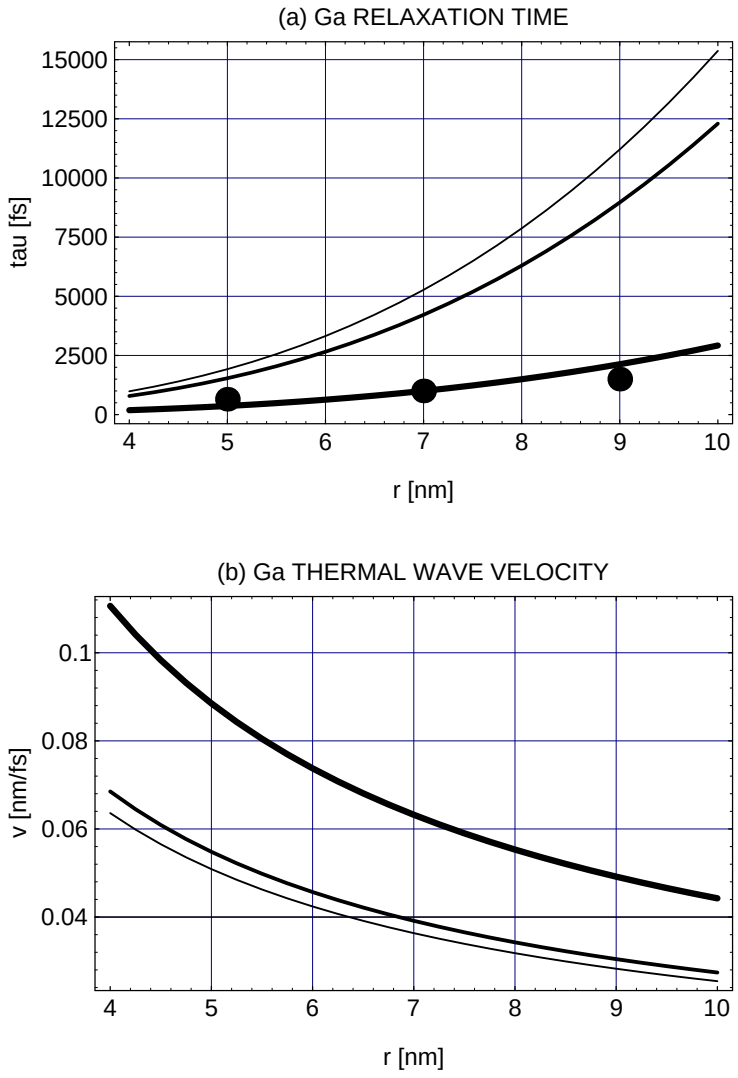

Figure 2.9: (a) Experimentally determined relaxation times for Ga nanoparticles [2.34]. Curves denote the calculated relaxation times for $d = 0.19$ (—), $d = 0.8$ (—) and $d = 1$ (—). (b) Calculated thermal wave velocities for nanoparticles with $d = 0.19$(—), $d = 0.8$ (—) and $d = 1$ (—).

Fig. 2.9(a) shows the calculations of the τ^f for $d = 0.19, 0.8$ (spheroid shape) and for $d = 1$ (sphere). As can be seen the fairly good agreement is obtained for spheroid with semiaxes $a = b = r$ and $c = 0.19r$. Fig. 2.9(b) shows the calculated velocities of the thermal waves. The reduction of the thermal wave velocity is caused by electron-electron scattering and reflecting of the thermal wave from the surface of the nanoparticles.

2.8 Velocity spectra of the relativistic electrons

The implementation of chirped pulse amplification (CPA) systems in high power lasers has made available new intensity regimes previously inaccessible in the laboratory. At intensities of $10^{18}\,\mathrm{W\,cm^{-2}}$ the electron oscillatory velocity for $1\,\mu$m radiation becomes relativistic and the radiation pressure reaches 300 Mbar. Interesting, new physical phenomena have been predicted in this regime, such as emission high energetic electrons, ions and MeV x-ray.

In the physical picture of a relativistic gas, we think of the *world lines* of the particles as a discrete complex. For a particle with mass m the four momentum relationships M_r fulfills the relations $M_r M_r = -m^2$ for massive particles and $M_r M_r = 0$ for photons. If η is the number of world lines for particles which cross the space volume element $dS = dx_1 dx_2 dx_3$ and momentum volume $d\Omega = dM_1 dM_2 dM_3$, then η equals [2.42]

$$\eta = N\, dS\, d\Omega, \tag{2.154}$$

N being independent of the sizes of dS and $d\Omega$. We call N the relativistic

distribution function. For massive particles with mass m, the four momentum components are related to three velocity component u_S by the equations

$$M_S = \frac{m\gamma u_S}{c}, \qquad \gamma = \left(1 - \frac{u^2}{c^2}\right)^{-1/2}, \tag{2.155}$$

where c is the velocity of light. The relation between $d\Omega$ and $dU = du_1 du_2 du_3$ reads

$$d\Omega = \frac{m^3\gamma^5}{c^3}\, dU. \tag{2.156}$$

In the rest frame of the relativistic gas container, the distribution function N has the form

$$N = \frac{N_0 T^{-1}}{4\pi m^2 K_2(\frac{m}{T})} \exp\left[-\frac{m\gamma}{T}\right]. \tag{2.157}$$

In formula (2.157), N_0 is the *numerical density* (number of particles per volume in the rest frame of the container), T is the relativistic gas temperature (in energy units) and $K_2(m/T)$ is the modified Bessel function of the second kind. From formulas (2.154) and (2.157), the number of particles in $dSdU$, in the rest frame of gas is

$$d\eta = \frac{N_0 m T^{-1}}{4\pi K_2(\frac{m}{T})}\, c^{-3}\gamma^5 \exp\left[-m\gamma T^{-1}\right]\, dSdU. \tag{2.158}$$

The number of particles in the volume dS in the range $(u, u+du)$ is obtained by equating $4\pi u^2\, dU$ to dU and is therefore

$$d\eta = N_0\, \frac{mT^{-1}}{K_2(\frac{m}{T})}\, c^{-3}\gamma^5 u^2 \exp\left[-m\gamma T^{-1}\right]\, dSdU. \tag{2.159}$$

If we define $\beta = u/c$, then formula (2.159) reads

$$d\eta = \frac{N_0 m T^{-1}}{K_2(\frac{m}{T})}\, \gamma^5\beta^2 \exp\left[-m\gamma T^{-1}\right]\, dSd\beta, \tag{2.160}$$

and describes the number of particles in the volume dS in the range $(\beta, \beta + d\beta)$.

For low temperatures, i.e., for $mT^{-1} \gg 1$, $K_2(m/T)$ has an approximate form

$$K_2(x) \cong \sqrt{\frac{\pi}{2x}} e^{-x}; \qquad x = mT^{-1}. \tag{2.161}$$

Considering formula (2.161), Eq. (2.160) reads

$$d\eta = \frac{4\pi}{\sqrt{8\pi^3}} N_0 \left(\frac{mc^2}{T}\right)^{3/2} \gamma^5 \beta^2 \exp\left[-\frac{mc^2(\gamma - 1)}{T}\right] d\beta, \tag{2.162}$$

where $E = mc^2(\gamma - 1)$ is the kinetic energy of the particle with mass m. Formula (2.162) is the relativistic analog of the Maxwell formula for non-relativistic particles, i.e. for particles with $T \ll mc^2$.

Since the exponential falls off rapidly with increasing T, u/c is small for vast majority of the particles and for them we may replace γ by 1 and E by nonrelativistic kinetic energy $E \sim 1/2mu^2$; then (2.162) reads

$$d\eta = \frac{4\pi}{\sqrt{8\pi^3}} N_0 \left(\frac{mc^2}{T}\right)^{3/2} \beta^2 \exp\left[-\frac{m\beta^2}{2T}\right] d\beta. \tag{2.163}$$

This is precisely a Maxwellian distribution and so we are assured that T is, in fact, the absolute temperature in the ordinary sense.

Note, however, that we obtained (2.163) from (2.162) merely in order to make contact with Maxwellian theory; formula (2.162) is a much better expression relativistically, because it corresponds to the range $(0, c)$ for u, whereas (2.163) corresponds to the range $(0, \infty)$. On account of this difference in ranges, it is not quite correct to say that for low temperatures the relativistic theory is reduced to the Maxwellian case. In the case of high temperatures $T \sim mc^2$, we derive from formula (2.160)

$$d\eta = \frac{N_0}{2} \left(\frac{mc^2}{T}\right)^3 \gamma^5 \beta^2 \exp\left[-\frac{m\gamma c^2}{T}\right] dS d\beta, \tag{2.164}$$

for $K_2(x) \sim 2x^{-2}$ when x is small.

Recent advances in high intensity sub-pico-seconds laser technology enables new regimes of hot dense matter to be investigated [2.43]–[2.48]. Dense high temperature plasmas are typically studied by x-ray spectroscopy. Time of flight (TOF) measurements have been used to determine suprathermal electron temperatures of plasmas produced by lasers with pulse length 1 ps [2.49] to 1 ns [2.50]. Spatially and temporally averaged x-ray spectra of sub-ps laser produced plasmas have shown electron temperatures of a few hundred eV [2.51]. Spatially and temporally localized measurements of 500 eV electron temperatures were reported in [2.52].

For electrons with temperatures of the order of hundred eV (10^6 K), the quantum heat transport equation (QHT)

$$\tau \frac{\partial^2 T}{\partial t^2} + \frac{\partial T}{\partial t} = \frac{\hbar}{m} \nabla^2 T \tag{2.165}$$

must be used for the description of the transport phenomena.

The solution of the QHT shows the temperature oscillations for the time period of the few relaxation times [2.25]. The predicted oscillations propagates as a thermal wave with velocity $v_{th} \sim \alpha c$ where α is the fine structure constant. The temperature oscillations as well as the thermal waves are a true relativistic effect. For a nonrelativistic transport description, c is infinite and relaxation time $\tau = 0$. In that case the quantum heat transport is the parabolic equation (QPT), viz

$$\frac{\partial T}{\partial t} = \frac{\hbar}{m} \frac{\partial^2 T}{\partial t^2}, \tag{2.166}$$

and oscillations as well as the thermal waves are completely attenuated. The relativistic oscillations of the temperature strongly influence the velocity of the emitted particles.

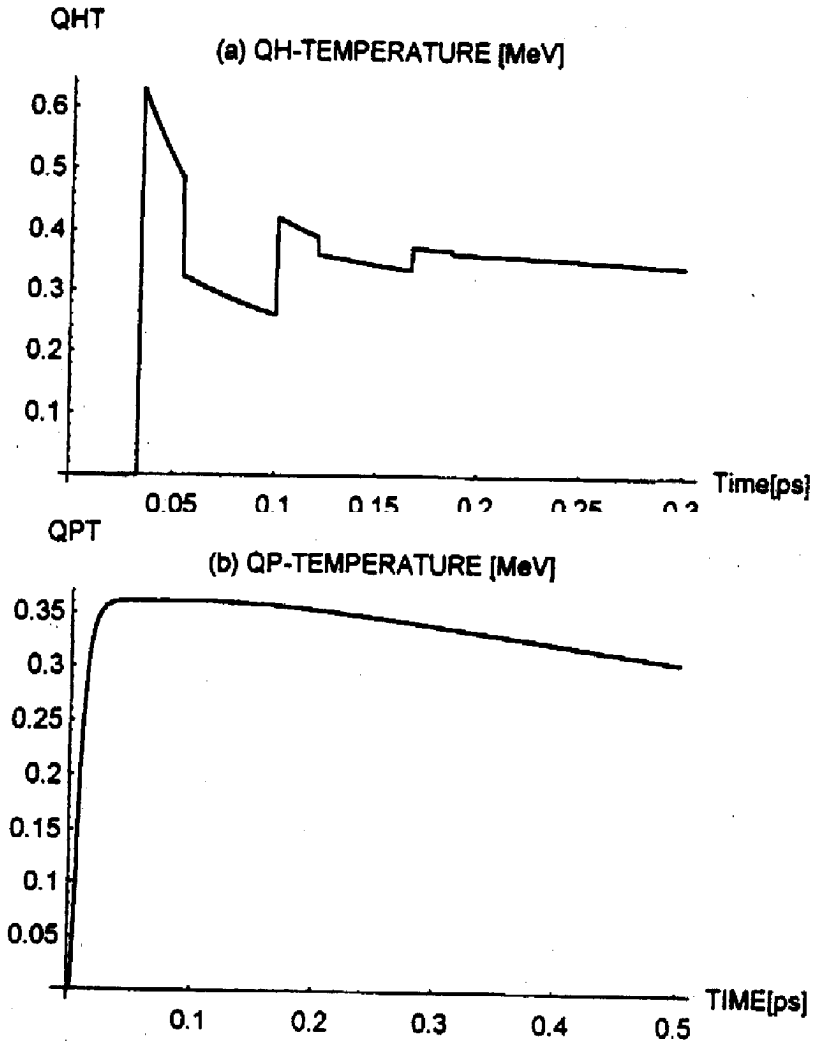

Figure 2.10: (a) The solution of the QHT equation (2.165) "QH-Temperature" for $v_h = 1.5\,10^2\,\mathrm{nm/ps}$ relaxation time 20 fs, Δt = pulse duration = τ, energy density $10^{16}\,\mathrm{W\,cm^{-2}}$. (b) The solution of QPT equation (2.166) "QP-Temperature" for the same value of v_h, τ and energy density.

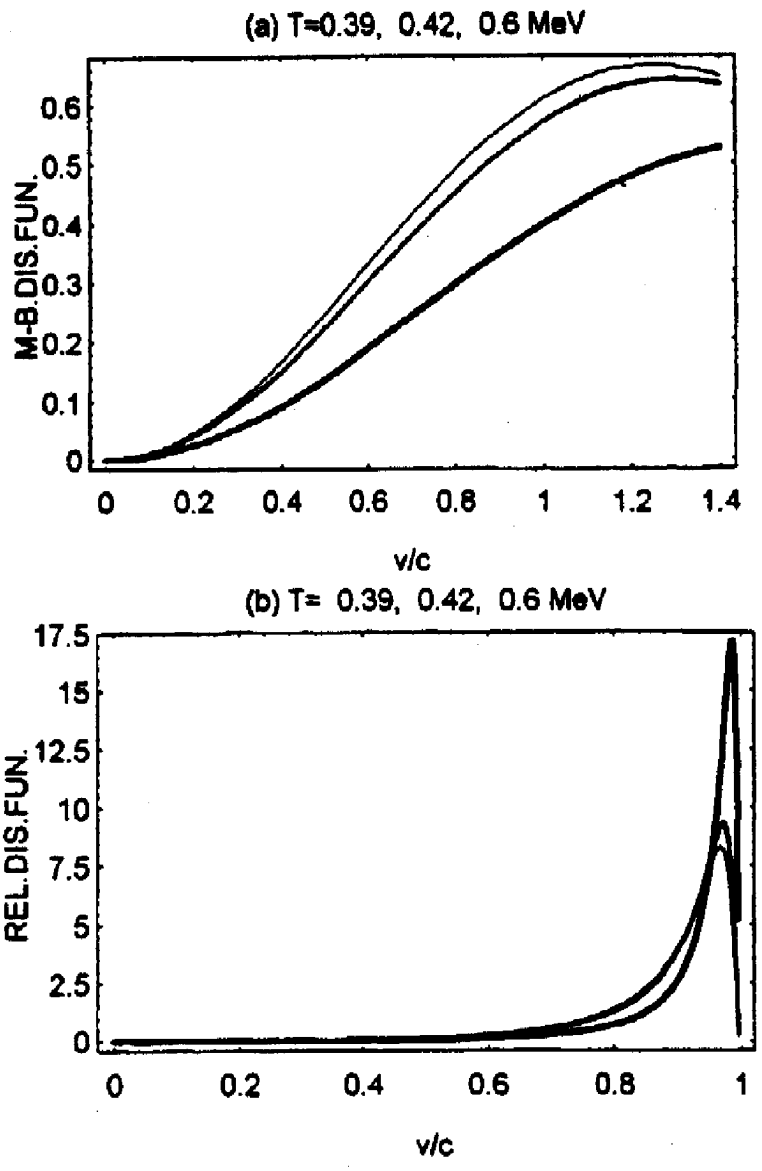

Figure 2.11: (a) The Maxwellian distribution function (2.163) for $t = 3.3\,10^{-2}$ ps (—), $t = 10^{-1}$ ps (—) and $1.7\,10^{-1}$ ps (—). (b) The relativistic distribution function (2.160) for the same values of time.

Subsequently the electron spectra emitted after irradiation of 5 nm Au film will be calculated. The following input parameters are assumed: initial energy density $10^{16}\,\mathrm{W/cm^2}$ and 15% of the light absorbed. The thermal wave velocity $v_h = 0.15\,\mu\mathrm{m\,ps^{-1}}$ [2.12] and relaxation time $\tau = 20\,\mathrm{fs}$.

Fig. 2.10(a) shows the solution of QHT equation (2.165) and Fig. 2.10(b) the solution of QPT. In Fig. 2.11 the velocity spectra of the particles emitted when the temperature is calculated from QHT equation for $t = 3.3\,10^{-2}$ ps, 10^{-1} ps and $1.7\,10^{-1}$ ps. Fig. 2.11(a) shows the velocity spectra calculated from formula (2.163) — Maxwell-Boltzmann distribution function and Fig. 2.11(b) the relativistic distribution function — formula (2.160). The Maxwellian distribution function gives the wrong result for particle spectra when the temperature T lies in the range of electron mass ($m_e = 0.511\,\mathrm{MeV}$) as the one obtains $u/c > 1$ for emitted electrons. On the other hand, the relativistic distribution function (2.160) shows the localization of the electron velocity in the vicinity $u \to c$. Moreover, the velocity spectra oscillate as the function of time.

2.9 Ballistic and diffusion thermal pulse propagation in the attosecond time domain

For the first few decades after the invention of the laser in 1960, the record for the shortest laser pulses fell by a factor of two every three years or so. Each development provided new insight into the microworld of atoms, molecules and solids. In 1986, however, this trend essentially stopped when the pulse length reached 6 femtoseconds. For visible light this corresponds

to just three oscillations of the electromagnetic field in the laser.

Since the mid - 1980's, there have been many advances in the laser science, but the minimum pulse duration has decreased only slightly. In order to break significantly the current record, a 4.5 femtosecond pulse from the laser with a wavelength of 800 nanometers, a completely different approach is needed. Physicists at the Foundation for Research and Technology – Hellas (FORTH) on Crete have recently demonstrated one such approach [2.53].

One place to look for inspiration is the method currently used to measure femtosecond pulses. Basically, we ask the pulse to measure itself. Practically this means that we take the pulse, split it in two, delay the replicas in the arms of an interferometer by amounts that we can control, and then direct each replica onto a material with nonlinear optical properties. If the two arms have exactly the same length, the pulses arrive at the same time and their intensity is higher than if the path are unbalanced and one pulse arrives before the other. Observing the nonlinear response allows us to measure the extent of the overlap as we change the difference between the two path lengths, Δx. The pulse duration τ, is simply $\tau = \Delta x/c$.

The FORTH group produced replica pulses by splitting the pulse when it is easy to do so – before the high harmonics are produced. And they use the ionizing gas which produces the high harmonics for a second purpose. It also serves as the nonlinear medium needed to measure the length of the pulses in the train. In a result, an isolated less than 100 as (1 as = 1 attosecond = 10^{-18} s) sharp feature, indicative for the production of the trains of sub-fs XUV pulses, is clearly observable in the resulting temporal trace [2.53].

In the paper [2.53], the time structure with the line width of the order of 100 as was obtained. This debut of attosecond science opens new avenues

for investigating atomic and molecular structures. As was shown in papers [2.54] and [2.55] for these two levels of complexity the relaxation times are of the order of $\tau_a \sim 70$ attosecond [2.54] and $\tau_m \sim 10^3$ attosecond [2.55]. In both cases the line width is of the order of/or longer than the relaxation times. For these circumstances the parabolic Fourier equation cannot be used [2.54, 2.55]. Instead, the new equation, QHT is the valid equation. The QHT can be written as

$$\frac{1}{v^2}\frac{\partial^2 T}{\partial t^2} + \frac{m}{\hbar}\frac{\partial T}{\partial t} = \frac{\partial^2 T}{\partial x^2}. \tag{2.167}$$

In Eq. (2.167) v denotes the velocity of the thermal pulse propagation, m is the heat carrier mass. In this paper, we will consider the Fermi gas of electrons and $m = 0.511$ MeV, $v = \frac{1}{\sqrt{3}}\alpha c$, where α is the electromagnetic fine-structure constant, $c =$ light velocity. The Cauchy initial condition for Eq. (2.167) can be written as

$$T(x,0) = 0, \qquad T(0,t) = f(t). \tag{2.168}$$

For initial conditions (2.168) the solution of Eq. (2.167) has the form [2.27]

$$\begin{aligned} T(x,t) \;=\; & \left\{ f\left(t - \frac{x}{v}\right) e^{-\frac{\rho x}{v}} \right. \\ & \left. + \frac{\sigma x}{v}\int_{\frac{x}{v}}^{t} f(t-y) e^{-y\rho} \frac{I_1[\sigma(y^2 - \frac{x^2}{v^2})^{\frac{1}{2}}]}{(y^2 - \frac{x^2}{v^2})^{\frac{1}{2}}}\, dy \right\} H(t - \frac{x}{v}). \end{aligned} \tag{2.169}$$

In formula (2.169) $\rho = \sigma = \frac{1}{2\tau}$, $\tau = \frac{\hbar}{mv^2}$ and $H(t - \frac{x}{v})$ is the UnitStep function:

$$\begin{aligned} H(t - \frac{x}{v}) &= 1 \qquad \text{for} \qquad t \geq \frac{x}{v}, \\ H(t - \frac{x}{v}) &= 0 \qquad \text{for} \qquad t < \frac{x}{v}. \end{aligned} \tag{2.170}$$

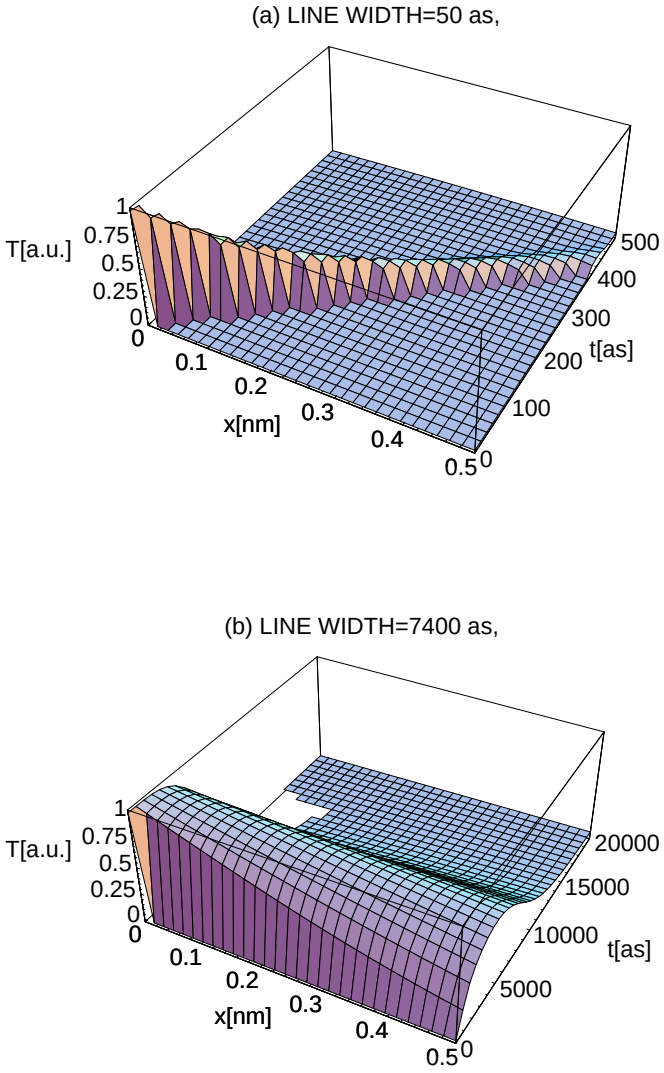

Figure 2.12: (a) The solution of QHT (Eq.2.169) for $t_s = 50$ as. (b) The solution of QHT for $t_s = 7400$ as.

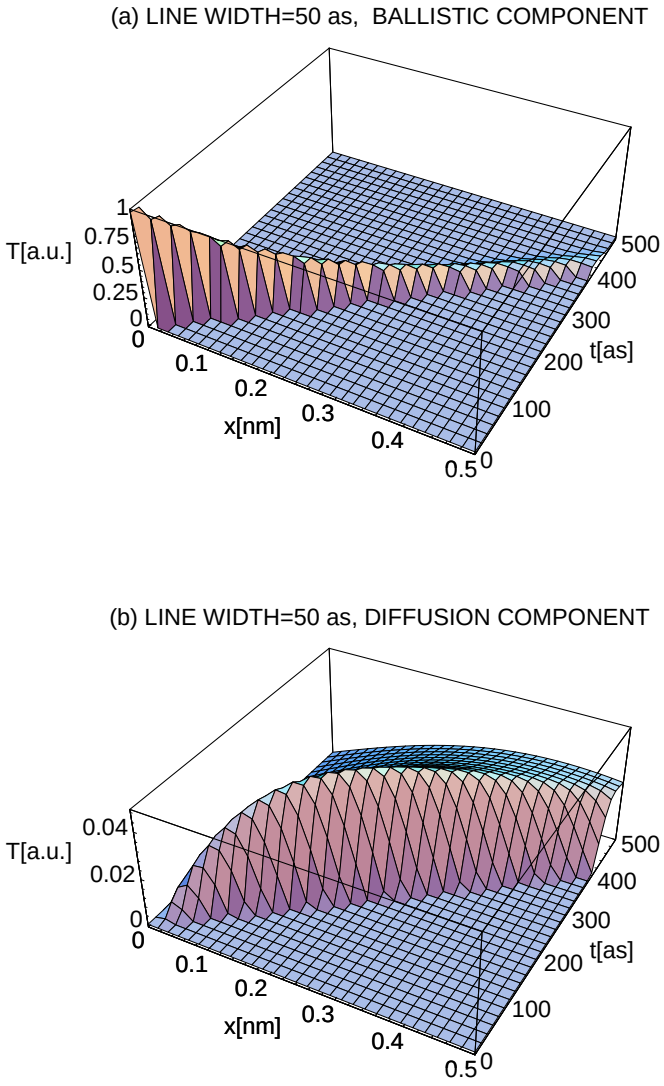

Figure 2.13: (a) The ballistic component of the heat pulse for $t_s = 50$ as. (b) The diffusion component for $t_s = 50$ as.

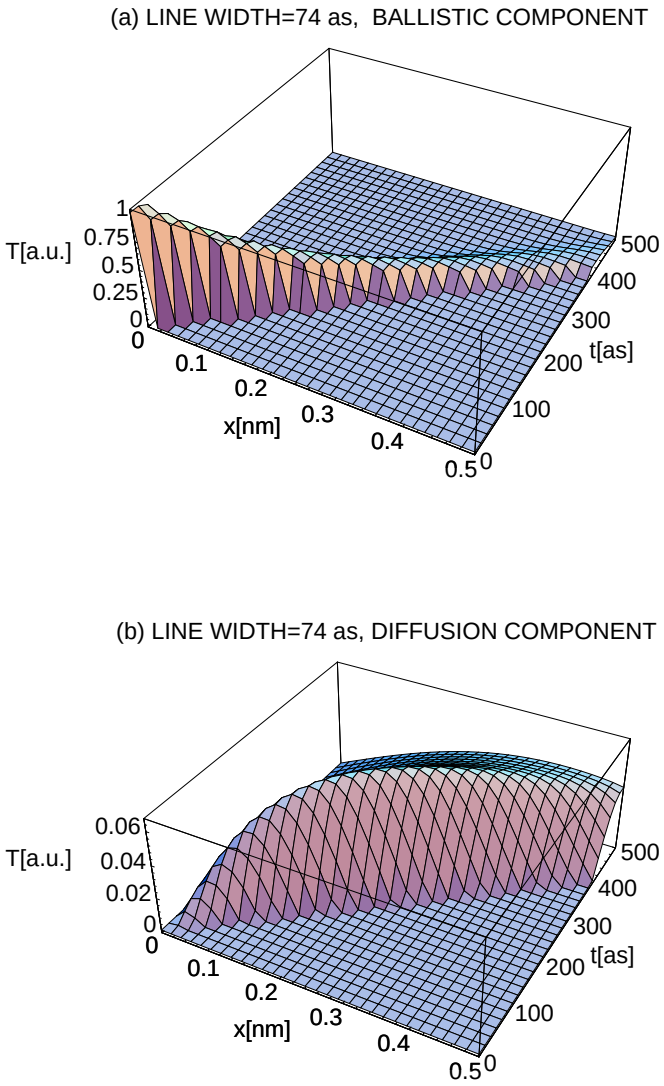

Figure 2.14: (a), (b) The same as in Fig. 2.13 but for $t_s = 74$ as.

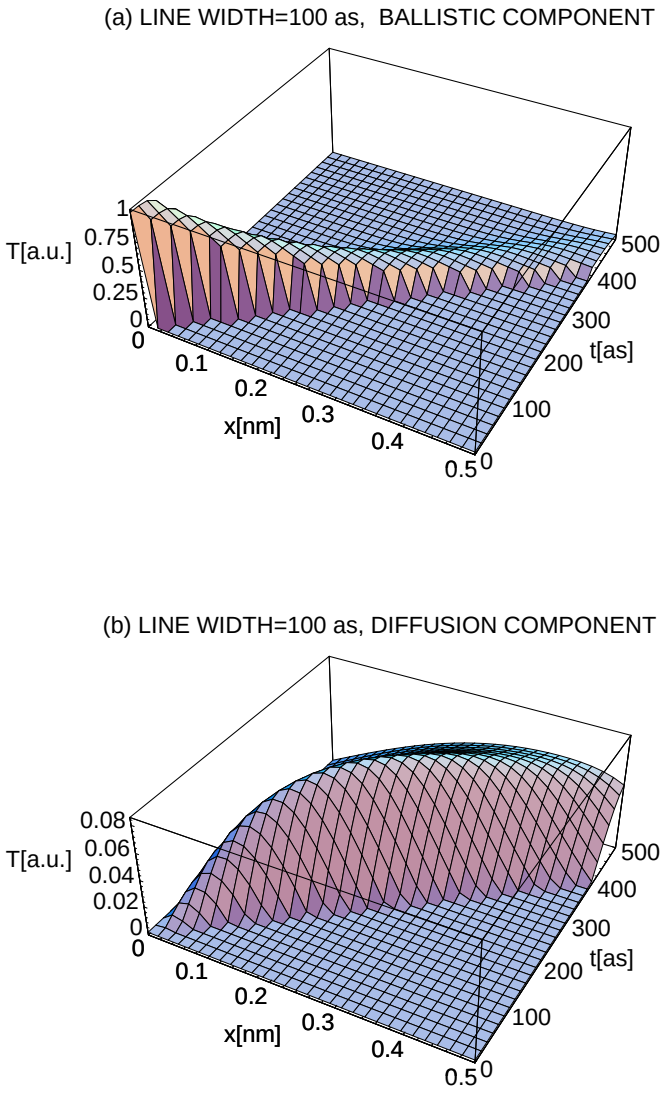

Figure 2.15: (a), (b) The same as in Fig.2.13 but for $t_s = 100$ as.

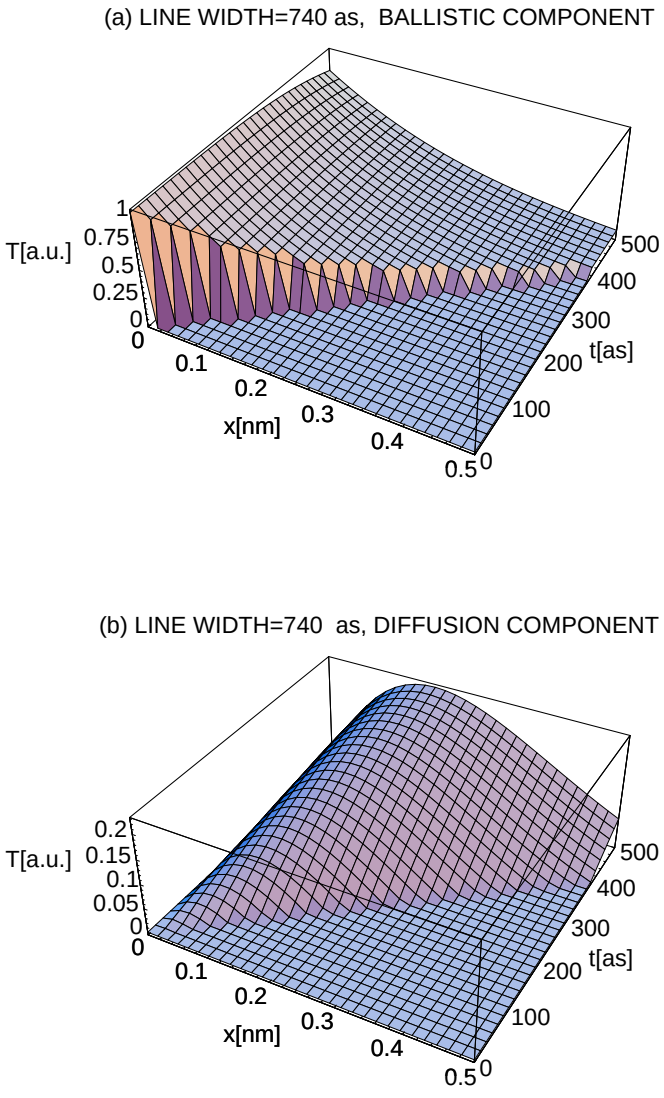

Figure 2.16: (a), (b) The same as in Fig. 2.13 but for $t_s = 740$ as.

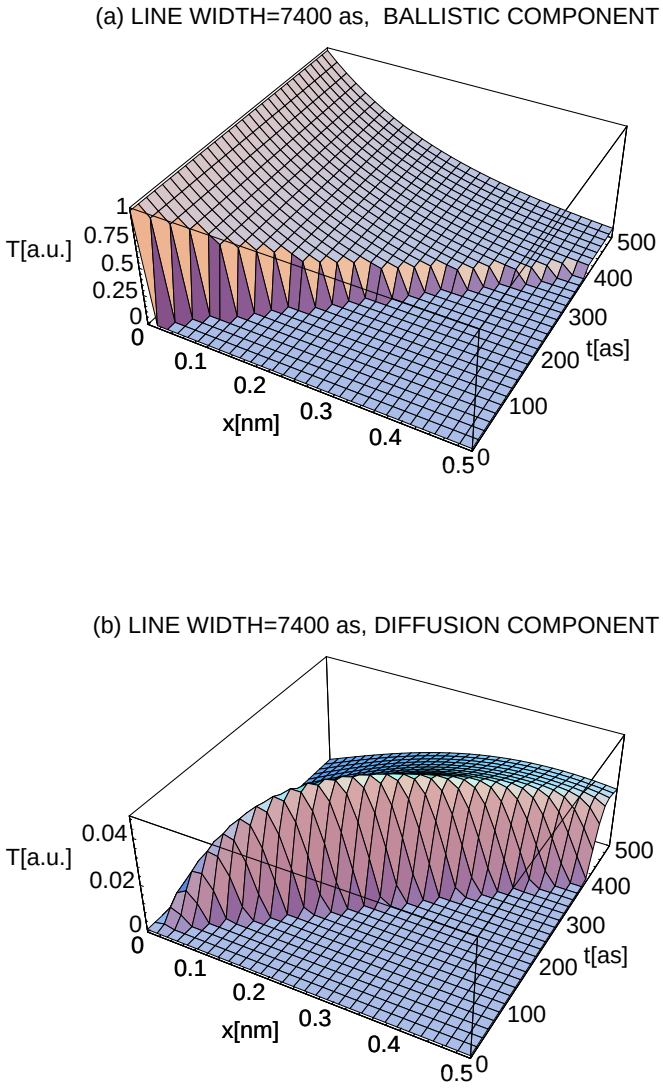

Figure 2.17: (a), (b) The same as in Fig. 2.13 but for $t_s = 7400$ as.

As can be seen from formula (2.169), the temperature field $T(x,t)$ has two components, $T_B(x,t)$–ballistic and $T_D(x,t)$–diffusion, i.e.,

$$\begin{aligned} T_B &= f(t-\frac{x}{v})e^{-\frac{\rho x}{v}}H(t-\frac{x}{v}), \\ T_D &= \left\{\frac{\sigma x}{v}\int_{\frac{x}{v}}^{t} f(t-y)e^{-y\rho}\frac{I_1[\sigma(y^2-\frac{x^2}{v^2})^{\frac{1}{2}}]}{(y^2-\frac{x^2}{v^2})^{\frac{1}{2}}}dy\right\}H(t-\frac{x}{v}). \end{aligned} \quad (2.171)$$

In the Figs. 2.12–2.17, the solution of the Eq. (2.169) for the initial condition (2.168) with [2.32]

$$f(t) = Sech^2\left[\frac{t}{t_s}\right] \quad (2.172)$$

are presented. The numerical integration in the formula (2.169) was performed with the *Mathematica* code, for $t_s = 50,\ 74,\ 100,\ 740$ and 7400 as. In Fig. 2.12 the solution of Eq. (2.169) for $t_s = 50$ as (Fig. 2.12(a)) and $t_s = 7400$ as (Fig. 2.12(b)) is presented. The line width $t_s = 50$ as is smaller than the relaxation time $\tau = 74$ as and $t_s = 7400 = 100\tau_s$. The change of the structure of the solutions is evidently seen. Figs. 2.13–2.17 represent the analysis of the heat pulse according to formula (2.171). The ballistic (Figs. 2.13(a) to 2.17(a)) and diffusion components (Figs. 2.13(b) to 2.17(b)) have quite different shapes.

The results presented in Figs. 2.12–2.17 describe the heat transport on the atomic scale ($x \sim 0.5$ nm). For times of the order of the atomic relaxation time (ballistic propagation), the heat pulse preserves its shape and only the amplitude is diminished due to scattering. On the other hand, for the longer time periods a new structure develops. Multiple scatterings distort the shapes of the initial pulse. One can says that for $t_s \gg \tau$ the information contained in the initial pulse is lost as the time $\to \infty$.

2.10 The polarization of the electrons emitted after ultrashort laser pulse interaction with spin active solids

Let us consider the quantum heat transport equation for dissipative medium with potential V (2.84)

$$\frac{1}{v^2}\frac{\partial^2 T}{\partial t^2}+\frac{m}{\hbar}\frac{\partial T}{\partial t}+\frac{2Vm}{\hbar^2}T=\frac{\partial^2 T}{\partial x^2}. \tag{2.173}$$

In Eq. (2.173), v denotes the velocity of heat propagation, m is the mass of heat carrier and T denotes the temperature. For quantum heat transport equation (2.173), we seek solution in the form

$$T(x,t)=e^{-\frac{t}{2\tau}}u(x,t), \tag{2.174}$$

where τ denotes the characteristic relaxation time

$$\tau=\frac{\hbar}{mv^2}. \tag{2.175}$$

After substitution of Eq. (2.174) into Eq. (2.173), one obtains

$$\frac{\partial^2 u(x,t)}{\partial t^2}=v^2\frac{\partial^2 u}{\partial x^2}+b^2u(x,t), \tag{2.176}$$

where

$$b=\sqrt{\left(\frac{mv^2}{2\hbar}\right)^2-\frac{2Vmv^2}{\hbar^2}}. \tag{2.177}$$

For particles with spin (e. g., electrons), potential V will contain the term describing the spin-orbit interaction. In that case, potential V equals

$$V(r)=V_{\text{central}}(r)+V_{ls}(r)\frac{<\boldsymbol{ls}>}{\hbar^2}, \tag{2.178}$$

where $V_{\rm central}(r)$ denotes the potential part which does not depend on spin. The combination of the orbital angular momentum $\boldsymbol{l}$ and electron spin $\boldsymbol{s}$ leads to a total angular momentum $j\hbar = l\hbar \pm \hbar/2$ and hence to the expectation values:

$$< \boldsymbol{ls} >= \begin{cases} \frac{l}{2} & \text{for} \quad j = l + \frac{1}{2} \\ -\frac{(l+1)}{2} & \text{for} \quad j = l - \frac{1}{2} \end{cases} \tag{2.179}$$

Substituting formula (2.179) to formula (2.178), one obtains the splitting for potential V:

$$\begin{aligned} V^+(r) &= V_{\rm central}(r) + V_{ls}(r)\frac{l}{2} \qquad \text{if} \qquad j = l + \frac{l}{2}, \\ V^-(r) &= V_{\rm central}(r) - V_{ls}(r)\frac{(l+1)}{2} \qquad \text{if} \qquad j = l - \frac{1}{2} \end{aligned} \tag{2.180}$$

and for parameter b (formula(2.177))

$$\begin{aligned} b^+ &= \sqrt{\left(\frac{mv^2}{2\hbar}\right)^2 - \frac{2V^+mv^2}{\hbar^2}}, \\ b^- &= \sqrt{\left(\frac{mv^2}{2\hbar}\right)^2 - \frac{2V^-mv^2}{\hbar^2}}. \end{aligned} \tag{2.181}$$

One concludes, that existence of the spin-orbit term splits the Eq. (2.176) into two equations:

$$\frac{\partial^2 u^+(x,t)}{\partial t^2} = v^2\frac{\partial^2 u^+(x,t)}{\partial x^2} + (b^+)^2 u^+(x,t), \tag{2.182}$$

$$\frac{\partial^2 u^-(x,t)}{\partial t^2} = v^2\frac{\partial^2 u^-(x,t)}{\partial x^2} + (b^-)^2 u^-(x,t). \tag{2.183}$$

In the following, we will consider the constant potentials: $V_{\rm central}$ and V_{ls}. The general solution of Eqs. (2.182) and (2.183) for Cauchy boundary conditions:

$$u(x,0) = f(x), \qquad \left.\frac{\partial u(x,t)}{\partial t}\right|_{t=0} = F(x)$$

has the form:

$$u^{+,-}(x,t) = \frac{f(x-vt)+f(x+vt)}{2} + \frac{1}{2}\int_{x-vt}^{x+vt} \Phi^{+,-}(x,t,z)dz,$$

where

$$\begin{aligned}\Phi^{+,-}(x,t,z) &= \frac{1}{v}F(z)J_o\left(\frac{b^{+,-}}{v}\sqrt{(z-x)^2-v^2t^2}\right) \\ &\quad + b^{+,-}tf(z)\frac{J_0'\left(\frac{b^{+,-}}{v}\right)\sqrt{(z-x)^2-v^2t^2}}{\sqrt{(z-x)^2-v^2t^2}} \qquad (2.184)\end{aligned}$$

and $J_o(z)$ denotes the Bessel function of the first kind. The interaction of laser beam with solid creates hot electrons with temperatures described by formulas (2.174) and (2.184):

$$\begin{aligned}T^+(x,t) &= e^{-\frac{t}{2\tau}}u^+(x,t), \\ T^-(x,t) &= e^{-\frac{t}{2\tau}}u^-(x,t). \qquad (2.185)\end{aligned}$$

The velocity spectra of the emitted hot electrons are described by formula

$$d\eta^{+,-} = N_0\frac{m(T^{+,-}(x,t))^{-1}}{K_2\left(\frac{m}{T^{+,-}(x,t)}\right)}\gamma^5\beta^2\exp\left[-m\gamma(T^{+,-}(x,t))^{-1}\right]\cdot dVd\beta. \quad (2.186)$$

In formula (2.186) $\beta = v/c, \gamma = 1/\sqrt{1-\beta^2}, N_0$ is the numerical density − initial number of particles per volume in the rest frame of the solid, and $K_2[m/T]$ is the modified Bessel function of the second kind. Formula (2.186) describes the number of particles with temperatures T^+, T^- in the volume dV in the range $(\beta, \beta+d\beta)$.

The particles with temperature T^+ have the total angular momentum $j = l + \frac{1}{2}$ and particles with temperature T^- have the total angular momentum $j = l - 1/2$. One can define the degree of the polarization of the

emitted electrons (after solid irradiation by an energetic laser beam)

$$P(x,t) = \frac{N^+(x,t) - N^-(x,t)}{N^+(x,t) + N^-(x,t)}, \tag{2.187}$$

where

$$N^{+,-} = \frac{d\eta^{+,-}}{dV\ d\beta}.$$

Considering formulas (2.186) and (2.187), one concludes, that existence of the spin-orbit term in potential V (formula(2.178)) creates the polarization of the emitted electrons. For $V_{ls}(r) = 0$, $N^+(x,t) = N^-(x,t)$ and P(x, t)=0.

Bibliography for Chapter 2

[2.1] C. Catteneo, *Atti Sem. Mat. Fis. Univ. Modena* 3, (1948) 3;
C. R. Acad. Sc. (Paris) 247, (1958) 431.

[2.2] A. V. Luikov, *Analytical Heat Diffusion Theory* (Academic Press, Inc., New York, 1968).

[2.3] D. D. Joseph, L. Preziosi, *Rev. Mod. Phys.* 61, (1989) 41;
62, (1990) 375.

[2.4] D. Jou, J. Casas-Vázques, and G. Lebon, *Extended Irreversible Thermodynamics*, (Springer-Verlag, Berlin, 1993).

[2.5] M. Kozłowski, *Nucl. Phys.* A492, (1989) 285.

[2.6] E. Nelson, *Phys. Rev.* 150, (1966) 1079.

[2.7] D. H. Perkins, *Introduction to High Energy Physics*, (Addison-Wesley, Menlo Park, California, 1987).

[2.8] M. Ivanov, P. B. Corkum, T. Zuo, and A. Bandrauk, *Phys. Rev. Lett,* 74, (1995) 2933.

[2.9] J. Marciak-Kozłowska, M. Kozłowski, *Lasers in Engineering* 6, (1997) 141

[2.10] B. B. Mandelbrot, *The Fractal Geometry of Nature* (W. H. Freeman and Company, San Francisco, 1989).

[2.11] L. F. Abbot, M. B. Wise, *Am. J. Phys.* 19, (1981) 37.

[2.12] B. Gaveau, T. Jacobson, M. Kac, and L. S. Schulman, *Phys. Rev. Lett.* 53, (1984) 419.

[2.13] S. C. Tiwari, *Phys. Lett. A* 133, (1988) 279.

[2.14] S. C. Tiwari, *Physics Essays* 2, (1989) 31.

[2.15] T. Jacobson, L. S. Schulman, *J. Phys. A Gen.* 17, (1984) 375.

[2.16] E. Zauderer, *Partial Differential Equations of Applied Mathematics*, (J. Wiley and Sons, New York, 1989).

[2.17] P. Debye, E. Hückl, *Phys. Z.* 24, (1923) 185.

[2.18] R. Balian, *From Microphysics to Macrophysics*, VOL. II, (Springer-Verlag, Berlin, 1992).

[2.19] B. Povh, K. Rith, Ch. Scholz, and F. Zetsche, *Particles and Nuclei*, (Springer-Verlag, Berlin, 1995).

[2.20] T. H. R. Skyrme, *Proc. R. Soc. London, Ser. A* 247, (1958) 260; Ch. Nayak, F. Wilczek, *Phys. Rev. Lett.* 77, (1996) 44.

[2.21] M. D. Perry, G. Mourou, *Science* 264, (1994) 917.

[2.22] T. Ditmire, T. Donnelly, R. W. Falcone, and M. D. Perry, *Phys. Rev. Lett.* 75, (1995) 3122.

[2.23] Y. L. Shao, T. Ditmire, J. W. G. Tisch, E. Springate, J. P. Marangos, and M. M. R. Hutchison, *Phys. Rev. Lett.* 77, (1995) 3343.

[2.24] T. Ditmire, J. W. G. Tisch, E. Springate, M. B. Mason, N. Hay,R. A. Smith, J. P. Marangos, and M. H. R. Hutchison, *Nature* 386, (1997) 54.

[2.25] J. Marciak–Kozłowska, M. Kozłowski, *Lasers in Engineering* 5, (1996) 79.

[2.26] J. Marciak–Kozłowska, M. Kozłowski, *Lasers in Engineering* 6, (1997) 141.

[2.27] H. S. Carslaw, J. C. Jaeger, *Operational Methods in Applied Mathematics*, (Oxford University Press, Oxford, 1953).

[2.28] C. Cohen-Tannoudji, B. Diu, and F. Laloe, *Quantum Mechanics* (J. Wiley and Sons, New York, 1977).

[2.29] B. R. Mottelson, The Study of the Nucleus as a Theme in Contemporary Physics in J. de Boer, E. Dal, O. Ulfbeck, Eds, *The Lesson of Quantum Theory*, (North Holland Physics Publishing, Amsterdam, 1986).

[2.30] J. R. Barker, *Molecular Electronics – Science and Technology*, A. Aviram, Eds. Engineering Foundation, 1989, p. 213

[2.31] J. R. Barker, *Parallel Processing in Neural Systems and Computer*, (edited by R. Eckmiller, G. Hartmann and G. Hauske, North-Holland Physics Publishing, Amsterdam, 1990), p. 519.

[2.32] J.-C. Diels, W. Rudolph, *Ultrashort Laser Pulse Phenomena*, (Academic Press, Inc., San Diego, 1996).

[2.33] Fang Li Zhi, Li Shu Xian, *Creation of the Universe*, (World Scientific, Singapore, 1989).

[2.34] M. Nisoli, S. Stagira, S. De Silvestri, A. Stella, P. Tognini, P. Cheyssac and R. Kofman *Phys. Rev. Lett.* 78, (1997) 3575.

[2.35] U. Bockelmann, Ph. Roussignol, A. Filoramo, W. Heller, G. Abstreiter, K. Brunner, G. Böhm, and G. Weimann *Phys. Rev. Lett.* 76, (1996) 3622.

[2.36] J-Y. Bigot, J.-C. Merle, O. Cregut, and A. Daunois, *Phys. Rev. Lett.* 75, (1995) 4702.

[2.37] R. F. Service, *Science* 271, (1996) 920.

[2.38] C. B. Murray, C. R. Kagan, and M. G. Bawendi, *Science* 270, (1995) 1335.

[2.39] J. Marciak-Kozłowska, M. Kozłowski, *Int. J. of Thermophys.* 17, (1996) 1099.

[2.40] M. Kozłowski, J. Marciak-Kozłowska, *Lasers in Engineering* 7, (1998) 13.

[2.41] J.-M. Lévy-Leblond, F. Balibar, *Quantics*, (North Holland Physics Publishing, Amsterdam, 1990).

[2.42] J. L. Synge, *The Relativistic Gas*, (North Holland, Amsterdam, 1957).

[2.43] D. Strickland, G. Mourou, *Opt. Commun.* 56, (1985) 219.

[2.44] R. M. More et al., *J. Phys. (Paris) Colloq.* 49, (1988) 7.

[2.45] A. Ng. et al., *Phys. Rev.* E51, (1995) 5208.

[2.46] H. M. Milchberg et al., *Phys. Rev. Lett.* 61, (1988) 2364.

[2.47] D. F. Price et al., *Phys. Rev. Lett.* 75, (1995) 252.

[2.48] J. C. Kieffer et al., *Phys. Fluids* B5, (1993) 2676.

[2.49] D. D. Meyerhofer et al., *Phys. Fluids* B5, (1993) 2584.

[2.50] S. J. Gitomer et al., *Phys. Fluids* 29, (1986) 2679.

[2.51] U. Teubner et al., *Phys. Plasmas* 2, (1995) 972.

[2.52] G. Guethein et al., *Phys. Rev. Lett.* 77, (1996) 1055.

[2.53] N. A. Papadogiannis et al., *Phys. Rev. Lett.* 83, (1999) 4289.

[2.54] M. Kozłowski, J. Marciak-Kozłowska, *Lasers in Engineering* 7, (1998) 81.

[2.55] M. Kozłowski, J. Marciak-Kozłowska, *Lasers in Engineering* 9, (1999) 39.

[2.56] D. D. Awschalom, J. M. Kikkawa, *Phys. Today* 52, (1999) 33.

[2.57] M. Kozłowski, J. Marciak-Kozłowska, *Hadronic Journal* 20, (1997) 289.

[2.58] NA44 Collaboration, *Phys. Rev. Lett.* 78, (1997) 2080.

Chapter 3

Causal thermal phenomena in a Planck Era

3.1 The Time Arrow in a Planck Gas

The enigma of Planck era i.e., the event characterized by the Planck time, Planck radius and Planck mass, is very attractive for speculations. In this paragraph, we discuss the new interpretation of the Planck time. We define Planck gas — a gas of massive particles all with masses equal the Planck mass $M_p = (\hbar c/G)^{1/2}$ and relaxation for transport process equals the Planck time $\tau_p = (\hbar G/c^5)^{1/2}$. To the description of a thermal transport process in a Planck gas, we apply the quantum heat transport equation (QHT) derived in Chapter 2. The QHT is the specification of the hyperbolic heat conduction equation HHC [3.1, 3.2] to the quantum limit of heat transport i.e., when the de Broglie wave length λ_B equals the mean free path, λ.

In the following, we will describe the thermal properties of

the Planck gas. To that aim, we use the hyperbolic heat transport equation (HHC) (2.31), (2.32)

$$\frac{\lambda_B}{v_h}\,\frac{\partial^2 T}{\partial t^2}+\frac{\lambda_B}{\lambda}\,\frac{\partial T}{\partial t}=\frac{\hbar}{M_p}\,\nabla^2 T. \tag{3.1}$$

In Eq. (3.1), M_p is the Planck mass, λ_B the de Broglie wavelength, and λ – mean free path for Planck mass. The HHC equation describes the dissipation of the thermal energy induced by a temperature gradient ∇T. Recently, the dissipation processes in the cosmological context (e.g., viscosity) were described in the frame of EIT (Extended Irreversible Thermodynamics) [3.2, 3.3]. With the simple choice for viscous pressure, it is shown that dissipative signals propagate with the light velocity, c [3.2]. Considering that the relaxation time τ is defined as [3.1]

$$\tau=\frac{\hbar}{M_p v_h^2}, \tag{3.2}$$

for thermal wave velocity $v_h=c$, one obtains

$$\tau=\frac{\hbar}{M_p c^2}=\left(\frac{\hbar G}{c^5}\right)^{1/2}=\tau_p, \tag{3.3}$$

i.e., *the relaxation time is equal to the Planck time* τ_p. The gas of massive particles with masses equal to the Planck mass M_p, and relaxation time for transport processes which equals Planck time τ_p we will define as the Planck gas.

According to the result of the paper [3.1], we define the quantum of the thermal energy, the *heaton* for the Planck gas, as

$$\begin{aligned} E_h &= \hbar\omega=\frac{\hbar}{\tau_p}=\left(\frac{\hbar c}{G}\right)^{1/2}c^2=M_p c^2, \\ E_h &= M_p c^2=E^{Planck}=10^{19}\ \mathrm{GeV}. \end{aligned} \tag{3.4}$$

With formula (3.2) and $v_h = c$ we calculate the mean free path, λ, viz.

$$\lambda = v_h \tau_p = c\tau_p = c\left(\frac{\hbar G}{c^5}\right)^{1/2} = \left(\frac{\hbar G}{c^3}\right)^{1/2}. \tag{3.5}$$

From formula (3.5), we conclude that mean free path for a Planck gas is equal to the Planck radius. For a Planck mass, we can calculate the de Broglie wavelength

$$\lambda_B = \frac{\hbar}{M_p v_h} = \frac{\hbar}{M_p c} = \left(\frac{G\hbar}{c^3}\right)^{1/2} = \lambda. \tag{3.6}$$

As it is defined in paper [3.1], Eq. (3.6) describes the quantum limit of heat transport. When formulas (3.5) and (3.6) are substituted in Eq. (3.1), we obtain

$$\tau_p \frac{\partial^2 T}{\partial t^2} + \frac{\partial T}{\partial t} = \frac{\hbar}{M_p} \nabla^2 T. \tag{3.7}$$

Equation (3.7) is the quantum hyperbolic heat transport equation (QHT) for a Planck gas. It can be written as

$$\frac{\partial^2 T}{\partial t^2} + \left(\frac{c^5}{\hbar G}\right)^{1/2} \frac{\partial T}{\partial t} = c^2 \nabla^2 T. \tag{3.8}$$

It is interesting to observe that QHT is the damped wave equation, and gravitation influences the dissipation of the thermal energy. In paper [3.4], P. G. Bergman discussed the conditions for the thermal equilibrium in the presence of the gravitation. As it was shown in that paper, the thermal equilibrium of spatially extended systems is characterized by the "global" temperature and a "local" temperature which is sensitive to the value of the gravitational potential.

On the other hand, Eq. (3.8) describes the correlated random walk of Planck mass. For mean square displacement of random walkers we have

$$< x^2 >= \frac{2\hbar}{M_p} \left[t/\tau_p - \left(1 - e^{-t/\tau_p}\right) \right]. \tag{3.9}$$

From formula (3.6), we conclude that for $t \sim \tau_p$,

$$< x^2 > \cong \frac{\hbar}{M_p \tau} t^2 \tag{3.10}$$

or

$$< x^2 > \cong c^2 t^2, \tag{3.11}$$

and we have thermal wave with velocity c. For $t >> \tau_p$ we have

$$< x^2 > \sim \frac{2\hbar\tau}{M_p} (t/\tau_p - 1) = \frac{2\hbar}{M_p} t = 2D^{Planck} t, \tag{3.12}$$

where

$$D^{Planck} = \frac{\hbar}{M_p} = \left(\frac{\hbar G}{c}\right)^{1/2} \tag{3.13}$$

denotes the diffusion coefficient for a Planck mass.

We can conclude that, for time period of the order of the Planck time, QHT describes the propagation of a thermal wave with velocity equal c and, for a time period much longer than τ_p, QHT describes the diffusion process with diffusion coefficient dependent on the gravitation constant G.

The quantum hyperbolic heat equation (3.7), as a hyperbolic equation sheds light on the time arrow in a Planck gas. When QHT is written in the equivalent form

$$\tau_p \frac{\partial^2 T}{\partial t^2} + \frac{\partial T}{\partial t} = \left(\frac{\hbar G}{c}\right)^{1/2} \nabla^2 T, \tag{3.14}$$

then, for a time period shorter than τ_p, we have preserved time reversal for thermal processes, viz,

$$\frac{1}{c^2} \frac{\partial^2 T}{\partial t^2} = \nabla^2 T, \tag{3.15}$$

and for $t >> \tau_p$,

$$\frac{\partial T}{\partial t} = \left(\frac{\hbar G}{c}\right)^{1/2} \nabla^2 T \tag{3.16}$$

the time reversal symmetry is broken.

These new properties of QHT open up new possibilities for the interpretation of the Planck time. Before τ_p, thermal processes in Planck gas are symmetrical in time. After τ_p the time symmetry is broken. Moreover, it seems that gravitation is activated after τ_p, and it creates an arrow of time (formula (3.16)).

3.2 The smearing out of the thermal initial conditions created in a Planck era

In paper [3.5], the QHT for a Planck gas was discussed. On time scales of Planck time, black holes of the Planck mass spontaneously come into existence. Via the process of Hawking radiation, the black hole can then evaporate back into energy. The characteristic time scale for this to occur happens to be approximately equal to Planck time. Thus, the Universe at $t_p = 10^{-43}$ s in age was filled with a Planck gas.

In the subsequent paper, we develop the generalized quantum heat transport equation for Planck gas, which includes the potential energy term. The condition for conserving the shape of the thermal wave created at the Planck time is developed and investigated.

For a long time the analogy between the Schrödinger equation and the diffusion equation was recognized [3.6]. Let us consider, for the moment, the parabolic heat transport equation for a Planck gas, i.e., Eq. (3.16),

$$\frac{\partial T}{\partial t} = \frac{\hbar}{M_p}\nabla^2 T. \tag{3.17}$$

When the real time $t \to \frac{it}{2}$ and $T \to \Psi$, Eq. (3.17) has the form of the free

Schrödinger equation

$$i\hbar\frac{\partial\Psi}{\partial t} = -\frac{\hbar^2}{2M_p}\nabla^2\Psi. \tag{3.18}$$

The complete Schrödinger equation has the form

$$i\hbar\frac{\partial\Psi}{\partial t} = -\frac{\hbar^2}{2M_p}\nabla^2\Psi + V\Psi, \tag{3.19}$$

where V denotes the potential energy. When we go back to real time $t \to -2it$ and $\Psi \to T$, the new parabolic quantum heat transport is obtained

$$\frac{\partial T}{\partial t} = \frac{\hbar}{M_p}\nabla^2 T - \frac{2V}{\hbar}T. \tag{3.20}$$

Equation (3.20) describes the quantum heat transport in a Planck gas for $\Delta t > t_p$. For heat transport in the period $\Delta t < t_p$, one obtains the generalized hyperbolic heat transport equation [3.5] with potential term added

$$t_p\frac{\partial^2 T}{\partial t^2} + \frac{\partial T}{\partial t} = \frac{\hbar}{M_p}\nabla^2 T - \frac{2V}{\hbar}T. \tag{3.21}$$

Considering that $t_p = \hbar/M_p c^2$ [3.5], Eq. (3.21) can be written as

$$\frac{1}{c^2}\frac{\partial^2 T}{\partial t^2} + \frac{M_p}{\hbar}\frac{\partial T}{\partial t} + \frac{2VM_p}{\hbar^2}T = \nabla^2 T, \tag{3.22}$$

where c denotes light velocity in vacuum.

In the following, we consider the one-dimensional heat transport phenomena with constant potential energy $V = V_0$

$$\frac{1}{c^2}\frac{\partial^2 T}{\partial t^2} + \frac{M_p}{\hbar}\frac{\partial T}{\partial t} + \frac{2V_0M_p}{\hbar^2}T = \frac{\partial^2 T}{\partial x^2}. \tag{3.23}$$

For quantum heat transport equation (3.23), we seek a solution in the form

$$T(x,t) = e^{-t/t_p}u(x,t). \tag{3.24}$$

After substituting Eq. (3.24) in Eq. (3.23), one obtains

$$\frac{\partial^2 u(x,t)}{\partial t^2} = c^2 \frac{\partial^2 u}{\partial x^2} + b^2 u(x,t), \tag{3.25}$$

where

$$b = \sqrt{\left(\frac{M_p c^2}{2\hbar}\right)^2 - \frac{2V_0 M_p}{\hbar^2} c^2}. \tag{3.26}$$

The general solution of Eq. (3.26) for Cauchy initial conditions

$$u(x,0) = f(x), \qquad \left.\frac{\partial u(x,t)}{\partial t}\right|_{t=0} = F(x), \tag{3.27}$$

has the form [3.7]

$$u(x,t) = \frac{f(x-ct) + f(x+ct)}{2} + \frac{1}{2}\int_{x-ct}^{x+ct} \Phi(x,t,z)dz, \tag{3.28}$$

where

$$\begin{aligned} \Phi(x,t,z) &= \frac{1}{c} F(z) J_0\left(\frac{b}{c}\sqrt{(z-x)^2 - c^2t^2}\right) \\ &\quad + btf(z)\frac{J_0'\left(\frac{b}{c}\sqrt{(z-x)^2 - c^2t^2}\right)}{\sqrt{(z-x)^2 - c^2t^2}} \end{aligned} \tag{3.29}$$

and $J_0(z)$ denotes the Bessel function of the first kind. Considering formulas (3.24 – 3.27), the solution of Eq. (3.23) describes the propagation of the initial state $f(x)$ of the Planck gas as the thermal wave with velocity c. It is quite interesting to formulate the condition at which these waves propagate without the distortion, i.e., conserving their shapes. The conditions for this to happen can be formulated as

$$b = \sqrt{\left(\frac{M_p c^2}{2\hbar}\right)^2 - \frac{2V_0 M_p}{\hbar^2} c^2} = 0. \tag{3.30}$$

When Eq. (3.30) holds, Eq. (3.25) assumes the form

$$\frac{\partial^2 u(x,t)}{\partial t^2} = c^2 \frac{\partial^2 u}{\partial x^2}. \tag{3.31}$$

Equation (3.31) is the wave equation with the solution (for Cauchy initial conditions (3.27))

$$u(x,t) = \frac{f(x-ct) + f(x+ct)}{2} + \frac{1}{2c}\int_{x-ct}^{x+ct} F(z)dz. \tag{3.32}$$

Equation (3.30), the distortionless condition, can be written as

$$V_0 t_p = \frac{\hbar}{8} \sim \hbar. \tag{3.33}$$

We can conclude that in the presence of the potential V_0, one can "observe" the undisturbed quantum thermal wave (created at $t = 0$) only when the *Heisenberg uncertainty* relation (3.33) is fulfilled.

On combining Eq. (3.24) and (3.32), the complete solution of Eq. (3.23) (for $b = 0$) can be written as

$$T(x,t) = e^{-t/2t_p}\left[\frac{f(x-ct) + f(x+ct)}{2} + \frac{1}{2c}\int_{x-ct}^{x+ct} F(z)dz\right]. \tag{3.34}$$

One can say that the formula (3.34) is a very pessimistic one, because the initial conditions (which operate at the Beginning) are smeared out over a time scale of the order of the Planck time.

3.3 Klein-Gordon thermal equation for a Planck Gas

As was shown in paper [3.5], the thermal properties of the Planck gas can be described by hyperbolic quantum heat transport equation, viz.,

$$\frac{1}{c^2}\frac{\partial^2 T}{\partial t^2} + \frac{M_p}{\hbar}\frac{\partial T}{\partial t} + \frac{2VM_p}{\hbar^2}T = \nabla^2 T. \tag{3.35}$$

In Eq. (3.35), t_p denotes Planck time, M_p is the Planck mass and V denotes the potential energy.

For the uniform Universe it is possible to study only one-dimensional heat transport phenomena. In the following ,we will consider the thermal properties of a Planck gas for constant potential $V = V_0$. In that case, the one-dimensional quantum heat transport equation has the form

$$\frac{1}{c^2}\frac{\partial^2 T}{\partial t^2} + \frac{M_p}{\hbar}\frac{\partial T}{\partial t} + \frac{2V_0 M_p}{\hbar^2}T = \frac{\partial^2 T}{\partial x^2}, \tag{3.36}$$

where formula for $t_p = \hbar/M_p c^2$ was used [3.5]. In Eq. (3.36) c denotes the light velocity. As $c \neq \infty$, we cannot omit the second derivative term and consider only Fokker-Planck equation

$$\frac{M_p}{\hbar}\frac{\partial T}{\partial t} + \frac{2V_0 M_p}{\hbar^2}T = \frac{\partial^2 T}{\partial x^2} \tag{3.37}$$

for heat diffusion in the potential energy V_0, or free heat diffusion

$$\frac{\partial T}{\partial t} = \frac{\hbar}{M_p}\frac{\partial^2 T}{\partial x^2}. \tag{3.38}$$

It occurs that only if we retain the second derivative term we have the chance to study the conditions in the Beginning.

Some implications of the forward and backward properties of the parabolic heat diffusion equation were beautifully described by J. C. Maxwell [3.7]:

> *"Sir William Thompson has shown in a paper published in the Cambridge and Dublin Mathematical Journal in 1844 how to deduce, in certain cases the thermal state of a body in past time from its observed conditions at present.*
> *If the present distribution of temperature is such that it may be expressed in a finite series of harmonics, the distribution of temperature at any previous time may be calculated but if (as in generally case) the series of harmonics is infinite, than the temperature can be calculated only when this series is convergent. For present and future time it is always convergent, but for past time it becomes ultimately divergent when the time is taken at a sufficiently remote epoch. The negative value of t for which the series becomes ultimately divergent, indicates a certain date in past time such that the present state of things cannot be deduced from any distribution of temperature occurring previously to the date, and becoming diffused by ordinary conduction. Some other event besides ordinary conduction must have occurred since that date in order to produce the present stage of things".*

As can be easily seen, the second derivative term in Eq. (3.35) carriers the memory of the initial state which occurred at time $t = 0$. If we pass with $c \to \infty$ we lose the possibility of studying the influence of the initial conditions at the present epoch as it is explained above by J. C. Maxwell. It means that by limiting procedure $c \to \infty$ *we cut off the memory of the Universe.*

For hyperbolic quantum heat transport, Eq. (3.36), we seek a solution of the form

$$T(x,t) = e^{-t/2t_p} u(x,t). \tag{3.39}$$

After substitution of Eq. (3.39) in Eq. (3.36), one obtains

$$\frac{1}{c^2}\frac{\partial^2 u}{\partial t^2} - \frac{\partial^2 u}{\partial x^2} + qu = 0, \tag{3.40}$$

where

$$q = \frac{2V_0 M_p}{\hbar^2} - \left(\frac{M_p c}{2\hbar}\right)^2. \tag{3.41}$$

In the following, we shall consider positive values of V_0, $V_0 \geq 0$, i.e., as well as the potential barriers and steps.

The structure of the Eq. (3.40) depends on the sign of the parameter q. Let us define the Planck wall potential, i.e., potential for which $q = 0$. From Eq. (3.41), one obtains

$$V_P = \frac{\hbar}{8t_P} = 1.25\ 10^{18}\ \text{GeV}, \tag{3.42}$$

where t_P is a Planck time. In Fig. 3.1, the parameter q is calculated as the function of V_0. For $q < 0$, i.e., when $V_0 < V_P$ Eq. (3.40) is *the modified telegrapher equation*(MTE) [3.3]. For the Cauchy initial condition

$$u(x,0) = f(x), \qquad \frac{\partial u(x,0)}{\partial t} = g(x), \tag{3.43}$$

and the solution of Eq. (3.39) has the form [3.3]

$$\begin{aligned} u(x,t) &= \frac{f(x-ct)+f(x+vt)}{2} + \frac{1}{2c}\int_{x-ct}^{x+ct} g(\zeta) I_0\left[\sqrt{-q(c^2t^2-(x-\zeta)^2)}\right] d\zeta \\ &+ \frac{(c\sqrt{-q})t}{2}\int_{x-ct}^{x+ct} f(\zeta)\frac{I_1\left[\sqrt{-q(c^2t^2-(x-\zeta)^2)}\right]}{\sqrt{c^2t^2-(x-\zeta)^2}} d\zeta. \end{aligned} \tag{3.44}$$

In Eq. (3.44), I_0, I_1 denotes the Bessel modified function of the zero and one, respectively.

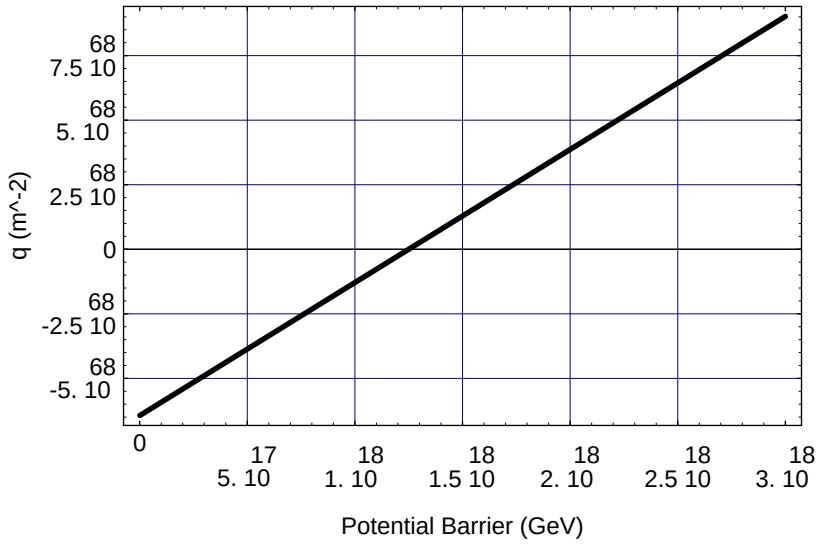

Figure 3.1: Parameter q (formula 3.36) as the function of the barrier height (GeV).

When $q > 0$, i.e., for $V_0 > V_P$ Eq. (3.40) is reduced to *the Klein-Gordon Equation* (K-GE), well known from its application in elementary particle and nuclear physics.

For the Cauchy initial condition (3.43), the solution of K-GE can be written as [3.3]

$$\begin{aligned} u(x,t) &= \frac{f(x-ct)+f(x+ct)}{2} \\ &+ \frac{1}{2c}\int_{x-ct}^{x+ct} g(\zeta) J_0\left[\sqrt{q(c^2t^2-(x-\zeta)^2)}\right] d\zeta \\ &- \frac{(c\sqrt{q})t}{2}\int_{x-ct}^{x+ct} \frac{J_1\left[\sqrt{q(c^2t^2-(x-\zeta)^2)}\right]}{\sqrt{c^2t^2-(x-\zeta)^2}} d\zeta. \end{aligned} \tag{3.45}$$

The case for $q = 0$ was discussed in paper [3.5] and described the distortionless quantum thermal waves.

Both solutions (3.44) and (3.45) exhibit the domains of dependence and influence on the modified telegrapher's equation and Klein-Gordon equation. These domains, which characterize the maximum speed, c, at which the thermal disturbance travels are determined by the principal terms of the given equation (i.e., the second derivative terms) and do not depend on the lower order terms. It can be concluded, that these equations and the wave equation have identical domains of dependence and influence. Both solutions (3.44) and (3.45) represent the distorted thermal waves in the field of potential barrier or steps V.

Bibliography for Chapter 3

[3.1] J. Marciak-Kozłowska, M. Kozłowski, *Found. Phys. Lett.* 9, (1996) 235.

[3.2] D. Jou, J. Casas-Vásquez, and G. Lebon, *Extended Irreversible Thermodynamics* (Springer-Verlag, Berlin, 1993).

[3.3] R. Maartens, *Class. Quantum Grav.* 12, (1995) 1455.

[3.4] P. G. Bergman, *Cosmology and Particle Physics* V. de Sabbata and H. Tso-Hain, Eds (Kluwer Academic, Dordrecht, 1994), p. 9.

[3.5] M. Kozłowski, J. Marciak-Kozłowska, *Found. Phys. Lett.* 10, (1999) 295.

[3.6] E. Nelson, *Phys. Rev.* 150, (1966) 1079.

[3.7] D. D. Joseph *Fluid Dynamics of Viscoelastic Liquids*, (Springer-Verlag, New York, 1990), p. 71

Chapter 4

Conclusions and perspectives

4.1 Quantum heat transport: from basics to applications

The development of ultraintense laser pulses will allow the study of new regimes of laser-matter interaction [4.1]. Lasers are now being designated [4.2] which will eventually lead to light intensities, such that $I\lambda_\mu^2 >> 10^{19}\,\mathrm{W}\mu\mathrm{m}^2/\mathrm{cm}^2$. Here I is the laser intensity of the laser light and λ_μ is the wavelength in microns. In such intensities, the electron jitter velocity in the laser electric field becomes relativistic: $p_0/mc > 1$, where p_0 is jitter momentum, m is electron rest mass and c is the light velocity in vacuum. When such lasers interact with an overdense plasma, it has been shown, that a large number of relativistic superthermal electrons with

energy E_{hot}

$$E_{hot} \sim \left[\sqrt{1 + \frac{I\lambda_\mu^2}{1.4\,10^{18}}} - 1\right] mc^2 \tag{4.1}$$

are produced [4.3]. Hence, $E_{hot} > mc^2$ for $I\lambda_\mu^2 > 4\,10^{18}$. For even higher $I\lambda_\mu^2$, E_{hot} can exceed the pair (e^+, e^-) production threshold. In the result, the interaction of ultraintense laser beams with matter can produce copious electron-positron pair, which represents a new state of matter with new thermal and radiative properties drastically different from ordinary plasma [4.4]. For the moment, the production of electron-positron pair was realized in SLAC experiment [4.5]. In that experiment a signal of 106 ± 14 positrons above background has been observed in collisions of a low-emittance 46.6 GeV electron beam with terawatt pulse from a Nd: glass laser at 527 nm wavelength. The positrons are interpreted as arising from a two step process in which laser photons are backscattered to GeV energies by the electron beam followed by a collision between the high energy photon and several laser photons to produce an electron-positron pair.

The creation of superthermal electron-positron pair is a relativistic effect. Both because the conversion of mass $\Leftrightarrow$ energy and the relativistic energies of created particle-antiparticle pairs. The natural frame to analyze the relativistic gases of particles is the quantum heat transfer equation (QHT) [4.6].

The GeV energy of laser photons emitted in SLAC experiment are precursors of a new field of interdisciplinary applications of laser femtosecond beams. This superenergetic photons can, in principle, create not only electron and nucleon fermionic gases but also the free quark-gluon gas (if it exists!).

In Chapter 2, the quantum heat transport equation (QHT) was formulated. For electron and nucleon gases, the QHT has the form:
for electrons:

$$\tau^e \frac{\partial^2 T^e}{\partial t^2} + \frac{\partial T^e}{\partial t} = \frac{\hbar}{m_e} \nabla^2 T^e, \tag{4.2}$$

for nucleons:

$$\tau^N \frac{\partial^2 T^N}{\partial t^2} + \frac{\partial T^N}{\partial t} = \frac{\hbar}{m} \nabla^2 T^N. \tag{4.3}$$

In Eqs. (4.2) and (4.3), m_e and m are the masses of electron and nucleon respectively and

$$\tau^e = \frac{\hbar}{m_e \alpha^2 c^2}, \qquad \tau^N = \frac{\hbar}{m(\alpha^s)^2 c^2}, \tag{4.4}$$

where τ^e and τ^N are the relaxation times for electrons and nucleons respectively. The constants $\alpha = e^2/\hbar c, \alpha^s = m_\pi/m$ (m_π denotes the π meson mass), are the fine-structure constants for electromagnetic and strong interactions.

As was shown in Chapter 2, static spherically symmetric solutions of Eqs. (4.2) and (4.3) potentials has the form

$$V^e(r) = -\frac{g^e}{r} e^{-\frac{r}{R_e}}, \qquad g^e = \alpha \ hbarc \tag{4.5}$$

$$V^N(r) = -\frac{g^N}{r} e^{-\frac{r}{R_N}}, \qquad g^N = \alpha^s \hbar c, \tag{4.6}$$

where the ranges of electromagnetic interaction (in solids) and strong interaction in nucleus equal

$$R_e = \frac{2\hbar}{m_e \alpha c}, \tag{4.7}$$

$$R_N = \frac{2\hbar}{m \alpha^s c}. \tag{4.8}$$

The potentials $V^e(r)$, $V^N(r)$ are the Debye-Hückl potential and Yukawa potential respectively [4.6].

It is quite natural to pursue the study of the thermal excitation to the subnucleon level, i.e. quark matter. Analogously as for electron and nucleon gases, for quark gas the QHT has the form

$$\frac{1}{c^2}\frac{\partial^2 T^q}{\partial t^2} + \frac{1}{c^2\tau}\frac{\partial T^q}{\partial t} = \frac{(\alpha_s^q)^2}{3}\nabla^2 T^q, \tag{4.9}$$

with α_s^q the fine-structure constant for strong quark-quark interaction. In paper [4.7], α_s^q was calculated, $\alpha_s^q = 1$. The *heaton* energy [4.6] for quark gas can be defined as

$$E_h^q = \frac{m_q}{3}\left(\alpha_s^q\right)^2 c^2, \tag{4.10}$$

where m_q denotes the average quark mass and $m_q = 417$ MeV [4.7]. With formula (4.10), the *heaton* energy for quark gas equals

$$E_h^q \cong 139\,\mathrm{MeV} = m_\pi. \tag{4.11}$$

It occurs that when we attempt to "melt" the nucleons in order to obtain the free quark gas, the energy of the *heaton* is equal to the π - meson mass. This is the thermodynamics presentation for the quark *confinement*. Moreover, we conclude that only from hyperbolic quantum heat transport equation we obtain finite mass for particle which mediates the strong interaction. For parabolic heat transport equation $\tau^N \to 0$, i.e. (formula 4.4)

$$\tau^N = \frac{\hbar}{m(\alpha^s)^2 c^2} = \frac{\hbar m}{m_\pi^2 c^2} \to 0, \tag{4.12}$$

hence, $m_\pi \to \infty$. Analogously from Fourier equation one can conclude, that due to the fact that $v_h \to \infty$, all interactions must have zero range as from formulas (4.7) and (4.8)

$$R^{e,N,q} = \frac{2\hbar}{m v_h^{e,N,q}} \to 0,$$

when $v_h \to \infty$.

Table 4.1: Ranges of interactions and *heaton* energies for quark, electron and nucleon gases

	Range [m]		*Heaton* energy [eV]	
particles	QHT	Fourier	QHT	Fourier
quarks	10^{-16}	0	$1.39\,10^{8}$	∞
electrons	10^{-10}	0	9	∞
nucleons	10^{-15}	0	$7\,10^{6}$	∞

In Table 4.1, the results for calculations of the ranges of interactions and *heaton* energies for electron, nucleon and quark gases are presented. From the inspection of the Table 4.1, we conclude that the Fourier equation cannot be applied to study of the thermal processes on the atomic, nuclear and quark scales.

4.2 Hierarchical structure of the thermal excitation

In the book, the structure of thermal excitation induced by femtosecond laser pulses was investigated. It was shown, that quantum of temperature field, *heaton*, has the energy which depends on the two constants of nature $\alpha = e^2/\hbar c$, (fine-structure constant for electromagnetic infractions) and $\beta = m_e/m_p$, where m_e is the electron mass and m_p is the proton mass.

Recently, the new field of thermal investigations of nanoparticles (i.e., particles with radius r of the order of nanometer) was developed [4.9]. In paper [4.10] the model for the relaxation of thermal excitation of the nanoparticles was derived and obtained to the study of Ga nanoparticles. It was shown, that the thermodynamical properties of nanoparticle depend on its geometrical dimensions.

The fact that the femtosecond thermodynamical properties of nanoparticles depend on fine-structure constant α open the question: does the constant α is really constant? Recently, [4.11] the search for fine-structure constant was undertaken with positive results. It occurs that $\Delta\alpha/\alpha \sim 10^{-5}$.

In the paper [4.10], starting with atomic values of the relaxation time τ_e and velocity of thermal wave v_h, the microscopic model of the relaxation processes in nanoparticles was formulated. Considering the quantum heat transport equation

$$\tau^e \frac{\partial^2 T^e}{\partial t^2} + \frac{\partial T^e}{\partial t} = \frac{\hbar}{m_e} \nabla^2 T^e \tag{4.13}$$

and Pauli-Heisenberg inequality

$$\Delta r \, \Delta p \geq N^{1/3} \hbar, \tag{4.14}$$

the thermal velocity v_h^f and relaxation time τ^f were calculated for nanoparticles:

$$v_h^f = \frac{1}{N^{1/3}} v_h \tag{4.15}$$

$$\tau^f = N\tau. \tag{4.16}$$

In formulas (4.15) and (4.16), N denotes the number of particles (*"partons"*) in a nanoparticle. For a nanoparticle with radius r, the number of *"partons"*

equals

$$N = \frac{\frac{4\pi}{3} r^3 \rho A Z}{\mu}, \tag{4.17}$$

where ρ is the density of nanoparticles, A is the Avogardo number, Z is the number of the valence electrons and μ is the molecular mass of the nanoparticle material.

Two new interesting results can be concluded from formulas (4.15)–(4.17). First of all, the radius of a nanoparticle is proportional to the number of *partons* [4.9]:

$$r \sim N^{1/3}. \tag{4.18}$$

In this aspect, the nanoparticle resembles the atomic nucleus in which [4.2]:

$$r \sim A^{1/3}. \tag{4.19}$$

In that case, A is the mass number of the nucleus (but not Avogardo number!). The formula (4.16) describes the quantization rule for the relaxation time. It can be stated, that the τ (atomic relaxation time) is the *quantum* of relaxation time.

From the theoretical point of view there emerges a model of "free" electrons in clusters as a system of Fermi (spin one-half) particles being quantized in a global mean field. In a nanoparticle the global mean field is not the screened Coulomb potential around the positive charge of the point – like nucleus; it is more like cavity [4.10]. And the positive charge is smeared out through the whole volume. The nanoparticles constitute a new family of what may be called *quasi-atoms* or even more descriptively, *giant atoms*. The analogy between real atoms and metallic nanoparticles has its limits. First, the clusters can easily lose single atoms or be split into smaller clusters. They are not indivisible the way atoms are. Unlike the atoms, where

the positive charges are extremely hard frozen, the ionic charges in a cluster may be highly excited thermally. As a result, the quantized electronic motion is really taking place in a heat bath. The electrons may be thermally excited (for example by ultrashort laser pulses) out of their ground state [4.10] configuration and eventually build the thermal waves penetrating the nanoparticles.

Table 4.2: Hierarchical structure of the thermal excitation

Hierarchical structures	τ [s]	v_h [m/s]	E_h [eV]	References
Atom	$\frac{\hbar}{m_e v_h^2}$	$\alpha c, \quad \alpha = \frac{e^2}{\hbar c}$	$m_e v_h^2$	(a)
Molecule	$\frac{m_p}{m_e}\frac{\hbar}{m_e v_h^2}$	$\alpha c(\frac{m_e}{m_p})^2$	$\alpha^2 \frac{m_e}{m_p} m_e c^2$	(b)
Nanoparticle containing N particles	$N\frac{\hbar}{m_e v_h^2}$	$\frac{1}{N^{1/3}}\alpha c$	$\frac{m_e}{N^{2/3}}\alpha^2 c^2$	(c)
Atomic nucleus	$\frac{\hbar}{m_N v_h^2}$	$\alpha^s c$ $\alpha^s = \frac{2m_e}{\alpha m_p}$	$m_p(\alpha^S c)^2$	(d)

a) J. Marciak-Kozłowska, M. Kozłowski, *Lasers in Engineering* 5, (1996) 79; b) M. Kozłowski, J. Marciak-Kozłowska, *Lasers in Engineering* 9 (1999) 103; c) M. Kozłowski, J. Marciak-Kozłowska, *Lasers in Engineering* 10 (2000) 37; d) M. Kozłowski, J. Marciak-Kozłowska, *Lasers in Engineering* 7, (1998) 13.

At closer look, the giant atoms are conceptually hybrids between atomic and nuclear quantum systems. The constant density (ρ) and the deformability are nuclear characteristic but the quantized constituents are electrons,

as in atom. The *quasi-atom* can be looked at as an ordinary atom differing only by having the nuclear charge distributed essentially through the whole atom.

In Table 4.2, the hierarchical structure of the matter is presented. It occurs that starting with nucleus, through the atom, the molecule and the nanoparticle the relaxation time, the velocity of heat propagation and *heaton* energy can be described with the help of two constants $\alpha = e^2/\hbar c = 1/137$, and $\beta = m_e/m_p = 1/1836$.

We conclude, that despite the vast complexity of everything made out of atoms and molecules the thermal properties of all entities are determined by the values of just two numbers. Up to now we do not known why these two numbers take the precise values that they do. Were they different our Universe would be different, perhaps unimaginably different [4.12]. In paper [4.13], the "ambient temperature" important for biological cells was calculated

$$T_m \sim 10^{-3}\alpha^2 m_e c^2 \sim 316 \text{ K} = 40^0 \text{ C}. \tag{4.20}$$

In Fig. 4.1(a), the values of T_m for different α are presented. When α changes in the range -10% to 10%, the ambient temperature changes from -20^0 C to 100^0 C. The problem "How constants are constants" is not an academic one. A time-varying fine structure constant, α, can now be sought with a new technique [4.11]. The inherent strength of the electromagnetic force is characterized by α, the value of which determines how well atoms hold together when heated up (compare heaton energies in Table 4.2).

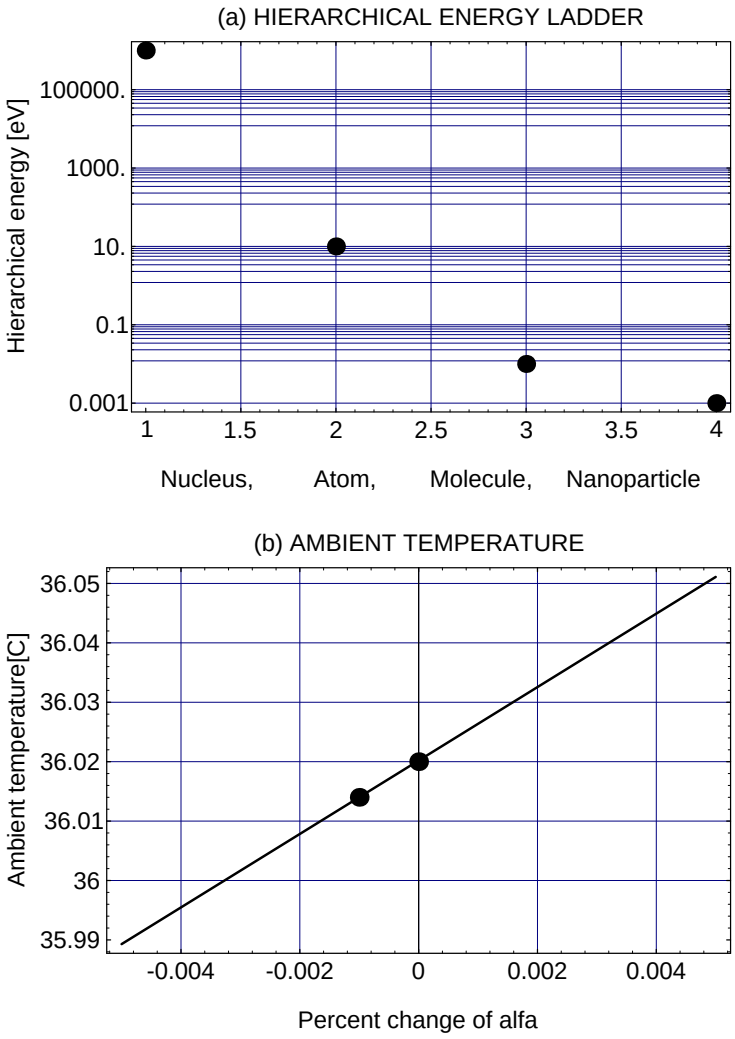

Figure 4.1: (a) Hierarchy of thermal excitation in nucleus, atom, molecule and nanoparticle. (b) The ambient temperature as the function of the change of fine structure constant. The experimental results of paper [4.11] is also presented (lower circle).

Now, a group of scientists led by John Webb has explored the possibility of sampling the ancient light emitted by ancient atoms and comparing it with modern light emitted by modern atoms. The researches looked at the relative spacing of multiplets of absorption lines in quasar spectra, comparing lines of ionized iron with those of ionized magnesium. After taking all corrections into account, the authors of the paper [4.11] place a limit on $\Delta\alpha/\alpha \sim -1.1\ 10^{-5}$. In Fig. 4.1(b) the values of ambient temperature for $\Delta\alpha/\alpha = 0$ ($\alpha = 1/137$) and the $\Delta\alpha/\alpha = 10^{-3}\%$ (paper [4.11]) are presented.

Bibliography for Chapter 4

[4.1] J. C. Diels, W. Rudolph, *Ultrashort Laser Pulse Phenomena*, (Academic Press, Inc., San Diego, 1996).

[4.2] M. D. Perry, G. Mourou, *Science* 264, (1994) 917.

[4.3] E. P. Liang et al., *Phys. Rev. Lett.* 81, (1998) 4887.

[4.4] R. Svenson et al., *Astrophys. J.* 283, (1984) 842.

[4.5] D. L. Burke et al., *Phys. Rev. Lett.* 79, (1997) 1626.

[4.6] M. Kozłowski, J. Marciak-Kozłowska, *Lasers in Engineering* 7, (1998) 81.

[4.7] M. Kozłowski, J. Marciak-Kozłowska, *Hadronic Journal* 20, (1997) 289.

[4.8] B. Povh, K. Rith, Ch. Scholz, F. Zetsche, *Particles and Nuclei*, (Springer-Verlag, Berlin, 1995).

[4.9] M. Nisoli et al., *Phys. Rev. Lett.* 78, (1997) 3575.

[4.10] M. Kozłowski, J. Marciak-Kozłowska, *Lasers in Engineering* 10, (2000) 37

[4.11] J. K. Webb et al., *Phys. Rev. Lett.* 82, (1999) 884.

[4.12] J. D. Barrow, *Theories of Everything*, (Fawcett Columbine, New York, 1991).

[4.13] M. Kozłowski, J. Marciak-Kozłowska, *Lasers in Engineering* 9, (1999) 103

Appendices

Appendix A

Elliptic, parabolic and hyperbolic equations

The hyperbolic heat transport equation

$$\frac{1}{v^2}\frac{\partial^2 T}{\partial t^2} + \frac{m}{\hbar}\frac{\partial T}{\partial t} + \frac{2Vm}{\hbar^2}T - \frac{\partial^2 T}{\partial x^2} = 0 \tag{A.1}$$

is the partial two dimensional differential equation (PDE). According to the classification of the PDE, QHT is the hyperbolic PDE. To show this, let us consider the general form of PDE, with only two independent variables ξ and η

$$\left(A\frac{\partial^2}{\partial \xi^2} + B\frac{\partial^2}{\partial \xi \eta} + C\frac{\partial^2}{\partial \eta^2}\right)\Psi(\xi,\eta) = \left(\text{function of } \xi, \eta, \Psi, \frac{\partial \Psi}{\partial \xi}, \frac{\partial \Psi}{\partial \eta}\right). \tag{A.2}$$

Then the equation is called

$$\text{elliptic} \quad \text{if} \quad B^2 - 4AC < 0,$$

$$\text{parabolic} \quad \text{if} \quad B^2 - 4AC = 0, \tag{A.3}$$

$$\text{hyperbolic} \quad \text{if} \quad B^2 - 4AC > 0.$$

For the Eq. (A.1) we have

$$A = \frac{1}{v}, \qquad B = 0, \qquad C = -1,$$

i.e. $B^2 - 4AC = 4\,v^{-1} > 0$ and according to (A.3) Eq. (A.1) is the hyperbolic equation.

On the other hand, for the Fourier equation with potential term

$$\frac{m}{\hbar}\frac{\partial T}{\partial t} + \frac{2Vm}{\hbar^2}T - \frac{\partial^2 T}{\partial x^2} = 0 \tag{A.4}$$

we have

$$A = 0, \qquad B = 0, \qquad C = -1,$$

i.e. $B^2 - 4AC = 0$ and Fourier equation is the parabolic PDE. One can say that for heat transfer, described by Fourier equation, the velocity of heat propagation v is infinite and $A = 0$.

Appendix B

Paradox of heat conduction

The fundamental problem of irreversible thermodynamics of fluids is the determination of the 5 fields:

$$\begin{array}{rl} \text{mass density} & \rho(x,t), \\ \text{velocity} & v_i(x,t), \\ \text{temperature} & T(x,t), \end{array} \tag{B.1}$$

in all points of the fluids and at all times. For this purpose, we need field equations and these are based upon the equation of balance of mechanism and thermodynamics, viz. the conservation laws of mass and momentum and the balance of internal energy

$$\dot{\rho} + \rho \frac{\partial v_j}{\partial x_j} = 0,$$

$$\rho\dot{v}_i - \frac{\partial t_{ij}}{\partial x_j} = 0, \tag{B.2}$$

$$\rho\dot{\epsilon} + \frac{\partial q_j}{\partial x_j} = t_{ij}\frac{\partial v_i}{\partial x_j},$$

where t_{ij} is the stress tensor, q_i is the heat flux and ϵ denotes a specific internal energy. Assuming only linear relations between forces and fluxes the phenomenological equations for heat flux can be written as

$$q_i = -\kappa\frac{\partial T}{\partial x_i}, \qquad \kappa > 0. \tag{B.3}$$

(In the subsequent we limit ourselves to the thermal phenomena only). Insertion of (B.3) into the balance equation (B.2) leads to the temperature field equation. The field equation is parabolic in character. In order to emphasize this fact we investigate two special cases:

- the case of the fluid at rest with constant density; and
- the case of the fluid with constant density and temperature and with velocity field of the form $\vec{v} = (0, v(x^1, t), 0)$.

In these cases the system of Eq. (A.2) is reduced to a single partial differential equation for $T(x,t)$. Neglecting non-linear terms in gradients and time derivatives, we obtain

$$\frac{\partial T}{\partial t} = \frac{\kappa}{\rho\epsilon_T}\Delta T, \tag{B.4}$$

where $\epsilon_T = (\frac{\partial \epsilon}{\partial T})_\rho$ is the specific heat at constant volume, a positive quantity. The Eq. (B.4) is the diffusion equation.

We may write the solution of (B.4) for an initial value problem in infinite space in the form

$$T(x,t) = \frac{1}{(4\pi Dt)^{\frac{3}{2}}}\int_{-\infty}^{\infty} T(y,0)\exp\left(-\frac{(y-x)^2}{4Dt}\right)dy, \tag{B.5}$$

where D stands for $\kappa/\rho\epsilon_T$. This solution implies that $T(x,t)$ is unequal to zero for all x and $t > 0$ even though $T(x,0)$ may have support on a finite interval only. Thus, the temperature spreads through the whole space *infinitely fast*, a phenomenon that has been called a paradox.

It is fair to say that few people had doubts about it, because the Eq. (B.5) perfectly reflected the engineers' and physicists' interests. However, the desire to have hyperbolic equation in thermodynamics and, hence, finite speeds was main motivation for the development of extended thermodynamics. It began with Cattaneo equation [1.1].

Cattaneo changed the formula for heat flux (B.3) and defined the non-stationary Fourier law

$$q_i = -\kappa \left(\frac{\partial T}{\partial x_i} - \tau \frac{\partial T}{\partial x_i} \right). \tag{B.6}$$

Finally, Cattaneo proceeds to modify Eq. (B.6), assuming that the operator $\tau \frac{d}{dt}$ is small such that

$$\left(1 - \tau \frac{d}{dt} \right)^{-1} \approx 1 + \tau \frac{d}{dt}. \tag{B.7}$$

In this approximation the Eq. (B.6) assumes the form (Cattaneo equation)

$$q_i + \tau \dot{q}_i = -\kappa \frac{\partial T}{\partial x_i}. \tag{B.8}$$

If we combine Cattaneo equation with energy balance equation (B.2), we obtain

$$\tau \frac{\partial^2 T}{\partial t^2} + \frac{\partial T}{\partial t} = \frac{\kappa}{\rho \epsilon_T} \nabla^2 T. \tag{B.9}$$

This is a hyperbolic heat transfer equation (if $\tau > 0$) and it predicts the propagation of heat pulses at the finite speed (Appendix A)

$$v = \pm \sqrt{\frac{\kappa}{\rho c_T \tau}}. \tag{B.10}$$

Index